MSC-E Technical Report 2/2001

September 2001

INTERCOMPARISON STUDY OF NUMERICAL MODELS FOR LONG-RANGE ATMOSPHERIC TRANSPORT OF MERCURY

Stage I. Comparison of chemical modules for mercury transformations in a cloud/fog environment

Alexey Ryaboshapko, MSC-East EMEP
Ilia Ilyin, MSC-East EMEP
Russell Bullock, US-EPA USA
Ralf Ebinghaus, GKSS Germany
Kristen Lohman, AER USA
John Munthe, IVL Sweden
Gerhard Petersen, GKSS Germany
Christian Seigneur, AER USA
Ingvar Wängberg, IVL Sweden

METEOROLOGICAL SYNTHESIZING CENTRE - EAST

Leningradsky prospekt, 16/2, Moscow 125040 Russia
tel./fax: 7 095 214 39 93
e-mail: msce@msceast.org
www. msceast.org

A B S T R A C T

The intercomparison study described in this Technical Note represents a first attempt to synthesize the current knowledge of atmospheric mercury chemistry into model systems which can be generally used to evaluate the atmospheric transport and mercury transboundary fluxes in Europe. At the first stage the comparison of modules for physico-chemical transformations of mercury species in a cloud/fog environment with prescribed initial mercury concentrations in ambient air and other physical and chemical parameters relevant for atmospheric mercury transformations has been realized. Five scientific groups involved in atmospheric mercury modeling have participated in the study: U.S. Environmental Protection Agency (USA), GKSS Scientific Research Center (Germany), Atmospheric and Environmental Research/EPRI (USA), Environmental Research Institute (Sweden), Meteorological Synthesizing Centre-East/EMEP (Russia).

Results of individual modules in terms of temporal evolution of mercury concentrations in cloud droplets for a variety of initial concentrations in ambient air have been intercompared. In general, results obtained by all modules agree within a factor of about two. It is confirmed that the modules are based on an adequate parameterization of main physico-chemical processes such as oxidation of mercury both in the gas and aqueous phase, simultaneously occurring reductive processes in the aqueous phase, and the adsorption of oxidized aqueous mercury on soot particles.

CONTENTS

INTRODUCTION

Environmental pollution by heavy metals (HM) more and more attracts attention on national and international levels. A range of projects related to the long-range atmospheric transport of these substances are being carried out by several international organizations and programmes such.

In June 1998 in Arhus (Denmark) 36 Parties to the Convention on Long-Range Transboundary Air Pollution (LRTAP) signed the Protocol on HMs. In accordance with the Protocol EMEP shall provide Executive Body with information on the long-range transport and deposition of HMs. EMEP results should promote further evaluating international abatement strategies and reviewing the implementation of the Protocol and compliance with Parties obligations. In addition to the fulfilment of the basic obligations Parties to the Protocol shall encourage research, monitoring and co-operation, in particular, in the fields of long-range transport modelling.

The Meteorological Synthesizing Centre - East (EMEP/MSC-E) has a responsibility to perform model calculations of transboundary transport and deposition of heavy metals in the EMEP region. Based on a decision of the 18th session of the Steering Body of EMEP (EB.AIR/GE.1/24, 1994) an intercomparison study of atmospheric long-range transport models had to be organized by MSC-E focusing on lead, cadmium and mercury defined by the Convention to be the priority metals of concern. The intercomparison study is considered by the Steering Body to be one of the essential prerequisites for application of heavy metal models for EMEP operational activity.

The model intercomparisons for lead and cadmium were carried out in 1996 (EMEP/MSC-E report 2/96, 1996) and 1998 (EMEP/MSC-E report 2/2000, 2000), respectively. As a follow up activity and in accordance with recommendations of EMEP/WMO workshops (Moscow 1996 and Geneva 1999) the mercury model intercomparison study has been started. There was a consensus among potential participants of the mercury model intercomparison study that this task would be far more comprehensive and complex, since unlike lead and cadmium, mercury:

- exists in ambient air predominantly in gaseous elemental form, which is estimated to have a global residence time of about one year making it subject to long-range atmospheric transport over hemispheric and global scales;
- is subjected to a variety of physical and/or chemical or photochemical processes and interactions;
- has a tendency to be readily re-emitted to the air once deposited to surfaces.

In this context a comparison of the EMEP/MSC-E model with the most advanced models of different scientific groups around the world provides a possibility for participants to reveal and eliminate shortcomings of their modelling approaches mercury models and to increase the reliability of their results.

The intercomparison will focus on:

- an evaluation of parameterization of the main physical-chemical processes of mercury transformations in the gaseous and the liquid phase;
- a comparison of modeling results with measurements obtained from both short-term campaigns and from the EMEP monitoring network and other international and national programs;
- a comparison of the main features of long-range transport of different mercury forms.

The model intercomparison study will be carried out in four stages:

Stage I. Comparison of modules for physico-chemical transformations of mercury species in a cloud/fog environment with prescribed initial mercury concentrations in ambient air and other physical and chemical parameters relevant for atmospheric mercury transformations.

Stage II. Comparison of model results with observations during 1-2 weeks episodes. Hourly and daily averages and event based averages of mercury concentrations in air and in precipitation, respectively, obtained from the joint Swedish/Canadian/German field campaign TRANSECT 1995 and from the European Union Environment & Climate project Mercury Species Over Europe (MOE) will be used.

Stage III. Comparison of model results with observed monthly and annual means of mercury concentrations in air and precipitation and deposition fluxes available from European monitoring stations in 1997.

Stage IV. Comparison of model predicted atmospheric budgets of mercury species in the entire EMEP domain and for selected European countries (UK, Poland and Italy), including dry and wet deposition within and outside the area of the countries.

Five scientific groups involved in atmospheric mercury modeling agreed to participate in Stage 1 of the mercury model intercomparison study:

- U.S. Environmental Protection Agency (USA), single volume version of the Community Multi-Scale Air Quality (CMAQ) model.

- GKSS-Forschungszentrum Geesthacht GmbH (Germany), Tropospheric Chemistry Module (TCM) extracted from the European mercury version of the Acid Deposition and Oxidants Model (ADOM).
- Atmospheric and Environmental Research / EPRI (USA), Mercury Chemistry Model (AER/EPRI).
- Swedish Environmental Research Institute (IVL) (Sweden), Chemistry of Atmospheric Mercury (CAM) process model.
- Meteorological Synthesizing Centre-East (Russia), Chemical Module of MSC-E Heavy Metal Model (MSCE-HM).

1. FIRST STAGE OF INTERCOMPARISON PROGRAM

It has been agreed by the participants that the modelling domain is presented by a fixed volume of a cloud. No atmospheric movements like advective or vertical transport are considered. Any exchange with surrounding air or with underlying surfaces is also neglected. Hence, only mercury transfer processes between the gas and liquid phase and chemical transformations in the gas and liquid phase are modelled.

The size spectrum of water droplets and the liquid water content in the system are assumed to be constant in time and within the modelled volume. Atmospheric pressure in the modelling system is 800 mbar corresponding roughly to 2 km height.

Since photochemistry can play a serious role in mercury transformations it was agreed to start model calculations at midnight for all participating models. Duration of day and night is assumed to be equal with solar radiation typical for Central Europe (the 55-th latitude) on September 15.

The time evolution of mercury concentrations in a cloud/fog environment for 48 hour period is considered. All participants should use their own individual values of reaction rates, water solubilities, Henry's law constants, etc.

Temporal resolution for output parameters is 10 min. The output parameters are the following:

Elemental mercury (Hg^0) in the gas phase

Oxidized mercury (Hg^{2+}) in the gas phase

Mercury in the aerosol particulate phase (all chemical forms)

Elemental mercury (Hg^0) in the liquid phase

Oxidized mercury (Hg^{2+}) dissolved (all chemical species in sum)

Mercury in the particulate phase within droplets (all chemical forms)

Four-valent sulfur in the liquid phase

Ozone in the liquid phase

Hydrogen-ion in the liquid phase.

All output parameters for mercury are expressed as mercury mass in the defined volume (one cubic meter). The other output parameters (sulfur, ozone, hydrogen-ion) are expressed in moles per liter.

It is commonly recognized that soot particles can play a key role in the liquid phase mercury chemistry. From the other hand, the knowledge on soot behavior and soot concentrations in

the atmosphere is rather poor. Bearing this in mind the participants have agreed to provide two modelling calculation sets – including soot and without soot.

To check sensitivity of the module to the values of initial concentrations of gaseous oxidized and particulate mercury it has been agreed to run the models at a set of different values of the initial concentrations of the mentioned mercury forms.

2. DESCRIPTION OF THE SCHEMES

As it was shown above, in the atmosphere mercury is represented by a great number of different reactive compounds. In the atmosphere oxidation reactions can take place both in the gaseous and liquid phase. Oxidants can be represented by a wide range of substances – ozone, halogens, different radicals. Along with oxidation reverse reactions of reduction to the elemental form are possible. The key question of atmospheric mercury chemistry lies in the evaluation of a relative importance of oxidation and reduction in the cloud liquid phase. The answer to this question depends on understanding of the role of clouds: whether they are chemical reactors of oxidation of mercury with subsequent scavenging from the atmosphere or they are reactors where oxidized mercury is reduced to the elemental form. In the latter case the availability of clouds leads to the increase of mercury life-time in the atmosphere.

At present in science there are two points of view on this problem the essence of which is illustrated in figure 2.1 by schemes in a very simplified form. According to scheme A [*Pleijel and Munthe*, 1995; *Petersen et al.,* 1998] the availability of the liquid phase in the atmosphere leads to the intensification of oxidation. Vice versa according to scheme B [*Seigneur et al.*, 1994, 1998; *Seigneur and Lohman*, 1999] clouds are reactors of mercury reduction to the elemental form.

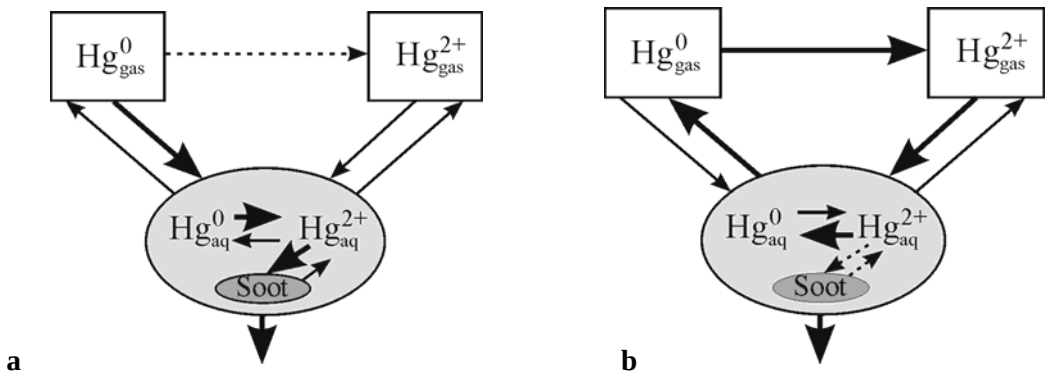

Figure 2.1. Possible pathways of mercury physical-chemical transformations

Most of mercury transport models currently in use or under development contain chemistry modules to describe physical-chemical transformations of mercury [*Pleijel and Munte*, 1995; *Lin and Pehkonen*, 1997; *Petersen et al.,* 1998; *Seigneur et al*., 1994]. In some models physical-chemical transformation schemes are very simple and can be solved analytically [*Ryaboshapko et al*., 1999]. Other schemes include a number of chemical reactions and physical processes [*Pai et al*., 1997]. In such cases the solution can be obtained only by numerical modelling. Consideration of these or those reactions in a model can drastically change final results. In this context the first stage of the campaign is devoted only to chemical transformations of mercury species.

It should be noted that the Tropospheric Chemistry Module (TCM) used by the GKSS does not correspond in full to the conditions of the intercomparison of mercury chemical schemes. The intercomparison conditions presumed to consider totally closed chemical systems. The GKSS scheme deals with entire cloudy layer of the atmosphere and it is open for exchange with the upper and lower layers. In other words, the GKSS scheme is intermediate between purely chemical schemes and schemes of mercury wet scavenging from the atmosphere. Moreover, the TCM is the only scheme with a capability to simulate real measurement data, i.e. concentration of precipitation as a function of precipitation amount.

2.1. CMAQ Model

The CMAQ-Hg model is being developed from the Community Multi-scale Air Quality model developed by the U.S. Environmental Protection Agency. The CMAQ model originally simulated the emission, transport, transformation and deposition of a variety of air pollutant species related to tropospheric ozone, acid deposition and aerosol particulate matter. The CMAQ-Hg model adds the capability to simulate the atmospheric pathway of elemental mercury and certain inorganic mercury compounds. Toward the development of the CMAQ-Hg model, a simplified single-volume version has been developed to simulate gas/liquid partitioning, cloud water chemistry and adsorption of mercury complexes to soot particles suspended in cloud water. A closed volume is assumed and a single cloud droplet size is simulated. Gas-phase chemistry is not simulated in the closed cloud-volume version of the model used for the intercomparison since current scientific evidence suggests that gas-phase mercury chemistry is very slow and operates on reaction time scales on the order of months or years. Gas/liquid partitioning of elemental mercury (Hg^0) and mercuric chloride ($HgCl_2$) is simulated using Henry's law equilibrium assumptions. The Henry's constants used for Hg^0 and $HgCl_2$ are 1.1×10^{-1} M atm^{-1} and 1.4×10^6 M atm^{-1}, respectively. Mercuric Oxide (HgO) is modelled as a solid aerosol in air and complete conversion to the liquid

phase is assumed to occur from cloud microphysics. However, since the test conditions specify no initial HgO, the concentration of HgO in air is always zero. HgO is the only gas-phase aerosol species in the CMAQ-Hg model.

Aqueous chemistry of mercury and its compounds is simulated simultaneously with the aqueous chemistry previously developed for the full scale CMAQ model. The schematic diagram below (figure 2.2) illustrates the physical chemistry system of the CMAQ-Hg single cloud volume model.

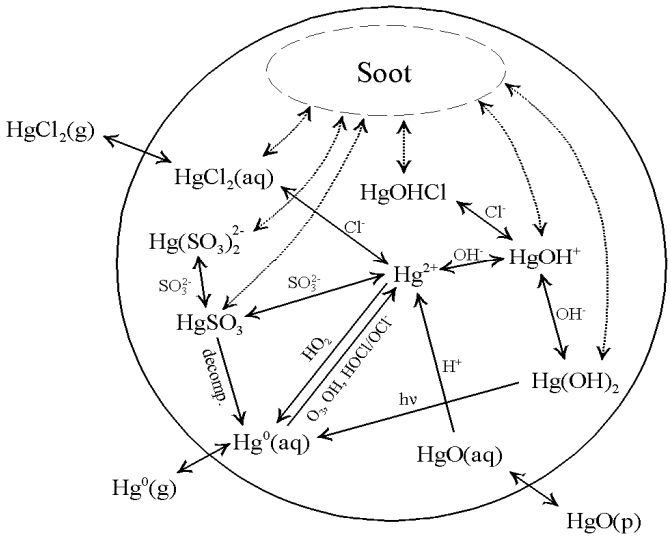

Figure 2.2. The physical chemistry system of the CMAQ-Hg single cloud volume model

Further testing and optimization will be performed on this cloud water model before its implementation into the full scale CMAQ-Hg.

Oxidation of Hg^0 by O_3

$$Hg^0_{(aq)} + O_{3(aq)} \xrightarrow{H^+} Hg^{2+}_{(aq)} + \text{Products}$$

$$R_1 = -\frac{d[Hg^0_{(aq)}]}{dt} = k_1[Hg^0_{(aq)}][O_{3(aq)}], \quad \text{where } k_1 = 4.5\times10^7 M^{-1}s^{-1}$$

The value for k_1 is taken from *K.Pleijel and J.Munthe* [1995].

Reduction of $HgSO_3$ to Hg^0 by decomposition

$$HgSO_{3(aq)} \xrightarrow{\text{decomp}} Hg^0_{(aq)} + \text{products}$$

$$R_2 = -\frac{d[HgSO_{3(aq)}]}{dt} = k_2[HgSO_{3(aq)}], \quad \text{where } \ln(k_2/T) = \frac{(31.971\times T) - 12595}{T}$$

where the temperature dependent function for k_2 is taken from [*Van Loon et al.,* 2000].

Photoreduction of $Hg(OH)_2$

$$Hg(OH)_{2(aq)} \xrightarrow{h\nu} Hg^0_{(aq)} + \text{products}$$

$$R_3 = -\frac{d[Hg(OH)_{2(aq)}]}{dt} = k_3[Hg(OH)_{2(aq)}], \quad \text{where } k_3 = 3\times10^{-7}s^{-1} \text{ at midday } 60^\circ\text{N latitude.}$$

The value for k_3 is taken from [*Xiao et al.,* 1994]. A simplification is made for the single volume cloud model where $k_3 = 2 \times 10^{-7}$ s^{-1} is used during all daylight hours.

Conversion of HgO to Hg^{2+} by H^+

$$HgO_{(aq)} \xrightarrow{H^+} Hg^{2+}_{(aq)} + \text{products}$$

$$R_4 = -\frac{d[HgO_{(aq)}]}{dt} = k_4[HgO_{(aq)}][H^+_{(aq)}], \text{ where } k_4 = 1\times 10^{10}\, M^{-1}s^{-1}$$

The value for k_4 is set close to the diffusion controlled limit as in [*Pleijel and Munthe*, 1995]. This reaction applies only to HgO particles captured from gas to liquid phase. HgO produced from Hg^0 oxidation in the liquid phase is assumed to be instantaneously converted to Hg^{2+}.

Oxidation of Hg^0 by OH radical

$$Hg^0_{(aq)} \xrightarrow{2OH} Hg^{2+}_{(aq)} + \text{products}$$

$$R_5 = -\frac{d[Hg^0_{(aq)}]}{dt} = k_5[Hg^0_{(aq)}][OH_{(aq)}], \quad \text{where } k_5 = 1\times 10^{9}\, M^{-1}s^{-1}$$

The value for k_5 is taken from [*Lin and Pehkonen,* 1997] as the limiting conversion rate of Hg^0 to Hg^+ which is followed by more rapid conversion of Hg^+ to Hg^{2+}.

Oxidation of Hg^0 by chlorine (HOCl and OCl^-)

$$Hg^0_{(aq)} + HOCl_{(aq)} \longrightarrow Hg^{2+}_{(aq)} + \text{products}$$

$$Hg^0_{(aq)} + OCl^-_{(aq)} \xrightarrow{H^+} Hg^{2+}_{(aq)} + \text{products}$$

$$R_6 = -\frac{d[Hg^0_{(aq)}]}{dt} = (k_{6a}\alpha_0 + k_{6b}\alpha_1)\times[Hg^0_{(aq)}][Cl(I)_{(aq)}]$$

where $k_{6a} = 2.09\times 10^6\, M^{-1}s^{-1}$; $k_{6b} = 1.99\times 10^6\, M^{-1}s^{-1}$; $\alpha_0 = \dfrac{[H^+]}{[H^+]+K_a}$; $\alpha_1 = \dfrac{K_a}{[H^+]+K_a}$;

$K_a = 10^{-7.5}$ is the equilibrium constant for $HOCl \Leftrightarrow H^+ + OCl^-$

and $[Cl(I)_{(aq)}]$ = total aqueous Cl_2 concentration calculated from an effective Henry`s law constant

$$H_{eff} = H_{int}\left(1 + \frac{10^{-3.3}}{[Cl^-_{(aq)}][H^+_{(aq)}]} + \frac{10^{-10.8}}{[Cl^-_{(aq)}][H^+_{(aq)}]^2}\right), \text{ where } H_{int} = 7.61\times 10^{-2} \text{ M atm}^{-1}$$

This treatment for combined chlorine reaction is taken from [*Lin and Pehkonen*, 1998].

Reduction of Hg^{2+} by HO_2

$$Hg^{2+}_{(aq)} + HO_2 \longrightarrow Hg^{+}_{(aq)} + \text{products}$$

$$Hg^{+}_{(aq)} + HO_2 \longrightarrow Hg^{0}_{(aq)} + \text{products}$$

$$R_7 = -\frac{d[Hg^{2+}_{(aq)}]}{dt} = k_7[Hg^{2+}_{(aq)}][HO_{(aq)}], \text{ where } k_7 = 1.7 \times 10^4\ M^{-1}s^{-1}$$

The value for k_7 is taken from [*Pehkonen and Lin,* 1998].

Equilibria for aqueous phase Hg^{2+} speciation

$$Hg^{2+}_{(aq)} + SO^{2-}_{3(aq)} \xrightarrow{K_1} HgSO_{3(aq),} \text{ where } K_1 = 2 \times 10^{-13} M$$

$$HgSO_{3(aq)} + SO^{2-}_{3(aq)} \xrightarrow{K_2} Hg(SO_3)^{2-}_{2(aq)}, \text{ where } K_2 = 4 \times 10^{-12} M$$

$$Hg^{2+}_{(aq)} + 2Cl^{-}_{(aq)} \xrightarrow{K_3} HgCl_{2(aq)}, \text{ where } K_3 = 1 \times 10^{-14} M^2$$

$$Hg^{2+}_{(aq)} + OH^{-}_{(aq)} \xrightarrow{K_4} HgOH^{+}_{(aq)}, \text{ where } K_4 = 2.51 \times 10^{-11} M$$

$$HgOH^{+}_{(aq)} + OH^{-}_{(aq)} \xrightarrow{K_5} Hg(OH)_{2(aq)}, \text{ where } K_5 = 6.31 \times 10^{-12} M$$

$$HgOH^{+}_{(aq)} + Cl^{-}_{(aq)} \xrightarrow{K_6} HgOHCl_{(aq)}, \text{ where } K_6 = 3.72 \times 10^{-8} M$$

K_1 and K_2 are taken from *J.Munthe et al.* [1991] and K_3, K_4, K_5 and K_6 are taken from *R.M.Smith and A.E.Martell* [1976].

Adsorption of Hg^{2+} complexes to suspended soot in cloud water

The model used for the adsorption of aqueous Hg^{2+} species to suspended carbon aerosol in cloud water is adapted from Seigneur et al. [1998] which describes a partitioning coefficient K_p (liters per gram) from previous investigations of particle-bound mercury in rainwater, where $3 < K_p < 90$ for total atmospheric particulate matter. A value for $K_P = 45$ for total atmospheric particulate matter is adopted for the CMAQ model, and a value of $K_p = 900$ liters per gram is used to model the sorption of aqueous Hg^{2+} to suspended carbon based on the assumption of 5% carbon by weight in total atmospheric particulate matter. All aerosol soot in the gas-phase is transferred to the liquid phase based on the assumption that these particles would have acted as cloud condensation nuclei in the generation of the cloud. For the model intercomparison, the initial concentration of 5.0×10^{-7} grams of soot per cubic meter of air results in an aqueous concentration of 1.0×10^{-3} grams of soot per liter of cloud water. Adsorption and desorption rates are set based on the resulting equilibrium partitioning to yield a 1-hour e-folding time for the establishment of the adsorption equilibrium.

2.2. The GKSS Tropospheric Chemistry Module

The Tropospheric Chemistry Module (TCM) has been extracted from a comprehensive mercury model system using the Eulerian reference frame of the Acid Deposition and Oxidant Model (ADOM). The TCM is designed to simulate the meteorology and mercury chemistry over the entire depth of the troposphere to study cloud mixing, scavenging and chemical reactions associated with precipitation systems that generate wet deposition fluxes of atmospheric mercury species [*Petersen et al.,* 1998]. The chemistry components of the module are based on a systematic simplification of the detailed Chemistry of Atmospheric Mercury (CAM) process model, which incorporates the current knowledge of physico-chemical forms and transformation reactions of atmospheric mercury species [*Pleijel and Munthe*, 1995].

The main purpose of the TCM development was to test the aqueous chemistry equation set and the scavenging mechanisms for mercury species in cumulus and stratus clouds. The module has been extensively used to test the sensitivity of mercury wet deposition to various assumptions about the chemical reactions including the rate constants and the scavenging of mercury by water droplets. The sensitivity of the module to various cloud parameters such as cloud depth, vertical temperature and moisture profiles, the lifetime of clouds, cloud fractional coverage and the precipitation rate has also been examined. The module schematically depicted in figure 2.3 consists of one ADOM grid column with the same 12 vertical levels used in the full model. Initial concentration profiles of mercury species in ambient air as well as cloud-base height, cloud-top height, precipitation rates, and vertical profiles of temperature, pressure and relative humidity are needed as input. Moreover, a cloud fractional coverage is used to divide the grid cell into cloudy and clear regions. The module can be run for a single hour or for a sequence of hours with the clouds evaporated and the mercury species in the cloudy air averaged with the clear air concentrations to provide the starting concentration profiles for the next hour. A cumulus cloud is created only when lifting of an air parcel from cloud base can support convection. Otherwise the stratiform cloud module is used. Because the cumulus cloud module only uses cloud-base height and ambient temperature, pressure and humidity profiles to create a cloud, it can treat both precipitating and non-precipitating clouds. The stratiform module is driven by the surface precipitation rate. To simulate non-precipitating stratiform clouds, a minimum precipitation rate of 0.029 mm h^{-1} is used to generate cloud water/ice profiles but no deposition is calculated.

The initial conditions selected for the first stage of the mercury model intercomparison are such that the TCM creates a cumulus cloud with a life time of one hour which is identical with

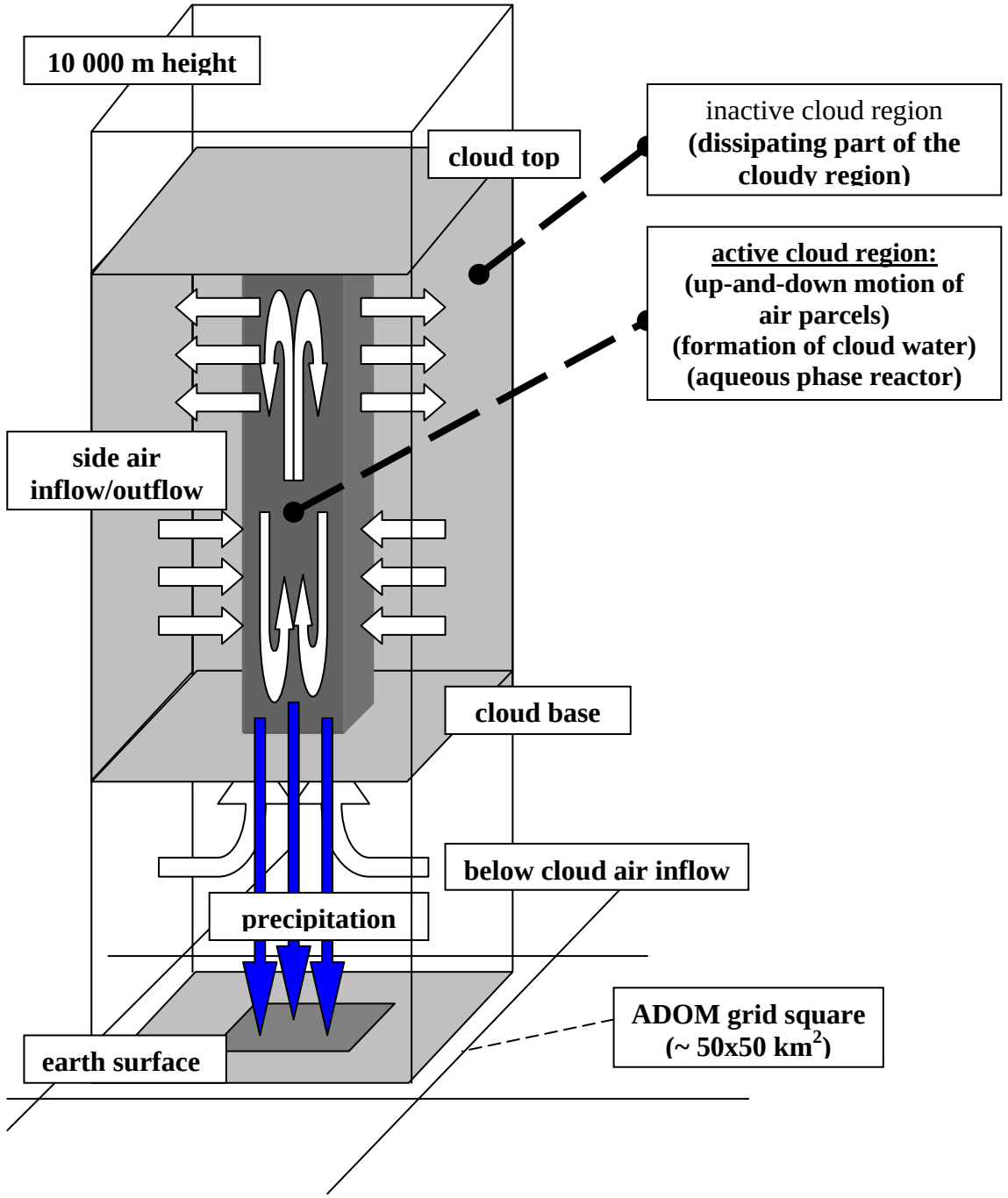

Figure 2.3. Schematic view of the Tropospheric Chemistry Module (TCM) for cumulus clouds

the basic model time step. The formulation of the cumulus cloud physics module is based on the model of *D.J.Raymond and A.M.Blyth* [1986]. There it is assumed that the observed cloudy region consists of active and inactive regions. The up-and-down motion of air parcels occurs in the active region. This motion is accompanied by the formation of cloud water and the redistribution of air and mercury species. The active region also represents the aqueous phase reactor. The inactive regions represent the dissipating part of the cloudy region. The

active region of the cloud is a transient phenomenon which is formed by the ingestion of air from the surrounding inactive region. The ingested mercury species participate in aqueous phase reactions in the cloud water formed in the active region. Some of the aqueous phase products are removed through precipitation, which is assumed to occur at the end of the life time of the active region. The remaining products are then put back into the cloudy (inactive and active region) which then redistributes them through vertical advection. At any time, the active region of the cloud is assumed to occupy a fraction of the cloudy region, which in turn occupies a fraction of the ADOM grid square.

The cloud physics sub-module calculates the mixing parameters (i. e. vertical profiles of air inflow and outflow) and the vertical distribution of liquid water and ice in the active cloud volume. Concentration profiles of mercury species during cloud formation are created using the air inflow profiles. Average concentrations in the active cloud volume, which are being used as input for the aqueous phase processes sub-module are determined from the properties of the environmental air and the cloud-base air using the inflow of air into the cloud from each level as the weighting factor. The aqueous phase processes sub-module comprises scavenging, chemistry and wet deposition. Scavenging in the active region is accomplished by dividing this region into a liquid-water and an ice reactor. Both aqueous phase chemistry and mass transfer processes are allowed to occur in the liquid water reactor. In the ice phase, only nucleation scavenging and equilibrium dissolution are considered. The scavenging components treat the reversible mass transfer of vapour- phase Hg^0 and Hg(II) to cloud water, irreversible scavenging of those two species by ice and irreversible particulate Hg scavenging by cloud water and ice.

In figure 2.4, the mercury chemistry scheme used with the TCM is depicted. It consists of four gas phase species, six dissolved aqueous species and four aqueous particulate phase species. The mass transfer and reaction rate expressions (R1-R21) derived from published data and assumptions of the rates of complex formation. A complete discussion can be found in *G.Petersen et al.* [1998]. As can be seen from figure 2.4, gas phase chemistry in the TCM is currently restricted to oxidation of Hg^0. Nevertheless this process may have a significant impact on mercury concentration levels since gas phase chemistry acts during each time step and in each grid cell over the entire TCM column.

The mass transfer/chemistry equations are solved once per time step of one hour using the Young and Boris predictor-corrector scheme [*Young and Boris,* 1977]. This is a complex but efficient solver well suited to the solution of the ‘stiff’ system of equations associated with chemical reactions. After scavenging and aqueous phase chemistry are simulated for the life cycle of the cloud, mercury species are removed from the cloud via wet deposition.

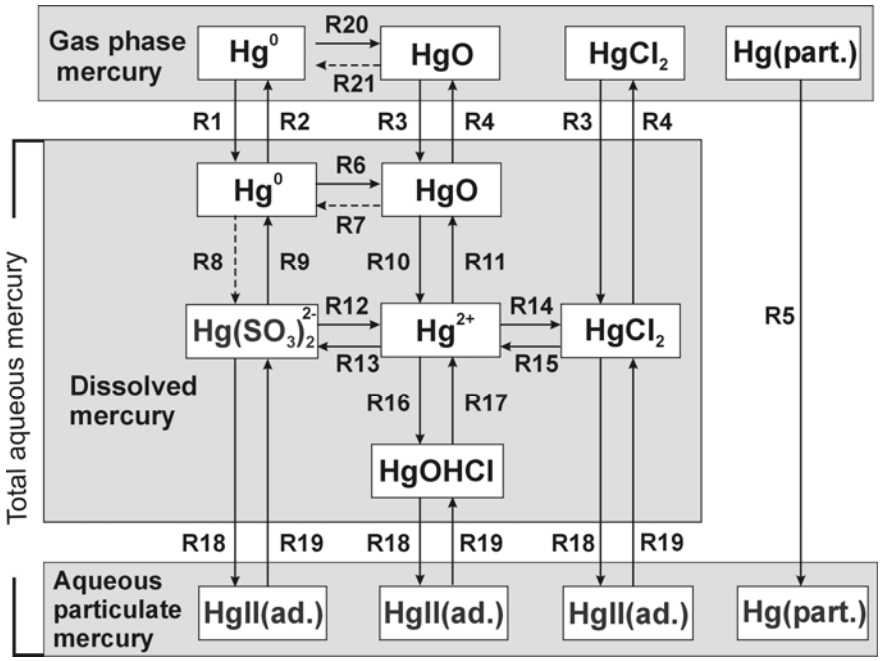

Figure 2.4. The mercury chemistry scheme used with the TCM

It should be noted that the Tropospheric Chemistry Module used by the GKSS does not correspond in full to the conditions of the intercomparison of mercury chemical schemes. The intercomparison conditions presumed to consider totally closed chemical systems. The GKSS scheme deals with entire cloudy layer of the atmosphere and it is open for exchange with the upper and lower layers. In other words, the GKSS scheme is intermediate between purely chemical schemes and schemes of mercury wet scavenging from the atmosphere.

2.3. AER/EPRI Mercury Chemistry Model

Figure 2.5 depicts the equilibria and reactions of mercury and other relevant species that are simulated. Table 2.1 lists the values of the equilibrium and kinetic parameters used for these processes along with the original references for those values. The formation of HgOHCl(aq) is not included because, at typical atmospheric pH values, the formation of $HgCl_2$(aq) dominates. The formation of $Hg(OH)_2$(aq) is included because it is important for Hg^{2+} complexation in the absence of chloride ions and it affects the gas/particle partitioning of Hg(II), even at low pH values. Temperature dependence is taken into account for the gas/liquid equilibria of O_3, SO_2, H_2O_2 and Cl_2. For the first three chemical species, the temperature dependence is described with the following relationship:

$$K(T) = K(298K)\exp\left(-\frac{\Delta H}{R}\left(\frac{1}{T}-\frac{1}{298}\right)\right),$$

where T is the temperature in Kelvin, ΔH is the enthalpy and R is the ideal gas law constant.

The values of $\left(-\frac{\Delta H}{R}\right)$ are 2300, 3020, and 6620 Kelvin for O_3, SO_2 and H_2O_2, respectively. For Cl_2, the relationship presented by *C.J.Lin and S.O.Pehkonen* [1998] was used.

This chemical kinetic mechanism is based on *R.L.Shia et al.* [1999] with the following modifications.

Two gas-phase reactions were added. Those are the oxidation of Hg(0) by hydrogen peroxide (H_2O_2) and molecular chlorine (Cl_2). The first oxidation reaction leads to a Hg(0) lifetime of 1.5 y for an H_2O_2 concentration of 1 ppb [*Tokos et al.,* 1998]. The second oxidation reaction is very slow and leads to a Hg(0) lifetime of over 20 years for a Cl_2 concentration of 10 ppt [*Calhoun and Prestbo*, 1998].

The kinetics of the intramolecular redox reaction of $HgSO_3$ leading to Hg(0) formation was updated to reflect new data published by *van Loon et al.* [2000]. The new rate parameter at 25° C is about 60 times lower than the previous value of *J.Munthe et al.* [1991]. Moreover, the new rate kinetics shows a strong dependence on temperature with a value of ΔH of 105,000 J/mol. Therefore, the kinetics of the reaction decreases sharply with decreasing temperature (e.g., it is about 20 times slower at 5° C than at 25° C).

Because SO_2 reacts with H_2O_2 within droplets, we also added this reaction. Since the aqueous reaction of HSO_3^- with H_2O_2 is very fast [*McArdle and Hoffman,* 1983], it is treated as an instantaneous titration. The product of this reaction is sulfuric acid (H_2SO_4), which is a strong acid. Therefore, we modify the initial pH based on the amount of H_2SO_4 produced. For example, titration of SO_2 by 0.5 ppb of H_2O_2 will lead to formation of 0.5 ppb of H_2SO_4, which corresponds to $4x10^{-5}$ M for a liquid water content of 0.5 g/m^3 at 1 atm and 298 K. The corresponding increase in H^+ concentrations is $8x10^{-5}$ M since dissociation of H_2SO_4 leads to two H^+. If the original pH value was 4.5 (i.e., H^+ concentration of $3.2x10^{-5}$ M), the new pH value is calculated to be 3.95 (i.e., H^+ concentration of $1.1x10^{-4}$ M).

Two other aqueous-phase reactions were added. These reactions correspond to the oxidation of Hg(0) by dissolved Cl_2. In solution, Cl_2 dissociates to form HOCl and OCl^-. These two chlorine species can oxidize Hg(0) to Hg^{2+} [*Lin and Pehkonen,* 1998].

Preliminary results of the kinetics of reactions of Hg(0) with OH radicals and with bromine (Br_2) in the gas phase [*Sommar et al.,* 1999] were presented at the Fifth International Conference on Mercury as a Global Pollutant. The preliminary value reported for the rate constant of the OH reaction was $2.6x10^{-12}$ cm^3 molec^{-1} s^{-1} which corresponds to a half-life of about 3 days for Hg(0) if one assumes a typical OH concentration of 10^6 molec cm^{-3}. Such a short half-life for Hg(0) in the absence of clouds or fog does not seem consistent with ambient measurements of Hg(0) and Hg(II). Since final data for these reactions have not yet been published in the peer-reviewed literature, they were not included in our mechanism.

The mercury chemistry module used here does not include the chemical reactions of nitrogen oxides (NO_x) and volatile organic compounds (VOC) that lead to the formation of oxidants (e.g., O_3, H_2O_2, OH and HO_2). It is designed to be imbedded into air quality models where concentrations of species other than Hg are either input by the user, as in our regional model [*Pai et al*., 1997] or our global model [*Shia et al.,* 1999], or simulated with a full chemical kinetic mechanism as in our plume model [*Constantinou et al*., 1995; *Seigneur et al*., 1997]. Therefore, the concentrations of the reactant species remained constant except for the species discussed below.

For species that are strongly dependent on solar irradiation, different diurnal and nocturnal concentrations were specified. Such species include OH, Cl_2 and HO_2. The daytime concentrations of OH, Cl_2, and HO_2 were specified to be 10^{-12} M, 0 ppt and $5x10^{-9}$ M, respectively. The night-time concentrations were specified to be 0 M, 5 ppt and 0 M, respectively.

Note that the oxidation of SO_2 is not treated in our mercury mechanism except for the reaction with H_2O_2; therefore, after the initial titration of SO_2 by H_2O_2, the concentration of sulfite ions and the pH remain constant. The initial concentrations of SO_2 and H_2O_2 were $1.88x10^{10}$ and $2.08x10^{9}$ molec. cm^{-3}, respectively. The titration of SO_2 by H_2O_2 reduced the SO_2 and H_2O_2 concentrations to $1.67x10^{10}$ and 0 molec. cm^{-3}, respectively. The associated formation of sulfuric acid reduced the pH from 4.5 to 4.34.

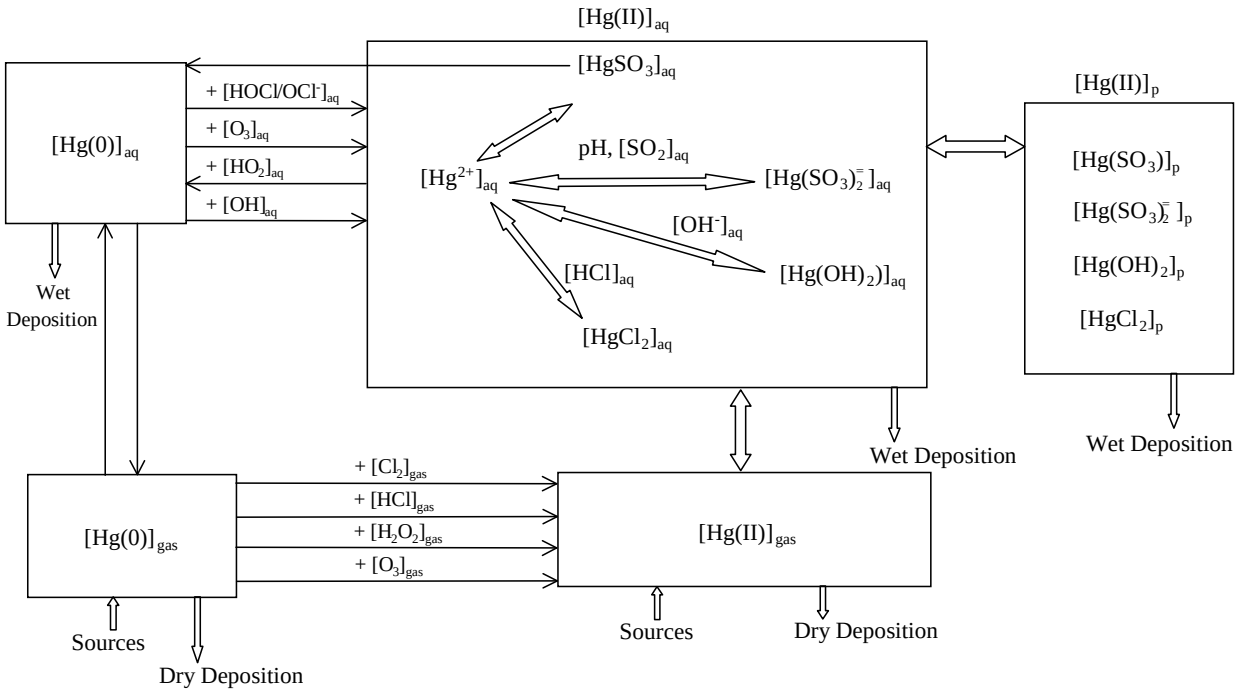

Figure 2.5. Schematic diagram of Hg atmospheric transformations, including gas/aqueous equilibria, ionic equilibria, solution/particle adsorption equilibrium, and gaseous and aqueous reactions

As shown in table 2.1, the adsorption of Hg(II) in droplets is defined with respect to total particulate matter rather than to soot. We assumed that soot constitutes 5% of particulate matter [*Seigneur et al.,* 1998] and, therefore, used a particulate matter concentration of 20 mg/l. The initial concentration of particulate Hg was assumed to be non-soluble Hg(II) and to be totally scavenged by the droplets.

Table 2.1. Equilibria and reactions of atmospheric Hg

Equilibrium process or chemical reaction	Equilibrium or rate parameter[a]	Reference
$Hg(0)\ (g) \leftrightarrow Hg(0)\ (aq)$	0.11 M atm^{-1}	*I. Sanemasa* [1975]
$HgCl_2\ (g) \leftrightarrow HgCl_2\ (aq)$	1.4×10^6 M atm^{-1}	*O. Lindqvist and H. Rohde* [1985]
$Hg(OH)_2\ (g) \leftrightarrow Hg(OH)_2\ (aq)$	1.2×10^4 M atm^{-1}	*O. Lindqvist and H. Rohde* [1985]
$O_3\ (g) \leftrightarrow O_3(aq)$	1.13×10^{-2} M atm^{-1}	*L.F. Kosak-Channing and G.R.Helz* [1983]
$HCl\ (g) \leftrightarrow HCl\ (aq)$	1.1 M atm^{-1}	*A.R.W. Marsh and W.J. McElroy* [1985]
$SO_2\ (g) \leftrightarrow SO_2\ (aq)$	1.23 M atm^{-1}	*R.M. Smith and A.E. Martrell* [1976]
$Cl_2\ (g) \leftrightarrow Cl_2\ (aq)$	0.076 M atm^{-1}	*J. Lin and S.O. Pehkonen* [1998]
$H_2O_2\ (g) \leftrightarrow H_2O_2\ (aq)$	7.4×10^4 M atm^{-1}	*J.A. Lind and G.L. Kok* [1986]
$HgCl_2\ (aq) \leftrightarrow Hg^{2+} + 2\ Cl^-$	10^{-14} M^2	*G.L. Sillen and A.E. Martell* [1964]
$Hg(OH)_2\ (aq) \leftrightarrow Hg^{2+} + 2\ OH^-$	10^{-22} M^2	*G.L. Sillen and A.E. Martell* [1964]
$HCl\ (aq) \leftrightarrow H^+ + Cl^-$	1.7×10^6 M	*A.R.W. Marsh and W.J. McElroy* [1985]
$Cl_2\ (aq) \leftrightarrow HOCl + Cl^- + H^+$	5.0×10^{-4} M^2	*J. Lin and S.O. Pehkonen* [1998]
$HOCl \leftrightarrow OCl^- + H^+$	3.2×10^{-8} M	*J. Lin and S.O. Pehkonen* [1998]
$SO_2\ (aq) + H_2O_2\ (aq) \rightarrow SO_4^{2-} + 2\ H^+$	instantaneous[b]	*J.V. McArdle and M.R. Hoffman* [1983]
$SO_2\ (aq) + H_2O\ (\ell) \leftrightarrow HSO_3^- + H^+$	1.23×10^{-2} M	*R.M. Smith and A.E. Martell* [1976]
$HSO_3^- \leftrightarrow SO_3^{2-} + H^+$	6.6×10^{-8} M	*R.M. Smith and A.E. Martell* [1976]
$Hg^{2+} + SO_3^{2-} \leftrightarrow HgSO_3$	5×10^{12} M^{-1}	*J. Munthe et al.* [1991]
$HgSO_3 + SO_3^{2-} \leftrightarrow Hg(SO_3)_2^{2-}$	2.5×10^{11} M^{-1}	*J. Munthe et al.* [1991]
$Hg(II)\ (aq) \leftrightarrow Hg(II)\ (p)$	34 l/g	*C. Seigneur et al.* [1998]
$Hg(0)\ (g) + O_3\ (g) \rightarrow Hg(II)\ (g)$	3×10^{-20} cm^3 $molec^{-1}$ s^{-1}	*B. Hall* [1995]
$Hg(0)\ (g) + HCl(g) \rightarrow\rightarrow HgCl_2(g)$	10^{-19} cm^3 $molec^{-1}$ s^{-1}	*B. Hall and N. Bloom* [1993]
$Hg(0)\ (g) + H_2O_2\ (g) \rightarrow Hg\ (OH)_2\ (g)$	8.5×10^{-19} cm^3 $molec^{-1}s^{-1}$	*J.J.S. Tokos et al.* [1998]
$Hg(0)\ (g) + Cl_2(g) \rightarrow HgCl_2(g)$	4.0×10^{-18} cm^3 $molec^{-1}s^{-1}$	*J.A. Calhoun and E.Prestbo* [1998]
$Hg(0)\ (aq) + O_3\ (aq) \rightarrow Hg^{2+}$	4.7×10^7 M^{-1} s^{-1}	*J. Munthe* [1992]
$Hg(0)\ (aq) + OH\ (aq) \rightarrow Hg^{2+}$	2.0×10^9 M^{-1} s^{-1}	*C.J. Lin and S.O. Pehkonen* [1997]
$HgSO_3\ (aq) \rightarrow Hg(0)\ (aq)$	0.0106 s^{-1}	*L. van Loon et al.* [1991]
$Hg(II)\ (aq) + HO_2\ (aq) \rightarrow Hg(0)\ (aq)$	1.7×10^4 M^{-1} s^{-1}	*S.O. Pehkonen and S.J. Lin* [1998]
$Hg(0)\ (aq) + HOCl\ (aq) \rightarrow Hg^{2+}$	2.09×10^6 M^{-1} s^{-1}	*S.O. Pehkonen and S.J. Lin* [1998]
$Hg(0)\ (aq) + OCl^- \rightarrow Hg^{2+}$	1.99×10^6 M^{-1} s^{-1}	*S.O. Pehkonen and S.J. Lin* [1998]
Hg(II) refers to all divalent Hg species		

[a] The parameters are for temperatures in the range of 20 to 25°C, see references for exact temperature; temperature dependence is included in the model for the Henry's law parameters of O_3, HCl, SO_2 [*Liu et al.,* 1997; *Seigneur and Saxena*, 1988], and Cl_2 [*Lin and Pehkonen*, 1998], and for the kinetic rate parameter of the $HgSO_3$ reaction.

[b] This reaction between HSO_3^- and H_2O_2 is fast and is treated as an instantaneous titration between SO_2 and H_2O_2. Since H_2SO_4 is a strong acid, the effect of this reaction on pH is taken into account.

2.4. MSCE-HM Model

Parameterisation of the liquid-phase mercury transformations is based on Tropospheric Chemistry Module (TCM) suggested by G. Petersen et al. [*Petersen et al*., 1998] (see 2.2). TCM includes 21 reactions. For the purposes of operational modelling the TCM was simplified. Some reactions (R10, R11) are very fast implying very short time step unsuitable for operational calculations. Some reactions (R8, R12, R17, R21) are assumed of the second priority unimportant and excluded from the consideration. Since many TCM reactions are both reversible and very fast, they were replaced by corresponding equilibrium ratios.

In this study three versions of the chemical scheme of the MSCE-HM operational model with different extent of simplification are used. In the first version the TCM has been simplified to analytical solution of the scheme [*Ryaboshapko et al.,* 1999]. The processes of washout of gaseous oxidized mercury and aerosol mercury are considered separately. The gas-phase oxidation process is not considered in this version. The second version is based on numerical solution of the scheme. It includes gas-phase oxidation, equilibrium between air and water for gaseous oxidized mercury compounds and washout process for aerosol mercury. The third version includes radical redox processes.

The first simplified version of the MSC-E scheme is shown in figure 2.6.

According to the scheme (figure 2.6.), Hg^0 is dissolved in a cloud drop following Henry's law. In a drop elemental mercury is oxidized by dissolved ozone (reaction R6) to the ionic state. Mercury oxide, the most probable intermediate product of the reaction, is very short-lived [*Petersen et al*., 1998] and it is not considered in the scheme. Mercury ion Hg^{2+} reacts with sulphite and chloride ions that leads to the formation of sulphite and chloride complexes (reaction). In the simplified scheme mercury chloride Hg_nCl_m is a "generalized substance" standing for various Hg-chloride and Hg-hydrochloride compounds. This mercury compound is assumed to take part in air-water

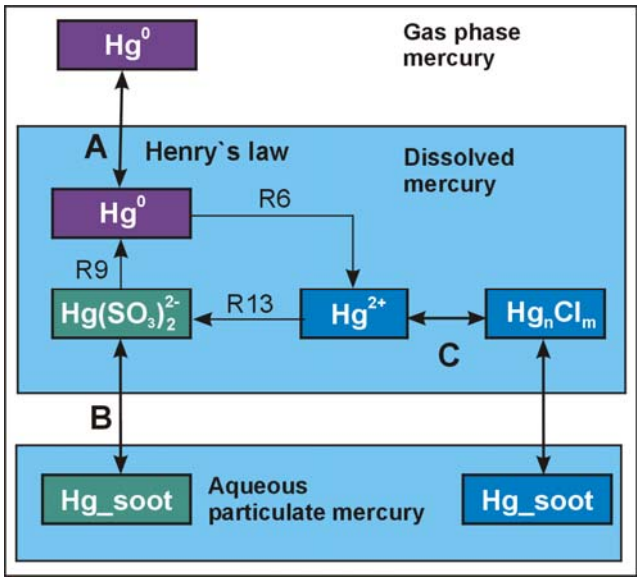

Figure 2.6. Simplified scheme (version 1) of mercury physical-chemical transformations in the liquid phase

exchange which rate obeys Henry's law. In the gaseous phase Hg_nCl_m is represented as $HgCl_2$ since it is usually assumed that $HgCl_2$ in the gaseous phase stands for a number of gas-phase oxidized inorganic mercury compounds. If at the first moment of a model run Hg_nCl_m is in excess in air a part of it is instantly transferred from air to water according to Henry's law.

Mercury sulphite is very unstable and readily decays resulting in reducing Hg^0 to the elemental state (reaction R9). This increases the pool of elemental mercury in a drop that prevents from dissolution of new portions of elemental mercury. Hence, the scheme implies negative feedback controlling elemental mercury uptake from the air.

Dissolution of elemental mercury and ozone to a great extent depends on temperature. The temperature dependence of Henry's law dimensionless constant (the ratio of concentration in liquid to that in gas) for gaseous elemental mercury was determined by *A.Ryaboshapko and V.Korolev* [1997]. Henry's law constant for ozone and temperature dependence is defined as the mean of all values published by *R.Sander* [1997].

Ratio R between concentration of mercury free ions and mercury concentration in the totality of chloride complexes in aggregate ($[HgCl^+] + [HgCl_2] + [HgCl_3^-] + [HgCl_4^=]$) can be found (without consideration of ion strength) by the following formula [*Lurie*, 1971]:

$$R = 1 : ([Cl^-]/1.82\ E\text{-}7 + [Cl^-]^2 / 6.03E\text{-}14 + [Cl^-]^3 /8.51\ E\text{-}15 + [Cl^-]^4 / 8.51\ E\text{-}16)$$

Typical concentrations of chloride in cloud water are within the range of 1E-5 - 1E-4 M [*Acker et al*., 1998] the bulk of mercury should be represented by different chloride-mercury complexes.

G.Petersen et al. [1998] considered mercury exchange in the aqueous phase between soot particles and solution as two reversible reactions. The rates of these reactions depend on soot particle size and concentration, and under realistic conditions the reactions are rather fast: practical equilibrium should be achieved in 10-15 min. Hence, the direct and reverse reactions (absorption and desorption) can be replaced by equilibrium E3 and equilibrium E4 for sulphite and chloride complexes, correspondingly. In the modelling scheme "dissolved: adsorbed" equilibrium ratio is adopted as 1:5 (equal to the ratio between the direct and reverse reaction rates in [*Petersen et al.,* 1998]) both for sulphite and chloride complexes.

The liquid phase oxidation rate (reaction R6) depends on ozone concentration in air and Henry law constant (as a function of temperature). The rate of sulhite complex formation (reaction R13) depends on sulfite ion concentration. In its turn, sulphite concentration depends on SO_2 concentration in air, Henry law constant (as a function of temperature) and pH value of solution. In acidic solutions (pH<5) S(IV) occurs mainly in the forms of $[H_2SO_3]$

and $[HSO_3^-]$. Sulphite ion becomes the dominating species at pH>7. Reaction of mercury sulphite decomposition (reaction R9) is the first order process. Equilibrium ratios and expressions for rate constants used in the scheme are compiled in table 2.2.

Table 2.2. Equilibrium ratios and rate constant expressions (s^{-1}) used in the chemical scheme

Expression	Notes	Reference
$H_{Hg}(T) = 0.00984 \times T \times \exp[2800 \times (1/T - 1/298)]$	Non-dimensional	*A.G. Ryaboshapko and V. Korolev* [1997]
$H_{O3}(T) = 0.000951 \times T \times \exp[2325 \times (1/T - 1/298)]$	Non-dimensional	*R. Sander* [1997]
$Hg^{2+}:HgCl_{2(aq)} = 1 : ([Cl^-]/1.82E\text{-}7 + [Cl^-]^2 / / 6.03E\text{-}14 + [Cl^-]^3 / 8.51E\text{-}15 + [Cl^-]^4 / 8.51E\text{-}16)$	Cl^- in [M]	*Yu.Yu. Lurie* [1971]
$Hg(SO_3)_2^{2-}{}_{(aq)} : Hg(SO_3)_2^{2-}{}_{(soot)} = 1:5$	At the prescribed conditions	*G. Petersen et al*. [1998]
$HgCL_{2(aq)}: HgCl_{2(soot)} = 1:5$	At the prescribed conditions	*G. Petersen et al*. [1998]
$R6 = k_6 \cdot H_{O3} \cdot [O_3(gas)]$	O_3 in [ppb]; $k_6 = 4.7E+7$ $[M^{-1}s^{-1}]$	*G. Petersen et al*. [1998]
$R9 = k_9$	$k_9 = 0.44E\text{-}3$ $[s^{-1}]$	*G. Petersen et al*. [1998]
$R13 = 1.1E\text{-}21 \cdot ([SO_2(gas)]/1.0E\text{-}(2 \cdot pH))^2$	SO_2 in [ppb]	*G. Petersen et al*. [1998]

As it follows from figure 2.6., one can distinguish three groups of mercury compounds being in equilibrium. The first group - elemental mercury in air and water, the second - mercury within sulphite complex in the water phase and on soot particles, the third group - free mercury ions and chloride complexes of mercury in the solution, on particles and in the gaseous phase. These three groups are denoted as A, B and C respectively:

$$A = Hg^0_{(liquid)} + Hg^0_{(gas)}$$

$$B = Hg(SO_3)_2^{2-}{}_{(liquid)} + Hg(SO_3)_2^{2-}{}_{(solid)}$$

$$C = Hg^{2+}_{(liquid)} + HgCl_{2(liquid)} + HgCl_{2(solid)} + HgCl_{2(gas)}$$

A, B and C can be considered as individual "substances" and the distribution inside A, B and C can be set up proceeding from equilibrium factors.

According to the simplified scheme and introduced notations, mercury behaviour in a drop can be described by a set of three equations of the first order:

$$\begin{cases} \frac{d[A]}{dt} = -R_6 \cdot \alpha \cdot [A] + \frac{1}{6} \cdot R_9[B] \\ \frac{d[B]}{dt} = -\frac{1}{6} \cdot R_9[B] + \gamma \cdot [C] \cdot R_{13} \\ \frac{d[C]}{dt} = R_6 \cdot \alpha \cdot [A] - \gamma \cdot [C] \cdot R_{13} \end{cases}$$

Here R_6, R_9, R_{13} are the rates of respective reactions, α - fraction of A mass in solution; according to Henry law $\alpha = H_{Hg} \times LWC/(1+H_{Hg} \times LWC)$, H_{Hg} - dimensionless Henry's law constant for mercury, LWC - liquid water content in cloud. Value γ is that fraction of mercury in C group, which is transferred to sulphite complex. Coefficient 1/6 obtained as a ratio of sorption-desorption reaction rates [*Petersen et al.,* 1998] expresses the equilibrium between mercury content on soot particles, on the one hand, and chloride or sulphite mercury complex on the other.

Parameter γ is calculated on the basis that:

$$\frac{[Hg^{2+}]}{[Hg_nCl_m(aq)]} = k_1, \qquad \frac{[Hg_nCl_m(aq)]}{[Hg_nCl_m(part)]} = k_2, \qquad W_{2+} = \frac{[Hg_nCl_m(aq)]}{[HgCl_2(gas)]}$$

where $k_1 = 1/R$, in our case $k_2 = 1/6$, W_{2+}. is dimensionless Henry's law constant for $HgCl_2$. It is easy to obtain that:

$$\gamma = \frac{k_1 \cdot k_2 \cdot W_{2+}}{k_1 \cdot k_2 \cdot W_{2+} + k_2 \cdot W_{2+} + W_{2+} + k_2}$$

The equation set above is reduced to one equation of the third order relative to A:

$$\frac{6}{R_9} \cdot \frac{1}{\gamma \cdot R_{13}} \cdot \frac{d^3A}{dt^3} + \left(\frac{6 \cdot \alpha \cdot R_6}{R_9 \cdot \gamma \cdot R_{13}} + \frac{1}{\gamma \cdot R_{13}} + \frac{6}{R_9} \right) \cdot \frac{d^2A}{dt^2} + \left(\frac{R_6 \cdot \alpha}{\gamma \cdot R_{13}} + \frac{6 \cdot R_6 \cdot \alpha}{R_9} + 1 \right) \cdot \frac{dA}{dt} = 0$$

It can be written in a simpler form:

$$a \cdot \frac{d^3A}{dt^3} + b \cdot \frac{d^2A}{dt^2} + c \cdot \frac{dA}{dt} = 0$$

Characteristic equation is written as:

$$a\lambda^3 + b\lambda^2 + c\lambda = 0 \qquad \text{or} \qquad \lambda (a\lambda^2 + b\lambda + c) = 0$$

Then the solution is found as:

$$A = C_1 \cdot \exp(\lambda_1 t) + C_2 \cdot \exp(\lambda_2 t) + C_3 \cdot \exp(\lambda_3 t)$$

Here λ_1, λ_2 and λ_3 - roots of square equations and λ_3 is equal to zero; constants C_1, C_2, C_3 are found from the initial conditions. Let initial values of A, B and C at time t = 0 be equal to A_0, B_0 and C_0 respectively. If we write the expression for A, dA/dt and d^2A/dt^2 at t = 0 then we obtain a set:

$$\begin{cases} C_1 + C_2 + C_3 = A_0 = RHS_1 \\ C_1(\lambda_1 + \alpha \cdot R_6) + C_2(\lambda_2 + \alpha \cdot R_6) + C_3 \cdot R_6 \cdot \alpha = \dfrac{R_9}{6} \cdot B_0 = RHS_2 \\ C_1(\lambda_1^2 + \alpha \cdot R_6 \cdot \lambda_1) + C_2(\lambda_2^2 + \alpha \cdot R_6 \cdot \lambda_2) = \dfrac{R_9 \cdot \gamma \cdot R_{13}}{6} \cdot C_0 - \dfrac{R_9^2 \cdot B_0}{36} = RHS_3 \end{cases}$$

From this set it is possible to obtain expressions for C_1, C_2, C_3.

The described above second version of the scheme includes some additional processes. This version is presented by figure 2.7.

The gaseous phase oxidation of elemental mercury by ozone is rather slow reaction. The rate of it depends on ozone concentration in air $\{O_3\}$ and is expressed as 7.4E-10 × $\{O_3\}$ s^{-1}, where $\{O_3\}$ is in ppb [*Petersen et al.,* 1998].

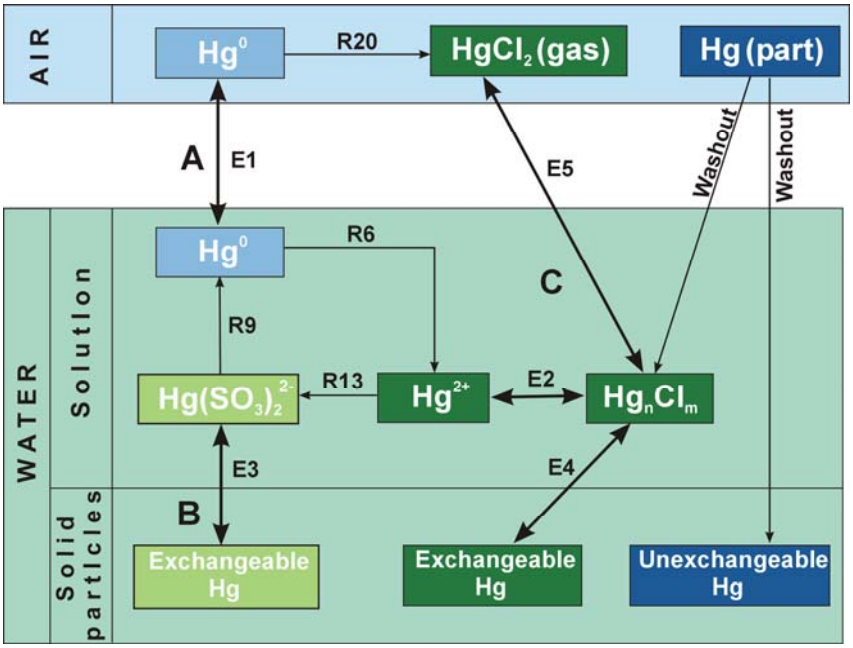

Figure 2.7. MSC-E mercury scheme

The Henry's law constant for dissolution of $HgCl_2$ is discussed in a few publications [*Lindqvist and Rodhe*, 1985, *Schroeder & Munthe*, 1998, *Seigneur et al.,* 1994, *Sommar et al,* 1999]. They demonstrate that the constant strongly depends on temperature. In this work the temperature dependence of Henry's law constant for mercury chloride has been derived (rather roughly) from the above publications:

$$H_{HgCl2}(T)=105369\times T\times\exp(5590\times(1/T-1/298)).$$

In air part of mercury occurs in particulate form. The scheme assumes that at the first moment of a modelling run particulate matter is totally transferred from air to water. It is believed that mercury on airborne particles is represented by both water-soluble compounds like $HgCl_2$ (50%) and water-insoluble forms (50%) [*Iverfeldt*, 1991]. Soluble compounds are included into physical-chemical cycle in the liquid phase. Insoluble part occurs in particulate form and cannot exchange with the liquid phase.

In addition to the processes described by the second version of the scheme, the third version includes two reactions with hydroxil ($OH^\bullet$) and hydroperoxide ($HO_2^\bullet$) radicals. Radical concentrations depend on solar radiation intensity and reach their maximum at noon [*Herrmann et al.*, 2000]. *S.Pehkonen and C.-J.Lin* [1998] showed that $OH^\bullet$ can oxidize elemental mercury in the liquid phase with reaction rate equal to 2E9 M^{-1} s^{-1}. Radical $HO_2^\bullet$ can react with both free mercury ions and dissolved mercury compounds reducing mercury to the elemental state. *S.Pehkonen and C.-J.Lin* [1998] found the rate constant of 1.7E4 M^{-1} s^{-1}.

Reaction rates and equilibrium ratios of the described chemical module of the MSCE-HM model are functions of initial conditions and concentrations of reactants. To check sensitivity of the system to this or that input parameters a sensitivity study is performed.

A cloud environment at pressure of 800 mbar (it corresponds to typical height of cloudiness) is simulated. Two mercury forms in air are considered: elemental gaseous mercury, [Hg(0)] and oxidized divalent mercury, [Hg(II)]. It is believed that oxidized mercury has physical-chemical properties of gaseous mercury chloride. Two sets of initial concentrations are considered: first, [Hg(0)] = 1.7 and [Hg(II)] = 0 ng/m^3; second, [Hg(0)] = 1.7 and [Hg(II)] = 0.05 ng/m^3. It is assumed that oxidized mercury can be easily dissolved in water. In the liquid phase the oxidized form exists in the dissolved state.

Variable input parameters are: liquid water content, temperature, sulphur dioxide concentration, ozone concentration, pH value and chloride concentration in droplet water. The range of variations is chosen to correspond to real conditions of cloud layer over moderately polluted areas of Europe.

Mercury concentration in the liquid phase is considered as an output result of the simulations. Each simulation period is 48 hours.

The range of LWC is taken from 0.05 to 5 g/m^3. The results of the simulation are shown in figures 2.8.a which presents the situation when initial [Hg(II)] concentration in gas is zero. Naturally, the higher LWC, the lower mercury concentration is in water. However, the dependence of accumulated mercury mass on LWC is not linear. It is determined by gas-phase oxidation: the same quantity of reaction products is solved in different volumes of water. It is especially important for low LWC values.

If the initial concentration [Hg(II)] in gas is 0.05 ng/m^3 the output concentration in water can be extremely high when LWC is low (fig. 2.8 a and b). The importance of chemical processes in the system is relatively low in this case. It should be mentioned that the total mass of dissolved mercury within the system is noticeably higher when LWC is higher. Hence, clouds with high LWC can remove mercury more effectively. It means that variability of LWC parameter should be taken into account in routine mercury modelling.

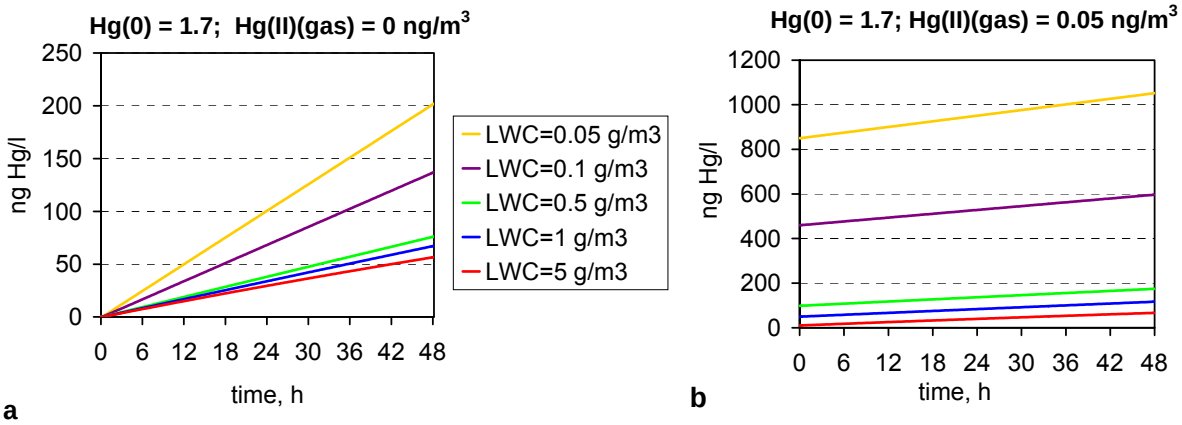

Figure 2.8. Sensitivity of mercury chemical module to liquid water content:
(a) – initially only elemental mercury in air;
(b) – initially elemental and oxidized mercury in air.

The investigated interval of temperature ranges from 268^{o}K (-5^{o}C) to 288^{o}K (+15^{o}C). This interval is typical of low cloudiness in Europe. At temperature of –5^{o}C cloud droplets are usually in the liquid state. Effects of temperature changing are determined by the fact that Henry law coefficients for elemental mercury, mercury chloride and ozone are exponential functions of temperature. As it is shown in figures 2.9 a and b the effect can be considerable (factor 2.5 within the investigated temperature range). Availability of initial mercury chloride makes this dependence relatively lower (fig. 2.9 b). However, in any case temperature dependence should be included into routine mercury modelling.

Figure 2.10 shows that the module is extremely sensitive to pH value when pH becomes higher than 5.0. At pH=5.5 and initial Hg(II)=0 (fig. 2.10.a) Hg concentration in water is stabilized on the level of 9 ng/l after 10 hours of simulation. When initially some Hg(II) is present in air the modelled system reduces mercury to the elemental form if pH is higher than 5.1 (fig. 2.10.b). The effect is explained by the fact that the rate of sulphite ion formation depends very strongly on pH.

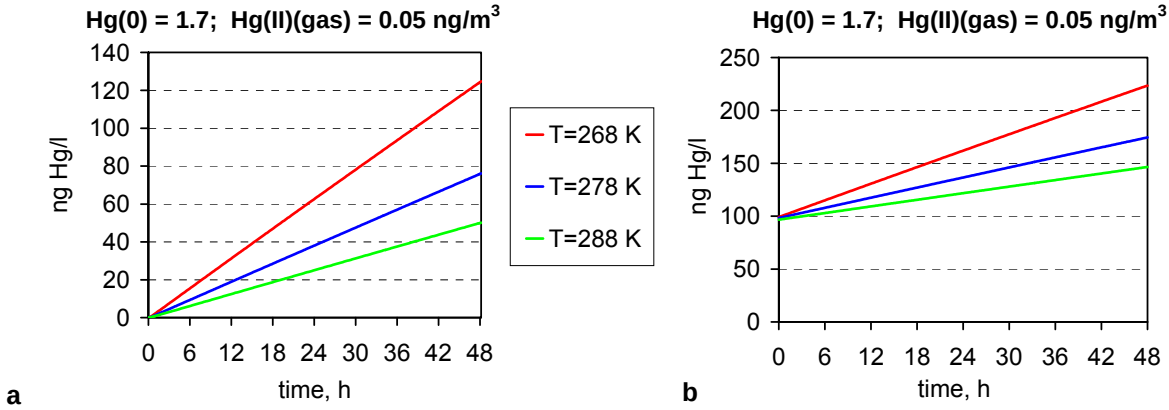

Figure 2.9. Sensitivity of mercury chemical module to temperature:
(a) – initially only elemental mercury in air;
(b) – initially elemental and oxidized mercury in air.

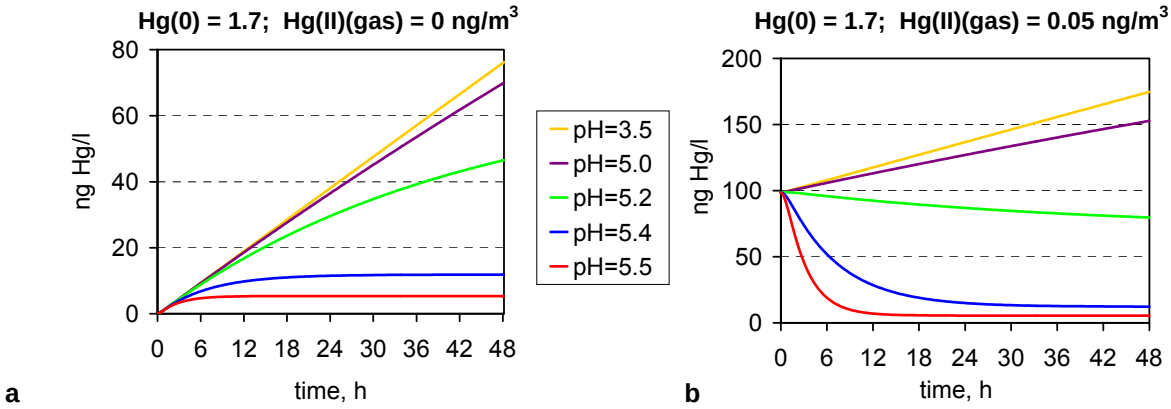

Figure 2.10. Sensitivity of mercury chemical module to pH of water:
(a) – initially only elemental mercury in air;
(b) – initially elemental and oxidized mercury in air.

At low pH values the chemical system works as an oxidation reactor. The output does not practically depend on pH value within the interval of 3.5-5.0. This interval of pH values corresponds to observations of pH of cloud water in Central Europe. From this viewpoint it is possible to conclude that for the real environmental conditions the module is not sensitive to pH values of cloud water.

Ozone concentration (both in air and in water) determines the oxidation rates of elemental mercury. The dependence of Hg concentration on ozone is practically linear: the higher ozone concentration, the higher concentration of oxidized mercury in water (figs. 2.11.a and b). The difference can be rather high when ozone variations are kept typical of Central Europe.

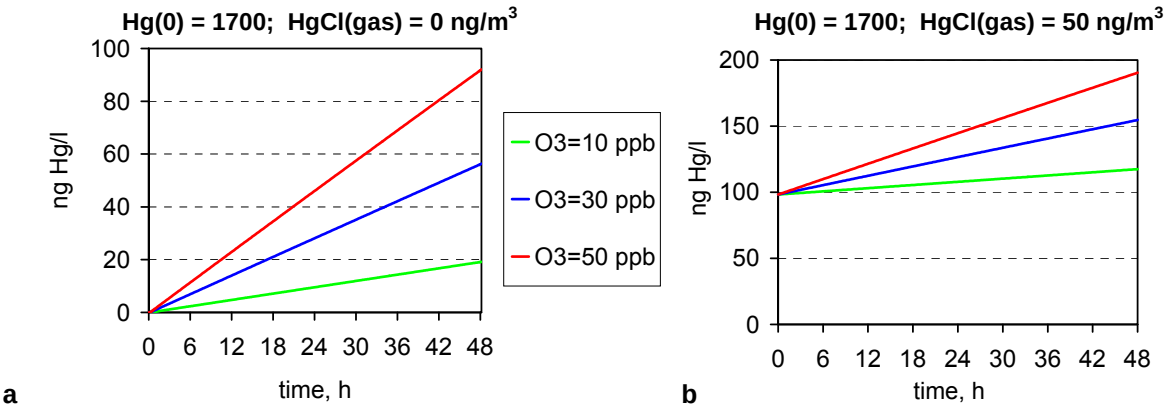

Figure 2.11. Sensitivity of mercury chemical module to ozone concentration:
(a) – initially only elemental mercury in air;
(b) – initially elemental and oxidized mercury in air.

Chloride-related mercury is the main reservoir of oxidized mercury in the liquid phase. Chloride content determines the capacity of the liquid phase to accumulate oxidized mercury. When chloride concentration is very low (1-2 μM) the increase of oxidized mercury concentration is limited (fig. 2.12.a). If initial concentration of oxidized mercury is rather high and chloride concentration is low the system works as a reduction reactor (fig. 2.12.b).

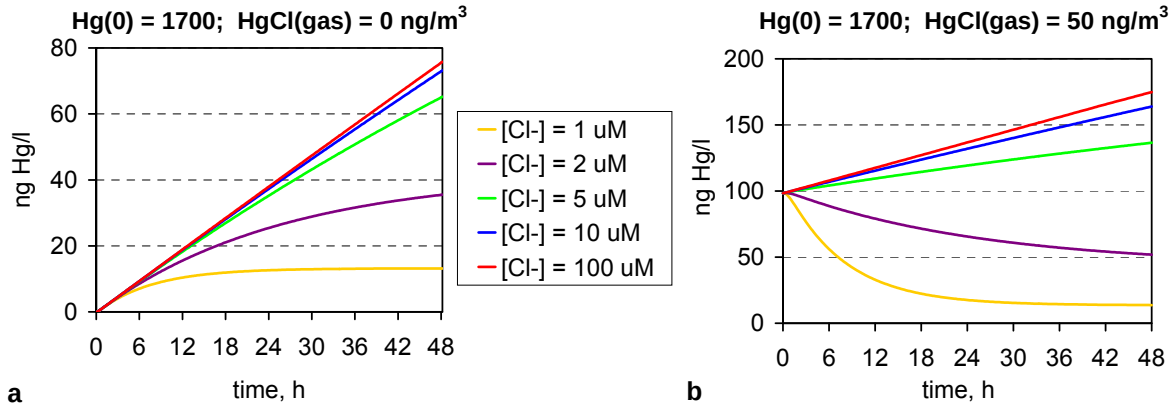

Figure 2.12. Sensitivity of mercury chemical module to chloride concentration:
(a) – initially only elemental mercury in air;
(b) – initially elemental and oxidized mercury in air

Normal concentrations of chloride in cloud water are rather high (10-100 μM) over Central Europe. Under this condition chloride provokes elemental mercury oxidation. However, the rate of oxidation depends on chloride in this concentration range rather slightly.

Sulphur dioxide can easily be solved in water and in chain of reactions produces sulphite ion. In the simplified scheme used the relation between SO_2 concentration in air and $[SO_3^{=}]$ concentration in water is linear. Sulphite ion acts as reducing agent. However, in the range of typical SO_2 concentrations in Central Europe (1-5 ppb) the influence of this agent is weak (fig. 2.13.a). Only in very polluted atmosphere elevated SO_2 concentrations can lead to reduction of mercury to the elemental form (fig. 2.13.b).

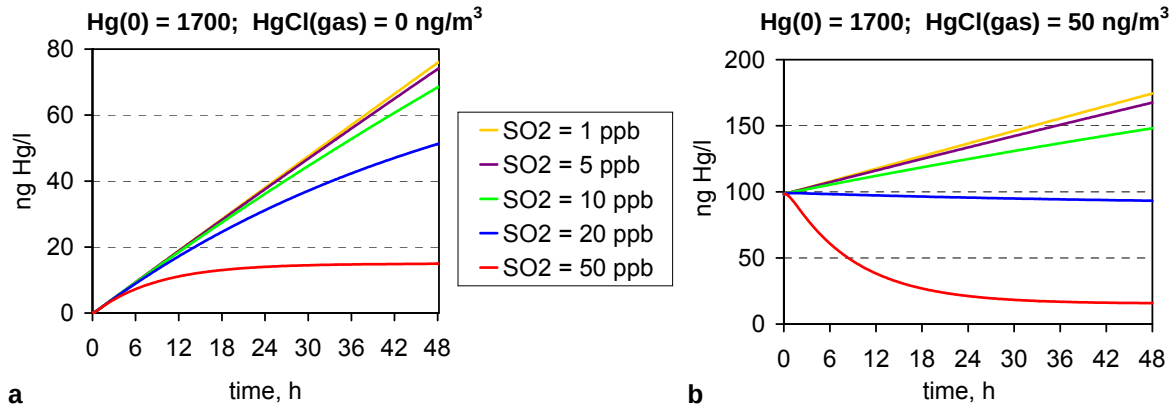

Figure 2.13. Sensitivity of mercury chemical module to SO_2 concentration:
(a) – initially only elemental mercury in air;
(b) – initially elemental and oxidized mercury in air.

2.5. IVL Mercury Chemistry Model

Chemistry of Atmospheric Mercury (CAM) model used for the calculations has been described by *K.Pleijel and J.Munthe* [1995]. The chemical scheme treats gas phase and aqueous phase chemistry using 90 species in 180 reactions.

The first version of the CAM presumed that in the initial oxidation step elemental mercury (Hg°) is oxidized by ozone to divalent mercury (Hg(II)). Divalent Hg complexes with available ligands is present in the aqueous phase as $HgSO_3$, $Hg(SO_3)_2^{2-}$, $HgCl^+$, $HgCl_2$, $HgOH^+$, $Hg(OH)_2$ and HgOHCl. Reactions leading to reduction of Hg(II) to Hg° indicate ways in which dissolved Hg(II) can be released from the droplet back to the gas phase. Adsorption of Hg(II)

by particles within the droplets is treated by means of an empirical relationship derived from field measurements of soot and particulate Hg in precipitation.

The following version of the model (IVL-Hg) included into consideration some new reactions both in gaseous and liquid phase. The original photo-oxidant chemistry has been exchanged for the EMEP chemistry package. As to chemistry of mercury in the gas phase the following reactions have been added:

$Hg^0 + OH^\bullet = HgO(g)$

In accordance to *J. Sommar* (personal communication) the constant of the reaction is $8 \cdot 10^{-14}$ $molec^{-1}$ s^{-1} cm^3. Experimental work on this reaction is currently on-going and the rate constant should be considered as preliminary.

$Hg^0 + O_3 = HgO(g)$

The reaction constant is $3 \cdot 10^{-20}$ $molec^{-1}$ s^{-1} cm^3 [*Hall*, 1995]. If global average ozone concentration is 30 ppb then global lifetime of elemental mercury only according to this reaction should be about 1 year.

$Hg^0 + Cl_2 = HgCl_2$

The reaction constant is 3.7×10^{-18} $molec^{-1}$ s^{-1} cm^3 [*Calhoun and Prestbo*, 1998]. It is assumed that the reaction is chemically dependent – during daytime Cl2 is photochemically destroyed, and its concentration at noon is 0.

The following reactions in aqueous phase were added to the scheme:

$Hg^0 + OH^\bullet = Hg^{2+}$

The reaction constant is 2.4×10^9 M^{-1} s^{-1} [*Gårdfeldt et al.*, 2001]. It is assumed that the reaction is chemically dependent – during daytime $OH^\bullet$ radical concentration is maximum.

Hg(II) + $HO_2^\bullet$ = Hg^0

The reaction constant is 1.7×10^4 M^{-1} s^{-1} [*Lin and Pekhonen*, 1997]. In this case Hg(II) represents all oxidized Hg species in aqueous phase. Again, the reaction is chemically dependent – during daytime $OH^\bullet$ radical concentration is maximum.

2.6. Similarities and Distinctions

It is seen that the different models use the different descriptions of mercury chemistry. In this section the basic distinctions and similarities are summarized.

All the models use the same basic principles – at each step of the calculations airborne species are in equilibrium with the liquid phase. The equilibrium between water droplets and the ambient air is settled instantly. The equilibrium ratios are determined in accordance with Henry law.

The models consider both oxidation and reduction processes for mercury compounds in the liquid phase. It means that a water droplet can be under different conditions both a sink and a source of mercury for the ambient air. Since the reactions proceeds simultaneously a water droplet can be considered as a chemical reactor with the negative feedback.

In all models one of the key species in mercury liquid phase oxidation process is dissolved ozone. As a reducing agent all models consider tetra-valence sulfur in the liquid phase. The precursor of this sulfur is sulfur dioxide in the ambient air. In all models this reduction process plays a significant role in preventing the accumulation of oxidized mercury within the liquid phase.

The most probable compound of mercury in the liquid phase is mercury chloride as adopted by all models. According to the theoretical schemes mercury chloride should be the main mercury compound in rain water under realistic assumptions on cloud water composition. All models but the MSCE-HG consider in addition compounds like $Hg(OH)_2$, $HgOH^+$, HgClOH.

It is commonly believed that all mercury compounds can be absorbed by solid particles within the liquid phase. Very probably that such particles consist of soot (partly or entirely). A mercury compound being absorbed cannot react with any reactant.

One of the main peculiarity which distinguishes the participating models is consideration of radical reactions in the liquid phase. These reactions were recently studied *by C.-J Lin and S.O.Pehkonen* [1997]. Hydroxyl radical $OH^\bullet$ serves as a strong oxidant while $HO_2^\bullet$ can reduce mercury to the elemental state. Hence the radicals are very short-lived compounds and are produced photochemically, it is natural that the reactions with mercury compounds are of pronounced daily cycle. The AER/EPRI, SMAQ and IVL-Hg models are taken these radical reactions into account. The TCM does not consider these reactions. The MSCE-HM have been used in different versions and one of them considered these radical reactions.

A certain role in oxidation of elemental mercury both in gaseous and liquid phases can be played by chlorine, chlorine-derived compounds ($HOCl/OCl^-$) and hydrochloric acid. These processes are taken into account by AER/EPRI, SMAQ and IVL-Hg models while TCM and MSCE-HM ignore them.

The participating models differently treat chemical processes in the gas phase. The AER/EPRI model takes into consideration four different oxidants while the CMAQ ignores all reactions in the gaseous phase. The AER/EPRI, TCM and IVL-Hg models treat the gas phase oxidation products as gases, most likely gaseous HgO or $HgCl_2$. In the MSCE-HM the products are considered as solid matter.

The main types of reactions and corresponding reactants used by all participating models are listed in table 2.3.

Table 2.3. Physical-chemical processes considered in the models

Processes / reactants	Models					
	AER / EPRI	CMAQ	TCM	MSCE-numeric.	MSCE-analytic.	IVL
Gas-phase oxidation						
O_3	+		+	+		+
Cl_2	+					+
HCl	+					
H_2O_2	+					
Liquid-phase oxidation						
O_3	+	+	+	+	+	+
OH^*	+	+				+
$HOCl/OCl^-$	+	+				
Liquid-phase reduction						
$HgSO_3$	+	+				+
$Hg(SO3)_2^{2-}$			+	+	+	+
$Hg(OH)_2$ + hv		+				
HO_2^*	+	+				+
Other reactants						
$[SO_3^{2-}]$	+	+	+	+	+	+
$[H^+]$	+	+	+			+
$[OH^-]$	+		+			+
$[Cl^-]$	+	+	+	+	+	+
Inter-phase equilibria						
Hg^0 (air-water)	+	+	+	+	+	+
O_3 (air-water)	+	+	+	+	+	+
$HgO_{(gas)}$ (air-water)			+			+
$Hg(II)_{(gas)}$ (air-water)	+	+	+	+	+	+
$HgO_{(solid)}$ (air-water)		+				
Cl_2 (air-water)	+					
HCl (air-water)	+					
$Hg(OH)_2$ (air-water)	+					
SO_2 (air-water)	+	+	+	+	+	+
H_2O_2 (air-water)	+					
Soot (air-water)	+	+	+	+	+	+
$[HgSO_3]$ (water-soot)	+	+				
$[Hg(SO_3)_2^{2-}]$ (water-soot)	+	+	+	+	+	+
$[Hg(OH)_2]$ (water-soot)	+	+				+
$[HgCl_2]$ (water-soot)	+	+	+	+	+	+
[HgOHCl] (water-soot)		+	+			+
$[HgOH^+]$ (water-soot)		+				+

3. DATA OF MEASUREMENTS

During last decades gaseous mercury has been measured in the atmosphere very widely. It was shown that at regional and global levels gaseous mercury form is represented mainly by elemental mercury (95-98%) and partly by volatile mercury compounds like mercury chloride. Routine measurements in industrialized regions of Central Europe revealed that the annually mean concentrations varied between 1.5 and 2.0 ng/m^3. In view of the fact it is possible to adopt the value of 1.7 ng/m^3 as a typical concentration of elemental mercury in Europe.

There are only few data on simultaneous measurements of different mercury forms in air and precipitation. In air mercury can occur not only in the gaseous phase but also within particulate matter. Chemical forms of particulate mercury are unknown. In precipitation mercury can be present as mercury compounds both in water solution and being absorbed on insoluble particles.

Very detailed simultaneous measurements of atmospheric mercury species in ambient air and precipitation were carried out during summer 2000 near Hamburg, Germany. Measurements have been carried out between July 6 to 27, 2000 at GKSS Research Centre Geesthacht. The study area is a rural site located in a wooded area. Metropolitan Hamburg is located approximately 30 km west of GKSS. Prevailing winds are coming from the south west. The following species have been measured:

a. in ambient air:

- gaseous elemental mercury
- reactive gaseous mercury
- total particulate mercury

b. in precipitation:

- total mercury
- reactive mercury.

3.1. Methods

Gaseous elemental mercury was detected with a Tekran gas-phase mercury analyser (Model 2537A). The instrument uses the gold amalgamation technique. The pre-filtered air stream is pulled through gold cartridges, then thermodesorbed and detected by Atomic Fluorescence Spectrometry (AFS). The instrument uses two cartridges in parallel, with alternating operation modes (sampling and desorbing/analysing) on a pre-defined time base of 5 minutes. A sampling flow rate of 1.5 l min^{-1} was used. Under these conditions a detectetion limit of

approximately 0.3 ng m^{-3} can be achieved. A 47 mm diameter Teflon pre-filter with a pore size of 0.2 µm protects the sampling cartridges against contamination with particulate matter.

In general, this system is sampling and analysing all gaseous fractions of atmospheric mercury, i.e. Total Gaseous Mercury (TGM). However, during this study the gold traps were preceded by an annular denuder which removes divalent inorganic Hg-species. Therefore, under background conditions it can be assumed that the remaining and measured fraction is elemental mercury only.

Two different approaches have been used for the determination of inorganic oxidized gaseous mercury species, operationally defined as Reactive Gaseous Mercury (RGM) – denuder system and mist chamber.

The Tekran mercury speciation unit (Model 1130) consists of a KCl coated annular denuder for the RGM collection, a denuder heating device and a pump unit. After sampling, RGM is released from the denuder by heating it up to 500^{o} C. At these temperatures oxidized mercury compounds on the denuder surface will be converted to Hg(0), released and can be subsequently detected with an on-line connected Tekran mercury vapor analyser. The limit of determination is 0.2 pg m^{-3} when a sampling time of 4 hours is used.

In the refluxing mist chamber sample air is pulled through a scrubber solution. The solution is partly nebulized by a nozzle inside the chamber and the soluble RGM species are effectively trapped by the nebulized mist. A hydrophobic filter at the top of the mist chamber separates the droplets from the air and allows the liquid fraction to drain back into the chamber. At the end of each run the trapped RGM is reduced with $SnCl_2$ to Hg(0) which is degassed from the aqueuous phase, preconcentrated on gold cartridges and detected by CV-AFS. For a sample volume of 1 m^3, the limit of determination is 4 pg m^{-3}.

Total Particulate Mercury has been sampled and analyzed according to a method published by *J.W.H. Lu et al.* [1998]. The analytical system basically consists of a miniaturized device, that serves as both particulate trap and pyrolyzer for airborne particulate mercury species. This device is used in combination with amalgamation/thermal desorption/cold vapor atomic fluorescence spectrometry detection for the determination of Total Particulate Mercury (TPM) associated with atmospheric aerosols. Since no sample preparation, no manual sample transfer or sample handling and no addition of chemicals or reagents is required, this method has a very low risk of contamination. The procedural detection limit of this method for a typical 24 h sample is ~ 2 pg m^{-3}.

Samples were taken using the GKSS bulk sampler (Teflon, 35 cm diameter) and brown glass bottles. Sampling intervals were 48 hrs, starting at 9:00 a.m. Sampling and analysis were

carried out according to the OSPAR guidelines for the sampling and analysis of mercury in precipitation.

Total mercury in precipitation was determined after an oxidative digestion with Cold Vapor Atomic Fluorescence Spectrometry (CV AFS). 10 mL of precipitation sample was treated with 0.25 ml of a 0.1M BrCl solution. The digestion was completed after 1 hour by addition of ascorbic acid. For AFS-determination, dissolved ionic mercury was reduced to Hg(0) by a stannous chloride solution.The blank performance of the entire method was 2.4 ng l^{-1} with a standard deviation of 0.17 ng l^{-1} (n=10). The corresponding limit of determination was 1.2 ng l^{-1}.

Reactive mercury was determined after direct reduction of the acidified sample with stannous chloride solution. The limit of determination is 0.6 ng l^{-1}.

3.2. Summary of Results

Table 3.1 and 3.2 are summarizing the average concentration values, the observed minimum and maximum concentrations and the number of samples for the individual species measured between July 6 to 27, 2000. Table 3.3 gives an overview on the meteorological parameters air temperature, relative humidity and precipitation rate for the study period.

Table 3.1. Summary of average concentrations of airborne mercury species

Species	Average concentration	Minimum concentration	Maximum concentration	Number of samples
Elemental Hg	1.59 ng m^{-3}	1.0 ng m^{-3}	2.4 ng m^{-3}	Ca. 5000
RGM; Denuder	4.0 pg m^{-3}	0.3 pg m^{-3}	90 pg m^{-3}	122
RGM; Mist Chamber	9.0 pg m^{-3}	Below DL	20 pg m^{-3}	25
TPM	40 pg m^{-3}	Below DL	275 pg m^{-3}	27

Table 3.2. Summary of average concentrations of mercury species in precipitation

Species	Average concentration	Minimum concentration	Maximum concentration	Number of samples
Total mercury	7.2 ng l^{-1}	5.0 ng l^{-1}	11.0 ng l^{-1}	7
Reactive mercury	2.2 ng l^{-1}	1.3 ng l^{-1}	3.5 ng l^{-1}	4

Table 3.3. Meteorological conditions

Parameter	Average value	Minimum value	Maximum value	Number of samples
Air temperature	15.4° C	9° C	27.5° C	
Relative humidity	77 %	31 %	96 %	
Precipitation rate	3.5 mm / 48 hrs	0.9 mm / 48 hrs	5.9 mm / 48 hrs	8

On the basis of information presented in tables 3.1 and 3.2 it is possible to use for the further model calculations as input initial parameters the value of 40 pg m^{-3} for particulate mercury and 5 pg m^{-3} for gaseous mercury compounds in air.

4. INPUT PARAMETERS

The initial concentrations and input parameters were defined at the MSC-E workshop held in Moscow on 13-14 April 2000. At the starting point they are characteristic values for regional atmospheric pollution levels [*CCC/EMEP,* 1998] and for cloud systems in Central Europe [*Acker et al.,* 1998]. The set of initial concentrations and parameters is presented in table 4.1.

Table 4.1. Initial concentrations and parameters for model calculations

Initial concentrations and parameters	Value, dimension
Liquid water content	0.5 g/ m^3
Water drop size, diameter	10 μm
Temperature	278°K
Elemental mercury in air	1.7 ng Hg / m^3
Elemental mercury in water	0 ng Hg /l
Gaseous oxidized mercury in air (as $HgCl_2$)	0.05 ng Hg /m^3
Particulate Hg in air	0.05 ng Hg /m^3
Oxidized mercury in water	0 ng Hg /l
Mercury adsorbed on soot particles in water	0 ng Hg /l
Sulphur dioxide in air	1 μg S /m^3
Sulphite ion in water, [$SO_3^=$]	0 M
Ozone in air, O_3	70 μg O_3 /m^3
Ozone in water, O_3	0 μg O_3 /l
pH of water	4.5
Chloride ion in water, Cl^-	2.5 mg/l
Soot content in air	0.5 μg C /m^3
OH radical in water, OH	0
Chlorine in air, Cl_2	5 ppt
Hydrogen peroxide in air, H_2O_2	100 ppt
Hydrogen peroxide in water, H_2O_2	0

Midday concentrations of photochemically dependent species are: OH radical – 10^{-12} M; HO_2 radical – 5×10^{-9} M; Cl_2 – 0 M.

To check sensitivity of the models to the values of initial concentrations of gaseous and particulate mercury chloride it was agreed to provide some additional model runs for 5 different cases:

Parameter/case	case 1	case 2	case 3	case 4	case 5
Hg^0, ng/m^3	1.7	1.7	1.7	1.7	1.7
$HgCl_2$ (gas), ng/m^3	0	0	0	0.005	0.005
$HgCl_2$ (part), ng/m^3	0	0	0.04	0	0.04
Soot	No	Yes	No	No	Yes

Duration of the time evolution of mercury concentrations is 48 hours. Output data step is 10 min. Duration of day and night is assumed to be equal with solar radiation typical for Central Europe (Lat. = 55 degree) on September 15. All participants have used their own values of reaction rates, water solubilities, Henry's law constants, etc.

The output parameters are:

Hg^0 in gas phase

Hg^{2+} in gas phase

Hg in aerosol particulate phase (all chemical forms)

Hg^0 in liquid phase

Hg^{2+} dissolved (all chemical species in sum)

Hg in particulate phase within droplets (all chemical forms)

S(IV) in liquid phase

O_3 in liquid phase

H^+ in liquid phase

5. RESULTS AND THEIR EXPLANATIONS

All participating groups have performed calculations in accordance with the agreed programme. Besides, two groups provided additional calculations. The GKSS group calculated three additional cases introducing occurrence of some precipitation of different intensity. The IVL group additionally calculated a version with a newly measured coefficient for elemental mercury solubility in water. The calculated volume of information is huge therefore in the analysis presented below the main attention is payed to the most important constituent – the evolution of constractions of different forms in the liquid phase. To facilitate the data comparison the basic calculation variant with the imput parameters listed in table 4.1 is called zero one. ("Case 0 with soot" and "Case 0 without soot"). The calculation variants used for examining the model sensitivity to initial concentrations of gaseous oxidized and paticulate mercury are represented as "Case 1", "Case 2", "Case 3", "Case 4", "Case 5". The additional variants of GKSS and IVL groups are represented as "Case 6", "Case 7" и "Case 8".

5.1. CMAQ Model

Case 0:

At the start of the simulation of case 0, most of the initial gaseous oxidized mercury (0.05 ng/m^3 as $HgCl_2$) and all of the particulate Hg (0.05 ng/m^3) is transferred to the cloud droplet liquid phase by the CMAQ-Hg model. $HgCl_2$ is partitioned strongly and immediately to the liquid phase based on its Henry's law constant (1.4×10^6 M/atm) and the assumption of an instantaneous Henry's equilibrium for 10 μm diameter cloud droplets. All of the particulate mercury is partitioned to the liquid phase based on the assumption that this Hg is bound to ambient aerosol particles which act as cloud condensation nuclei. The CMAQ-Hg model assumes this particulate Hg to be mercuric oxide, or HgO. The immediate transfer of 0.1 ng of Hg into 0.5 grams of cloud water results in an initial concentration of 200 ng Hg per litre, which is a very high concentration even for highly industrialised areas (see fig. 5.1 and 5.2).

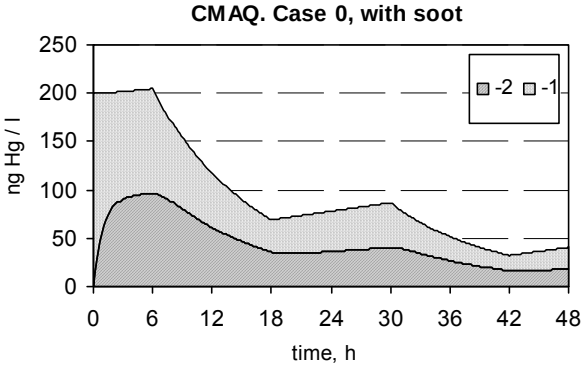

Figure 5.1. Hg liquid phase concentrations calculated by CMAQ. Case 0 with soot in air. 1 – dissolved mercury; 2 –absorbed on soot particles mercury

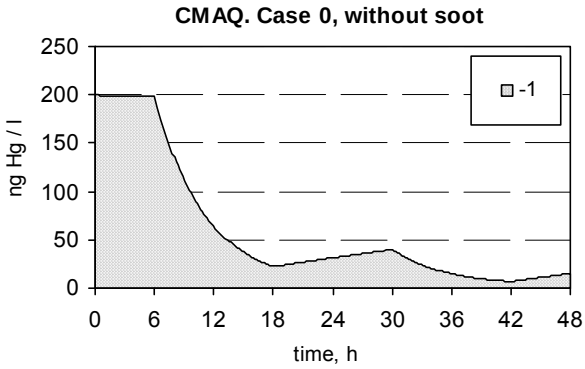

Figure 5.2. Hg liquid phase concentrations calculated by CMAQ. Case 0 without soot in air; 1 – dissolved mercury

Once the gaseous $HgCl_2$ and solid HgO have been dissolved into the cloud water, an aqueous chemical equilibrium is imposed and a variety of dissolved Hg(II) species exist in the simulation. These dissolved Hg(II) species are then allowed to sorb to any soot particles suspended in the cloud water based on the prescribed soot concentration in air, complete cloud water scavenging of the soot, and Hg(II) sorption and desorption rates. In the case 0 simulation with soot, the fraction of Hg(II) in cloud water which sorbs to suspended soot at equilibrium is about 47%, which has a noticeable effect on the redox balance and cloud-water Hg concentrations.

With the simulation beginning at midnight, the primary chemical reaction in cloud water is oxidation of Hg^0 by dissolved chlorine (HOCl and OCl^-). Oxidation of Hg^0 by ozone is second in importance, and reduction of Hg(II) by $HgSO_3$ decomposition is third. At the start of the

simulation, net oxidation of Hg is occurring and one might expect the cloud water concentration of Hg to increase significantly. However, $HgCl_2$ becomes the predominate species of dissolved Hg(II) over the first few hours due to the decline of SO_3^{2-} concentation from sulfur oxidation and lower pH, and the constant chloride ion concentration prescribed for the model intercomparison. The Henry's equilibrium transfers $HgCl_2$ from the dissolved phase to the gas phase, and from hour 0 to hour 6, total aqueous Hg(II) actually decreases slightly in case 0 without soot, and increases only slightly in case 0 with soot.

At sunrise, the HO_2 aqueous concentration of 5×10^{-9} M is imposed and all dissolved Hg(II) species are rapidly converted to Hg^0. The instantaneous onset of these reactions with HO_2 and suspension of oxidation by chlorine leads to a rapid loss of Hg(II) in cloud water beginning exactly at sunrise and continuing at a slowing pace until sunset at 18 hours into the simulation. By the time of first sunset, the rate of Hg reduction and outgassing of Hg^0 from cloud water is slowed to about one-half the rate of 12 hour before due mostly to depletion of dissolved Hg(II). Changing pH and oxidation of SO_3^{2-} to SO_4^{2-} from the co-existing CMAQ acid deposition and oxidant chemistry also slow the overall Hg reduction during this first daytime period and throughout the rest of the simulation. The loss of aqueous Hg is moderated by the presence of soot. The total aqueous Hg concentration is reduced to approximately 70 ng/l by sunset at hour 18 for the case with soot, compared to 23 ng/l for the case with no soot. At sunset, the reduction of Hg(II) by HO_2 ceases and the oxidation of Hg^0 by dissolved chlorine begins once again, and the overall redox system is once again showing net oxidation of Hg. It should be noted that Hg^0 oxidation by ozone and Hg(II) reduction by $HgSO_3$ decomposition both continue throughout the simulation, but these reactions which were the basis for earlier European and North American atmospheric mercury models are now secondary to the day-time reduction by HO_2 and night-time oxidation by aqueous chlorine in the cloud chemistry of the CMAQ-Hg model.

Beyond sunset at 18 hours into the simulation, net oxidation of Hg and increasing cloud-water concentration of Hg continues at night, and net reduction of Hg and decreasing cloud-water concentration of Hg continues during the day, with the overall trend showing about twice as much Hg in cloud water for the case with soot compared to the case without soot.

Case 1 and Case 2:

These test cases have a clean initial condition with regard to oxidized mercury in air and cloud water. Case 1 has no soot in air or cloud water, therefore sorption of Hg to soot does not occur in this case (fig. 5.3 and 5.4). For both cases, the initial condition of 1.7 ng/m^3 of Hg^0 in air and the model treatment of instantaneous Henry's equilibrium results in a very small concentration of dissolved Hg^0 which is available for oxidation at the start of the

simulation. Until the first sunrise at hour 6, the chlorine and ozone oxidation reactions dominate the slower reduction of Hg(II) by sulfite decomposition and approximately 8 ng/l of dissolved mercury accumulates in the cloud water in both cases. With sunrise, rapid reduction of all dissolved Hg(II) species by HO_2 starts and the oxidation of dissolved Hg^0 by chlorine ceases. For case 1, the total dissolved Hg concentration drops to about 4 ng/l by sunset at hour 18. For case 2, the dissolved Hg concentration is only reduced to about 7.5 ng/l. At sunset, the situation reverses once again and net oxidation of Hg continues for 12 hours, leading to a dissolved Hg concentration of just over 20 ng/l by the next sunrise at 30 hours for case 1 and just over 25 ng/l for case 2. The presence of soot in case 2 tends to moderate the reduction of Hg(II) by HO_2 during daytime and have no effect on oxidation of Hg^0 by chlorine at night, thus producing noticeably larger aqueous Hg concentrations after the first sunrise of the simulation period.

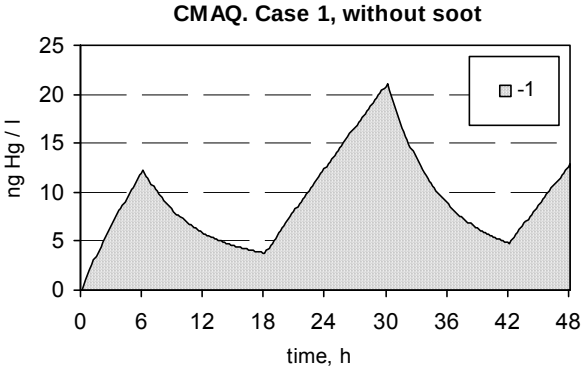

Figure 5.3. Hg liquid phase concentrations calculated by CMAQ. Case 1 without soot in air. 1 – dissolved mercury

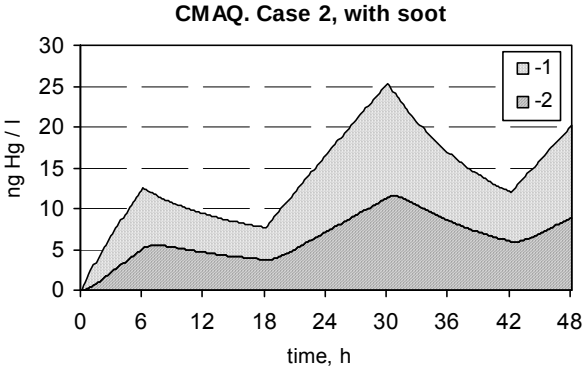

Figure 5.4. Hg liquid phase concentrations calculated by CMAQ. Case 2 with soot in air. 1 – dissolved mercury; 2 – absorbed on soot particles mercury

Case 3:

This case has no soot, but starts with 40 pg/m^3 of particulate mercury in air, which is assumed by the CMAQ model to be solid HgO which has acted as cloud condensation nuclei and dissolved during the formation of the cloud. This dissolved HgO is very rapidly converted to ionic Hg(II) which is distributed among the modeled Hg(II) species by the dissociation equilibria to form 80 ng/l of the total aqueous Hg concentration of 80.004 ng/l in the cloud water at the start of the simulation (fig. 5.5). Oxidation of dissolved Hg^0 by chlorine increases the total dissolved Hg concentration during the first night. However, $HgCl_2$ becomes the predominate dissolved Hg(II) species during this time, and transfer of $HgCl_2$ to the gas phase by Henry's equilibrium limits the build-up of total dissolved Hg concentration to around 86 ng/l. The reduction of Hg(II) by HO_2 beginning at hour 6 is very rapid and the aqueous Hg concentation has fallen to about 12 ng/l by the time of first sunset at hour 18. During the next

nighttime period, oxidation of Hg^0 results in an increase in dissolved Hg to slightly less than 30 ng/l, but the HO_2 reaction brings the dissolved Hg concentration down to around 6 ng/l by the end of the second day. By the end of the simulation, case 3 results appear to be developing an oscillation of dissolved Hg concentration with 20 ng/l at sunrise and 5 ng/l at sunset, similar to case 1.

Case 4:

This case has no soot, and starts with 5 pg/m^3 of gaseous $HgCl_2$ in air which partitions strongly to the aqueous phase at the start of the simulation. The Henry's equilibrium for $HgCl_2$, and to a much lesser degree that for Hg^0, produce an initial dissolved Hg concentration of around 10 ng/l (fig. 5.6). This dissolved Hg concentration is near the average value of the day/night oscillation indicated near the end of the simulation for previous test cases with no soot. Case 4 appears to show an oscillation between 20 ng/l at sunrise and 5 ng/l at sunset throughout the entire 48 hour simulation.

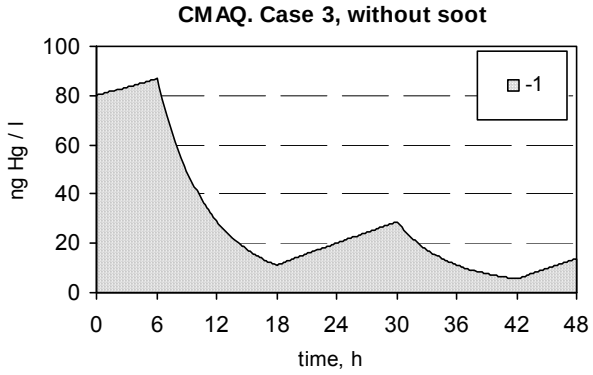

Figure 5.5. Hg liquid phase concentrations calculated by CMAQ. Case 3 without soot in air. 1 – dissolved mercury

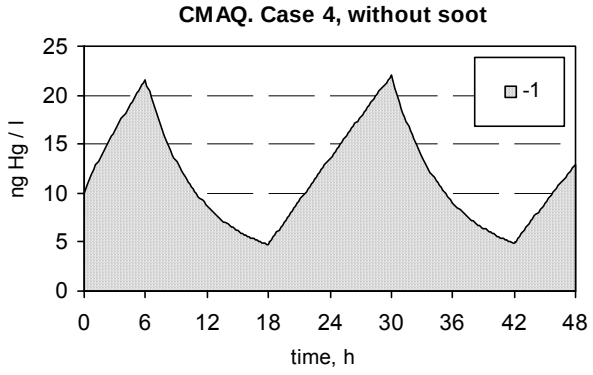

Figure 5.6. Hg liquid phase concentrations calculated by CMAQ. Case 4 without soot in air. 1 – dissolved mercury

Case 5:

This test case starts with air concentrations of 40 pg/m^3 of particulate Hg (as in case 3) and 5 pg/m^3 of $HgCl_2$ (as in case 4). Both of these Hg species partition strongly to cloud water, and an initial dissolved Hg concentration of approximately 90 ng/l is established (fig.5.7). This case also includes an initial

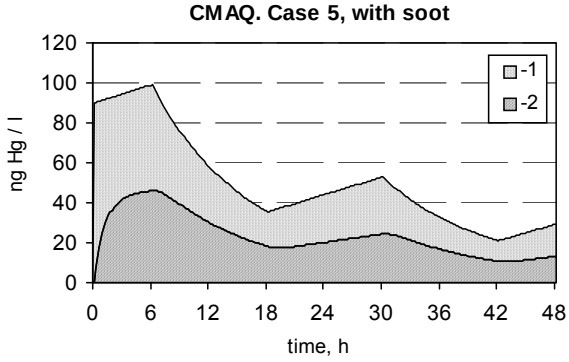

Figure 5.7. Hg liquid phase concentrations calculated by CMAQ. Case 5 with soot in air. 1 – dissolved mercury; 2 –absorbed on soot particles mercury

soot concentration of 0.5 $\mu g/m^3$ in air, similar to case 0 (with soot) and case 2, and a significant fraction of aqueous Hg(II) is similarly sorbed to soot suspended in the cloud water. The same cycle of nighttime oxidation and daytime reduction of Hg occurs in this case as with previous cases. The rate of oxidation of dissolved Hg^0 appears to be the same for all nighttime periods and is not affected by the sorption of Hg(II) to soot. The total aqueous Hg concentration is brought down rapidly during the first daytime period, from nearly 100 ng/l to around 35 ng/l, and less rapidly on the second day, from approximately 50 ng/l to 20 ng/l.

Discussion of all cases:

The concept of a cloud with temperature, pressure, liquid water content, cloud droplet size, and various dissolved ion concentrations holding steady over a 48-hour period is rather unnatural. Vertical velocity, cloud micro-physical processes and precipitation may all have complex effects on the overall chemical balance and loading of mercury in cloud water which are not treated in this simulation. However, these test simulations show which chemical reactions are important, and which are not, during various times of the day.

These test simulations show that a day/night oscillation of the aqueous Hg concentration occurs, driven mostly by the reaction of Hg^0 with chlorine (oxidation) during nighttime and reaction of Hg(II) with HO_2 (reduction) during daytime. It appears that all of the cases with no soot are approaching an equilibruim condition where the dissolved Hg concentration oscillates between 20 ng/l at sunrise and 5 ng/l at sunset. The presence of soot appears to moderate the reduction of Hg(II) during daytime and have little effect on oxidation of Hg^0 during nighttime, thus leading to an overall greater concentration of Hg in cloud water. These tests have also shown that the cloud chemistry mechanism in the CMAQ-Hg model is very sensitive to the concentrations of dissolved chlorine and hydroperoxyl radical. The rate constants used for their reactions with mercury have a strong effect on simulation results. An accurate determination of these rate constants, and those for any other important chemical reactions, is necessary before any confident modeling assessment is possible.

It should be noted that the cloud chemistry mechanism for Hg in the CMAQ model was modified during the course of this model intercomparison study based on newly published information about mercury chemistry.

5.2. The GKSS Tropospheric Chemistry Module

The TCM has been applied using the closest possible approximation to the input parameters described in Section 3, i. e. a non-precipitating cumulus cloud with a cloud base and top height of about 400 m and 4700 m, respectively. The environmental vertical profiles of temperature, pressure and relative humidity have been adjusted to generate a cloud with an average liquid water content of 0.5 g m^{-3}. The initial concentration profiles in the cloud region and in the above-cloud region for all three species are vertically constant with values corresponding to the values prescribed in Chapter 4. The initial concentrations in the below-cloud region are two orders of magnitude lower to avoid any substantial mercury inflow into the cloud from the below-cloud region, which would bias the mercury inventory in the cloud towards initial concentrations higher than the prescribed values.

Since the TCM is a system which incorporates atmospheric mercury chemistry together with cloud mixing, the results of the 48 hours simulations are affected by cloud formation and dissipation processes and by vertical up-and-down motion of air parcels and mercury species in the cloud resulting in pronounced vertical Hg^0, $HgCl_2$ and Hg(part.) concentration profiles after cloud evaporation at the end of each time step depicted in figure 5.8 (a, b, c) respectively.

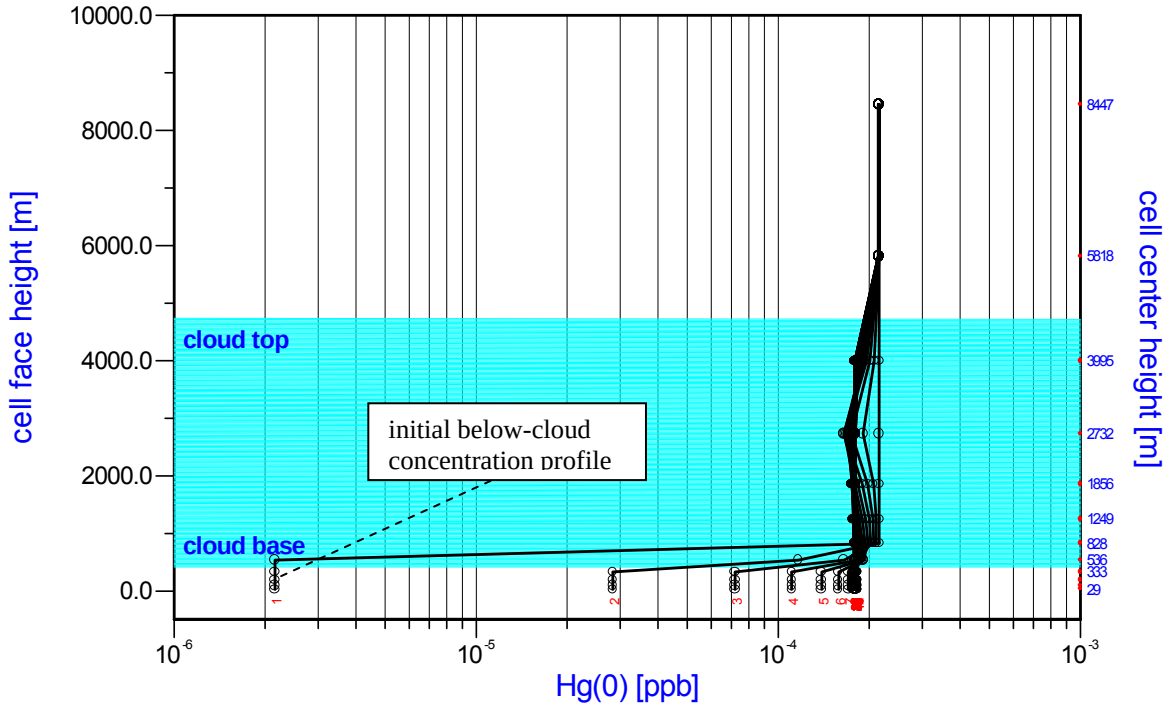

Figure 5.8.a. 48 hour time evolution of vertical Hg^0 concentration profiles at the end of each time step after cloud evaporation. (0.5 µg m^{-3} soot)

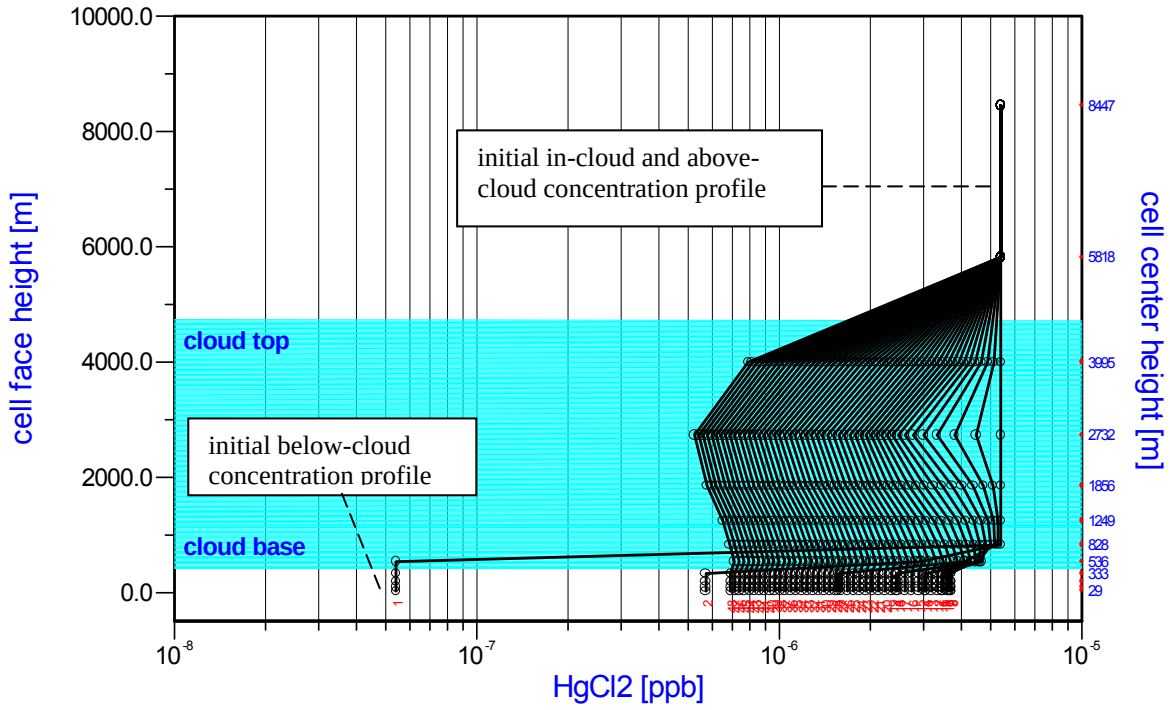

Figure 5.8.b. 48 hour time evolution of vertical $HgCl_2$ concentration profiles at the end of each time step after cloud evaporation. (0.5 μg m^{-3} soot)

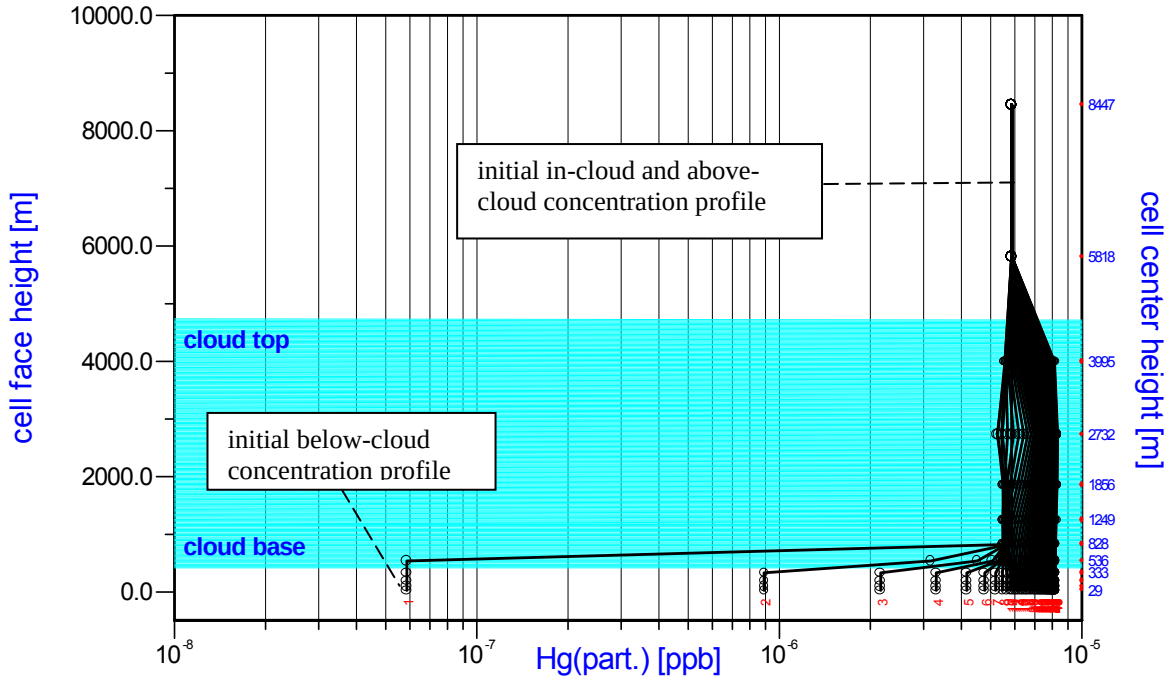

Figure 5.8.c. 48 hour time evolution of vertical Hg(part.) concentration profiles at the end of each time step after cloud evaporation. (0.5 μg m^{-3} soot)

These profiles are generated over the entire depth of the troposphere assuming a soot concentration in air of 0.5 μg m^{-3} including the regions below and above cloud base and cloud top. For all three species, changes in vertical profiles in the cloud area are due to vertical mixing together with aqueous phase chemistry, scavenging and back evaporation of the aqueous species at the end of each time step. Due to vertical redistribution after cloud dissipation below cloud concentrations of all three species are adjusting with time to cloud area concentrations, i.e. initial below cloud concentrations are increasing with time until they have reached the concentration level in the cloud and then closely follow in-cloud concentration changes.

Figure 5.8.a shows a relative small Hg^0 depletion in the cloudy area caused by mass transfer into the aqueous phase. The $HgCl_2$ depletion in figure 5.8.b is far more pronounced since this species is readily scavenged and subsequently adsorbed on soot particles. At the end of the time step, adsorbed $HgCl_2$ is evaporated back to Hg(part.) in air hence contributing to the increase of Hg(part.). concentration as a function of time shown in figure 5.8.c.

Concentration profiles generated by the TCM for the no-soot scenario are depicted in figures 5.9 (a,b,c).

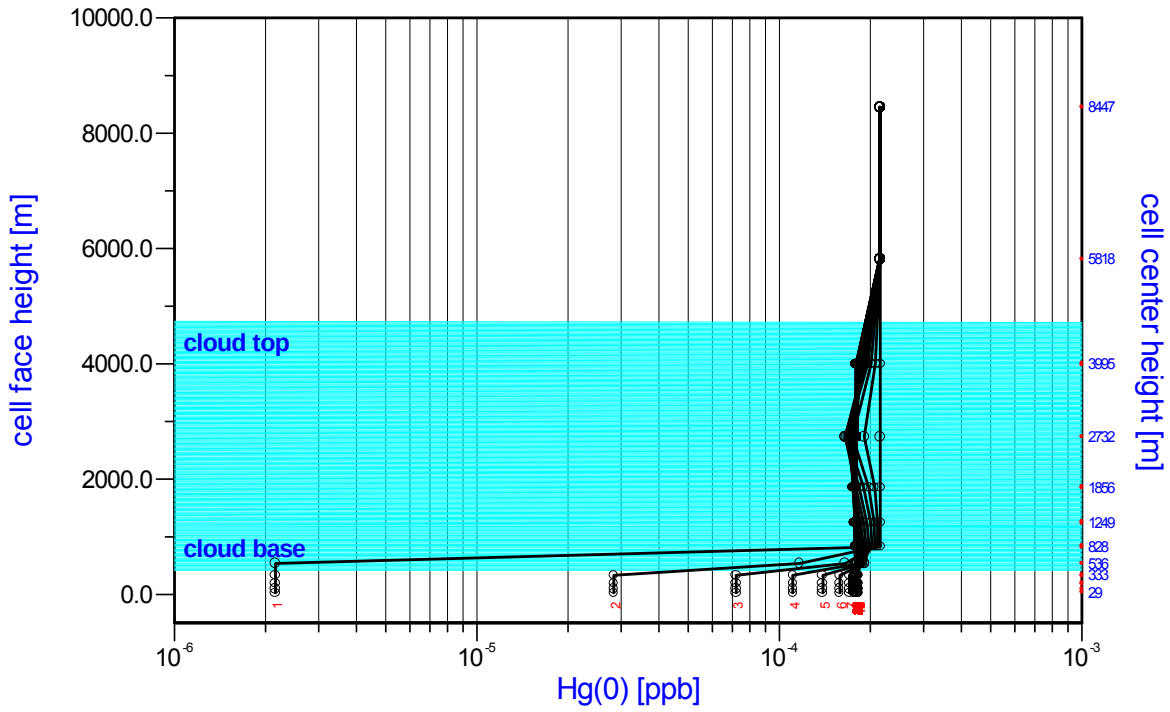

Figure 5.9.a. 48 hour time evolution of vertical Hg^0 concentration profiles at the end of each time step after cloud evaporation (no soot)

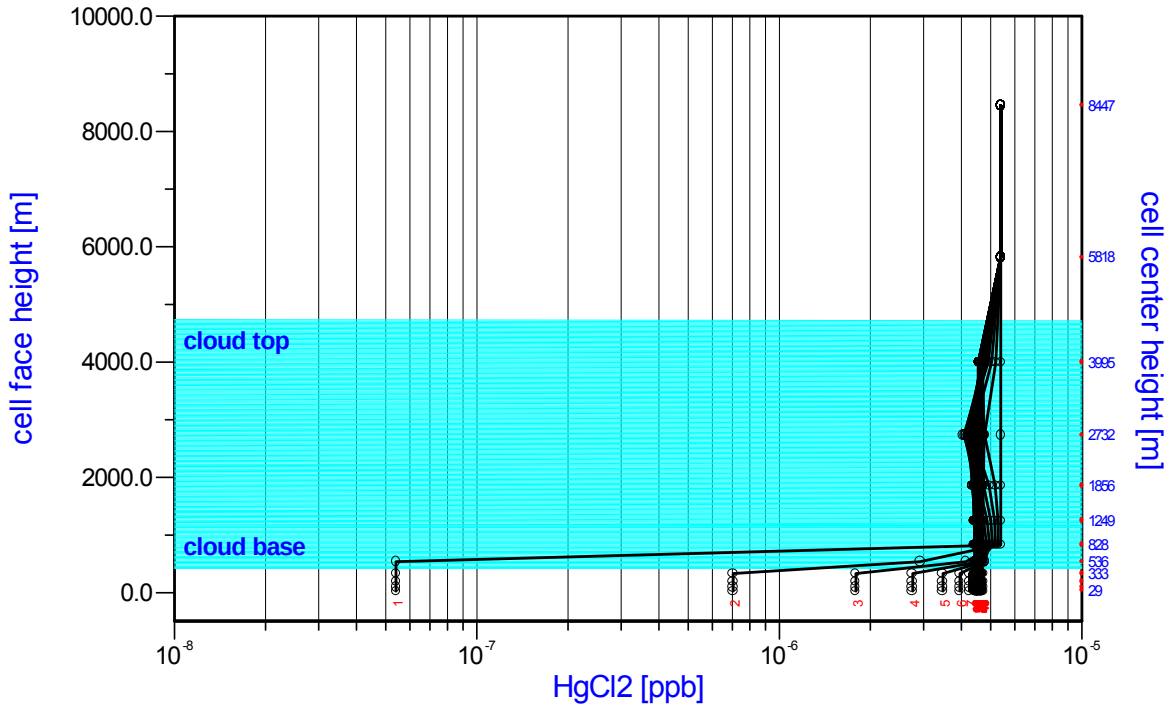

Figure 5.9.b. 48 hour time evolution of vertical $HgCl_2$ concentration profiles at the end of each time step after cloud evaporation (no soot)

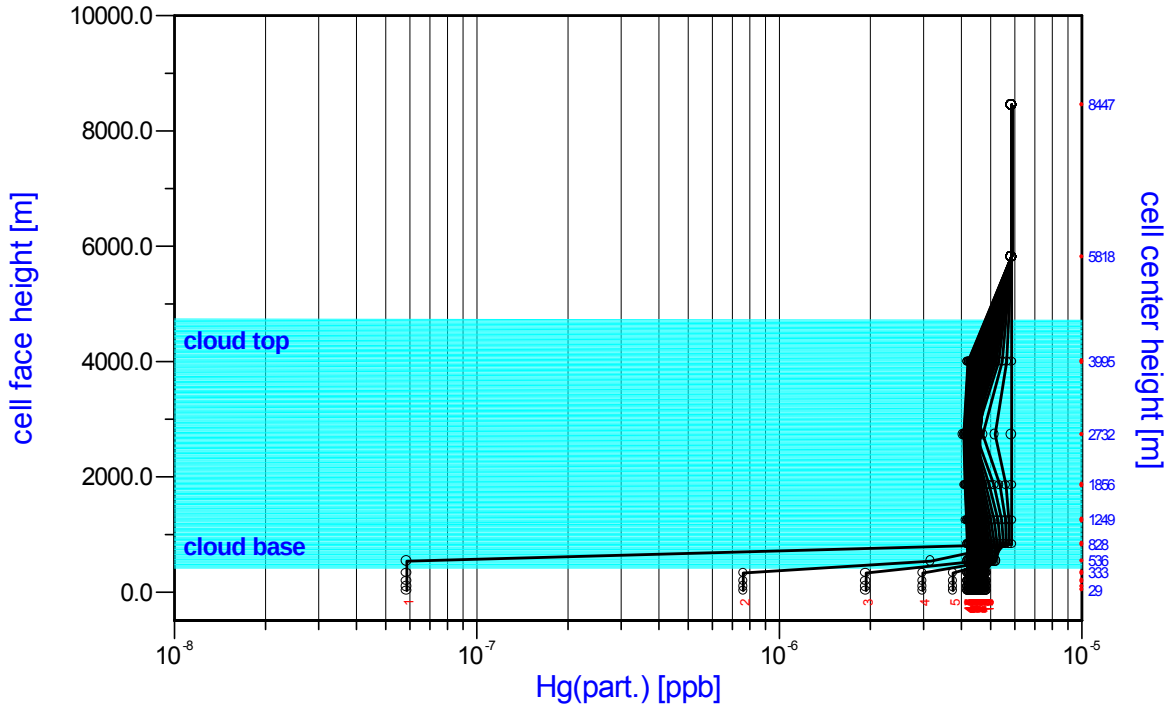

Figure 5.9.c. 48 hour time evolution of vertical Hg(part.) concentration profiles at the end of each time step after cloud evaporation (no soot)

A comparison of profiles in figure 5.8.a and 5.9.a reveals their similarities. Due to its low water solubility changes in Hg^0 concentrations are mainly determined by mass transfer processes into the aqueous phase and only to a minor extend by subsequent adsorption on soot particles. In the absence of soot $HgCl_2$ depletion is considerably slower (fig.5.9.b), because mass transfer of $HgCl_2$ from the gas phase to the aqueous phase is slowed down if a subsequent adsorption on soot particles is missing. This also affects the time evolution of Hg(part.) i.e. a smaller amount of adsorbed $HgCl_2$ is evaporated back and thus changing the Hg(part.) build up into a slight Hg(part.) depletion (see fig. 5.8.c and 5.9.c).

Figures 5.10 and 5.11 show time dependent average gas-phase and aqueous phase concentrations in the cloudy area after chemistry has taken place but before cloud dissipation and vertical redistribution of species for the 0.5 µg m^{-3} soot and for the no-soot scenario. It should be noted, that concentrations of all species undergo an initial spin-up period of about 6 hours according to the adjustment of below cloud concentrations to concentrations in the cloud area as illustrated in figures 5.8 and 5.9.

The low solubility of Hg^0 leads to the majority of Hg^0 to be present in the gas phase in both the 0.5 µg m^{-3} soot and the no-soot scenario (fig. 5.10.a and b). However, $HgCl_2$ and Hg(part.) gas phase concentrations behave significantly different in both scenarios: In case of the 0.5 µg m^{-3} soot scenario Hg(part.) concentrations are slightly increasing with time after the spin-up period, whereas $HgCl_2$ shows an opposite trend (fig. 5.10.a). This can be explained by an increasing ratio of adsorbed and dissolved aqueous species as a function of time and hence, after back evaporation at the end of the cloud life cycle, an increasing ratio of Hg(part.) and $HgCl_2$ gas phase concentrations. At the end of the 48 hours simulation the Hg(part.) concentrations are a factor of about 8 higher than $HgCl_2$ concentrations. If no soot is involved (fig. 5.10.b) less aqueous Hg is present in the adsorbed phase resulting in less back evaporation to Hg(part.) and at the end of the simulation period, in an $HgCl_2$ concentration slightly higher than Hg(part.) (fig. 5.10.b).

The Hg(dis.)aq and the Hg(ad.)aq. lines in figures 5.11.a and b represent the sum of all dissolved and adsorbed species, respectively, and the Hg(tot.) line is the sum of Hg(dis.) and Hg(ad.) (see fig. 2.4 in section 2.2). For both scenarios, the curves for Hg(dis.)aq and Hg(ad.)aq. concentrations show a shape very similar to $HgCl_2$ and Hg(part.) gas phase concentrations in figures 5.10.a and b. This occurs because the cloud system is not depleted by precipitation after aqueous phase chemistry has taken place and no mass of gas-phase species is added at the beginning of the next time step. Hence, the cloud system is governed by back evaporation i. e. most of Hg(dis.)aq and all of Hg(ad.)aq. is converted to gaseous $HgCl_2$ and Hg(part.) at the end of each time step and reaches almost steady-state conditions at the end of the simulation period with Hg(tot.) concentrations of about 110 ng l^{-1} for both

scenarios. In case of the 0.5 μg m^{-3} soot scenario about 95% of the aqueous species are associated with particles at the end of the simulation period, whereas for the no-soot scenario the major fraction (about 54 %) is in the dissolved phase, but a significant Hg(ad.)aq. of 46% is also present due to the initial Hg(part.). in the gas phase, which is chemically inert and just scavenged and evaporated back during the simulation period.

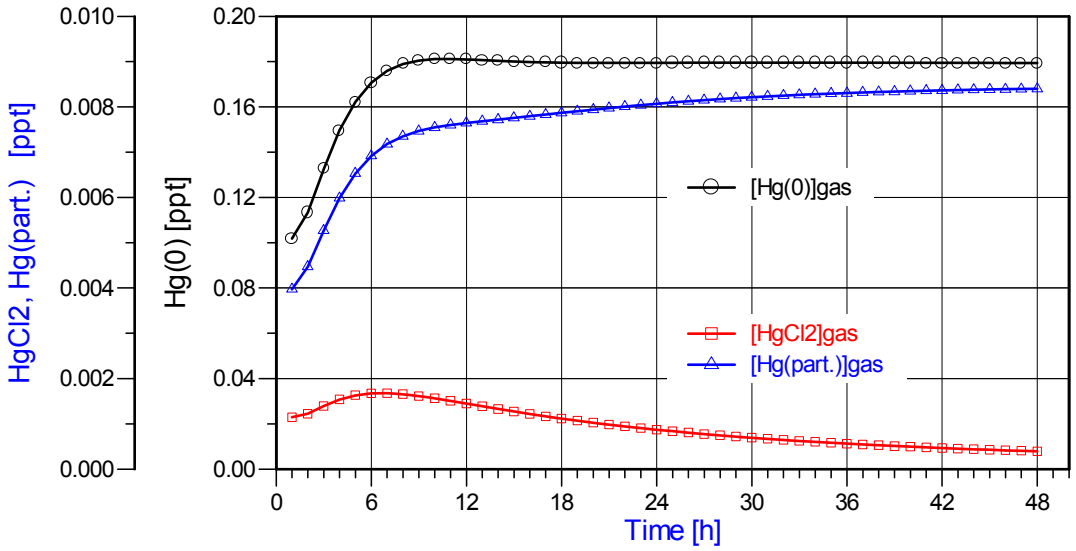

Figure 5.10.a. 48 hour time evolution of average gas-phase concentrations in the cloud area after aqueous-phase chemistry (0.5 μg m^{-3} soot)

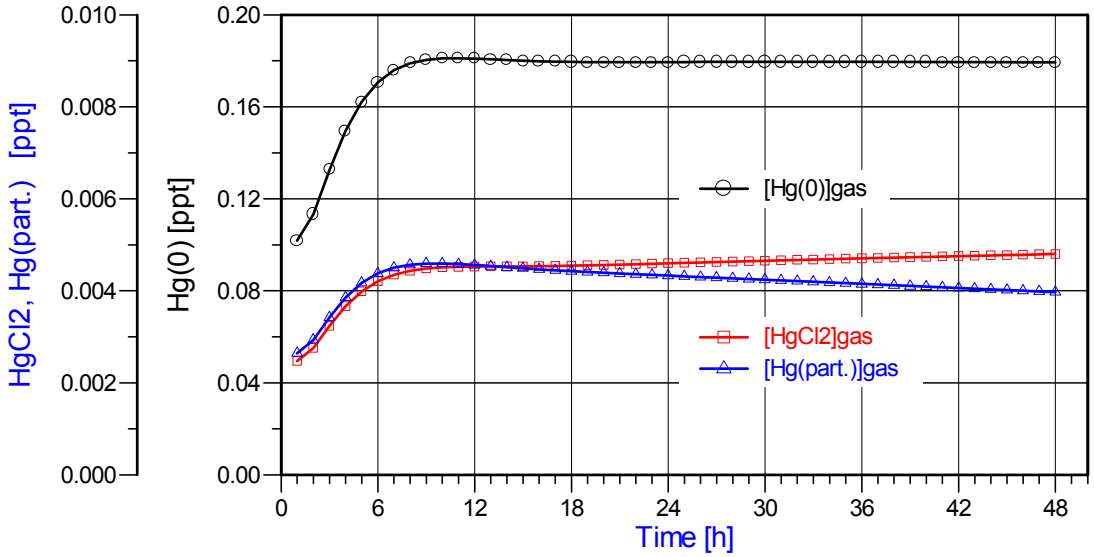

Figure 5.10.b. 48 hour time evolution of average gas-phase concentrations in the cloud area after aqueous-phase chemistry (no soot)

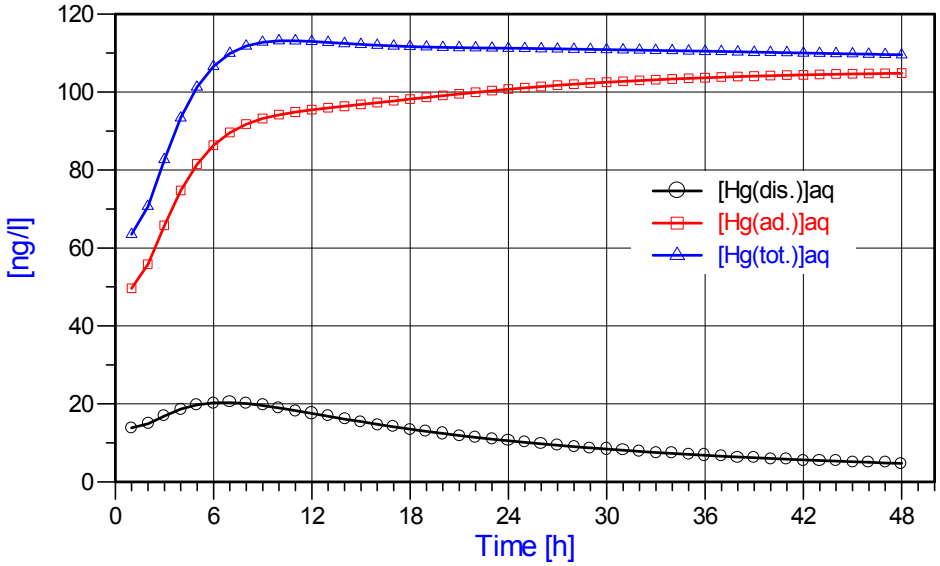

Figure 5.11.a. Case 0: 48 hour time evolution of average aqueous-phase concentrations in the cloud area after aqueous-phase chemistry (0.5 μg m^{-3} soot)

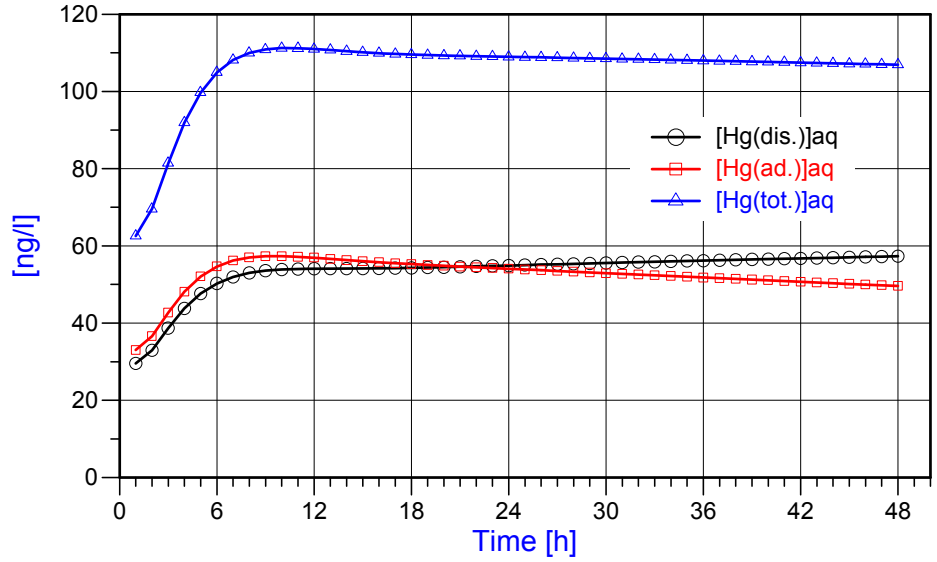

Figure 5.11.b. Case 0: 48 hour time evolution of average aqueous-phase concentrations in the cloud area after aqueous-phase chemistry (no soot)

Additional runs have been performed using input data from simultaneous measurements of mercury species at a site at the GKSS Research Centre Geesthacht, Germany (Chapter 3). These data form the basis for eight different cases defined in table 5.1. Results in terms of total aqueous mercury concentrations $Hg(tot.)_{aq.}$, i.e. the sum of Hg(dis.)aq and Hg(ad.)aq. as

a function of time and soot concentrations are summarized in figures 5.12.a and b. To demonstrate the impact of depletion effects by precipitation in more detail, $Hg(tot.)_{aq.}$ concentrations in these two figures have been generated without spin up during the first 6 hours as mentioned above and as shown in figures 5.8 – 5.11.

Table 5.1. Input parameters for model results depicted in figures 5.12.a and b

	Hg^0 [ng m^{-3}]	$HgCl_2$ [ng m^{-3}]	Hg(part.) [ng m^{-3}]	soot [µg m^{-3}]	precip. rate [mm $(48\ h)^{-1}$]
case 1	1.600	0.000	0.000	0.0	0.00
case 2	1.600	0.000	0.000	0.5	0.00
case 3	1.600	0.000	0.040	0.0	0.00
case 4	1.600	0.005	0.000	0.5	0.00
case 5	1.600	0.005	0.040	0.5	0.00
case 6	1.600	0.005	0.040	0.5	3.50
case 7	1.600	0.005	0.040	0.5	7.00
case 8	1.600	0.005	0.040	0.5	10.50

Figure 5.12.a shows the impact of $HgCl_2$ and Hg(part.) concentrations on $Hg(tot.)_{aq.}$ at a constant Hg^0 level of 1.6 ng m^{-3}. As expected, $Hg(tot.)_{aq.}$ shows minimum values, when $HgCl_2$ and Hg(part.) are set to zero, for both with soot and without soot (case 1 and 2, respectively). Adding 0.04 ng m^{-3} Hg(part.) results in an about fourfold increase of $Hg(tot.)_{aq.}$ (case 3) whereas an addition of 0.005 ng m^{-3} $HgCl_2$ only contributes about 10-15 % to $Hg(tot.)_{aq.}$ originating from Hg^0 (case 4). The input data for case 5 represent the observed average Hg concentrations in air but with a zero precipitation rate yielding a $Hg(tot.)_{aq.}$ concentration of about 80 ng l^{-1} (see fig. 5.12.a and b). If the TGM is depleted with the observed average precipitation rate of 3.5 mm ($48\ h^{-1}$) the concentrations is dropping to about 30 ng l^{-1} (case 6 in fig.5.12.b). Since the very minor observed precipitation rate is probably underestimated additional runs have been performed with precipitation rates increased by a factor of 2 and 3 (case 7 and 8, respectively). The results for $Hg(tot.)_{aq.}$ are in the range of 10 ng l^{-1} or less and hence rather close to the observed average $Hg(tot.)_{aq.}$ concentration of 7.2 ng l^{-1}.

There is evidence from these additional test runs (case 6-8) that the TCM has capabilities to reproduce observed field data in terms of concentrations in precipitation as a function of precipitation rates. Thus, calculated concentrations in cloudwater, i. e. cases 1-5 with no precipitation can be assumed to be in a realistic range as well.

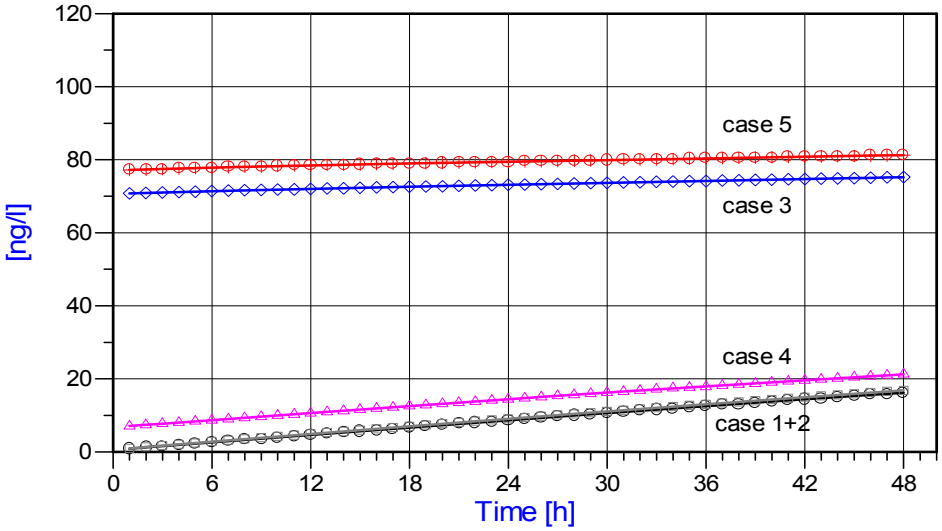

Figure 5.12.a. 48 hour time evolution of average aqueous-phase concentrations in the cloud area after aqueous-phase chemistry for 5 cases defined in table 5.1.

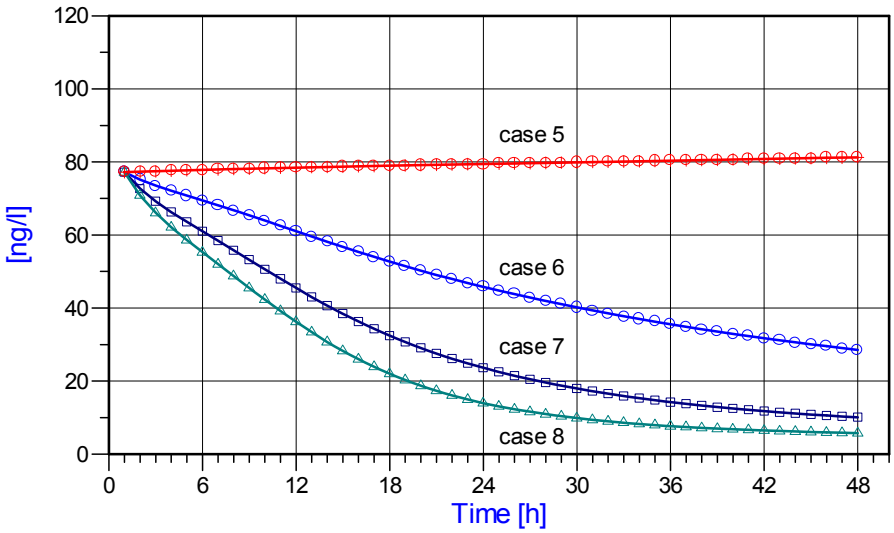

Figure 5.12.b. 48 hour time evolution of average aqueous-phase concentrations in the cloud area after aqueous-phase chemistry for 4 cases defined in table 5.1.

5.3. AER Mercury Chemistry Model

The 48-hour simulation for case 0 was initiated at midnight (i.e., using nocturnal concentrations for OH, Cl_2 and HO_2). It was assumed that daytime to occur from 8 a.m. to 8 p.m. Figure 5.13 shows the temporal variations of the aqueous concentrations of three mercury forms when soot particles occur in air: dissolved mercury species (Hg^0 and Hg(II)), absorbed Hg(II) on soot particles in droplets, insoluble particulate Hg(II) present in droplets.

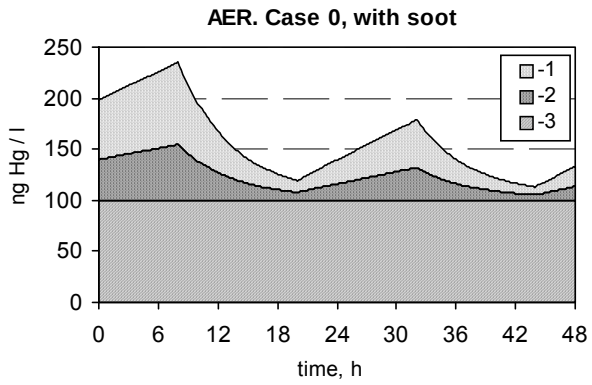

Figure 5.13. Hg liquid phase concentrations calculated by AER. Case 0 with soot in air
1 – dissolved mercury; 2 – absorbed on soot particles mercury; 3 – insoluble particulate mercury

Concentrations of Hg(II) species are greater at night than during the day because the oxidation of Hg(0) by Cl_2 is zero during the day and the reduction of Hg(II) by HO_2 is zero at night. The rate of the aqueous oxidation of Hg(0) by OH is too low to have a significant effect on the diurnal cycle of Hg chemistry. The result of this diurnal variation in the red-ox Hg reactions is increased oxidation of Hg(0) at night and increased reduction of Hg(II) during the day. Consequently, the Hg(II)/Hg(0) ratio increases at night and decreases during the day.

Generally, mercury content in the water drops is determined by initial concentration of particulate mercury in air. At noon (both the first and the second days) the contribution of this mercury to the total content in the liquid phase reaches about 80%.

Table 5.2 presents the distribution of Hg species for daytime and nighttime conditions. Concentrations are presented for all species in mass per volume of air (ng/m^3) and, for aqueous-phase species, in moles per volume of water (M). Partitioning between the gas and aqueous phases and Hg(II) speciation are also presented in percentage with respect to Hg(0) or Hg(II) as well as with respect to total Hg. Note that in table 5.2, particulate mercury is included in the droplet Hg(II) budget since it is assumed that all particles are scavenged by the droplets.

The low solubility of Hg(0) leads to the majority of Hg(0) to be present in the gas phase, only about 0.0001% is present in the aqueous phase. On the other hand, less than 2% of soluble Hg(II) is present in the gas phase. Note that most gas-phase Hg(II) is $Hg(OH)_2$ because it is more volatile (less soluble) than $HgCl_2$.

At night, reduction of Hg(II) occurs only via $HgSO_3$ since HO_2 concentrations are set to zero; however, the kinetics of this reaction as measured by *L.E. van Loon et al*. [2000] is slow. Oxidation of Hg(0) occurs via the aqueous reaction with HOCl (83%), the aqueous reaction with O_3 (11%) and the gas-phase reaction with O_3 (6%). During the day, reduction of Hg(II) is governed by HO_2 (98%) and the $HgSO_3$ reaction is minor (2%). Since the Cl_2 concentration is set to zero during the day, the oxidation of Hg(0) occurs solely by reaction with O_3 in the

aqueous phase (60%) and the gas phase (36%), and by reaction with OH in the aqueous phase (4%).

Table 5.2. Distribution of Hg species in the base case simulation[(a)]

Mercury species	Daytime[(b)]				Nighttime[(c)]			
	ng/m^3	M	% of Hg(0) or Hg(II)	% of total Hg	ng/m^3	M	% of Hg(0) or Hg(II)	% of total Hg
Total Hg(0)	1.74	NA	100.00	96.68	1.71	NA	100.00	95.01
Gas-phase Hg(0)	1.74	NA	100.00	96.68	1.71	NA	100.00	95.01
Droptlet Hg(0)	$2.34x10^{-6}$	$2.34x10^{-14}$	0.00	0.00	$2.30x10^{-6}$	$2.30x10^{-14}$	0.00	0.00
Total Hg(II)	$5.98x10^{-2}$	NA	100.00	3.32	$9.00x10^{-2}$	NA	100.00	5.00
Gas-phase Hg(II)	$1.46x10^{-4}$	NA	0.24	0.01	$5.93x10^{-4}$	NA	0.66	0.03
Droplet Hg(II)	$5.96x10^{-2}$	$5.95x10^{-10}$	99.76	3.31	$8.94x10^{-2}$	$8.91x10^{-10}$	99.34	4.97
Hg^{2+}	$7.03x10^{-9}$	$7.01x10^{-17}$	0.00	0.00	$2.88x10^{-8}$	$2.84x10^{-16}$	0.00	0.00
$HgSO_3$	$2.37x10^{-5}$	$2.37x10^{-13}$	0.04	0.00	$9.72x10^{-5}$	$9.61x10^{-13}$	0.11	0.01
$Hg(SO_3)_2^{2-}$	$4.01x10^{-3}$	$4.00x10^{-11}$	6.71	0.22	$1.64x10^{-2}$	$1.63x10^{-10}$	18.22	0.91
$HgCl_2$	$1.69x10^{-3}$	$1.68x10^{-11}$	2.83	0.09	$6.91x10^{-3}$	$6.83x10^{-11}$	7.68	0.38
$Hg(OH)_2$	$7.03x10^{-6}$	$7.01x10^{-14}$	0.01	0.00	$2.88x10^{-5}$	$2.84x10^{-13}$	0.03	0.00
Hg(p) (soluble)	$3.90x10^{-3}$	$3.88x10^{-11}$	6.52	0.22	$1.60x10^{-2}$	$1.58x10^{-10}$	17.78	0.89
Hg(p) (non-soluble)	$5.0x10^{-2}$	NA	83.61	2.78	$5.0x10^{-2}$	NA	55.55	2.78

(a) Concentrations are provided in mass per volume of air (ng/m^3) and, for the aqueous phase, in moles per volume of water (M); NA = not applicable; percentage numbers may not add to 100% due to round-off and percentage numbers less than 0.005% are reported as 0.00%

(b) At time = 20 h

(c) At time = 32 h

The speciation of Hg(II) does not change between day and night because it depends on the concentration of SO_2, Cl^-, H^+ and particles and these concentrations remain constant. About 40% of soluble Hg(II) is adsorbed to particles. In droplets, soluble Hg(II) is primarily present as $HgCl_2$ (18% of soluble Hg(II)), $Hg(SO_3)_2^{2-}$ (42%) and adsorbed Hg(II) (40%). However, most of Hg present in droplets is initial particulate Hg that we assumed to be non-soluble Hg(II). The particulate mercury concentrations are consistent with values reported by Frontier Geosciences in their sorption experiments with atmospheric particulate matter suspended in water [*Seigneur et al*., 1998]. In those experiments, dissolved Hg(II) accounted for 3 to 22% of total Hg(II) in water; the value simulated here is 16% at the end of the daytime period and 55% at the end of the nighttime period. The sorption experiments suggested that the soluble fraction of Hg(II) adsorbed to particles was in the range of 9 to 55%; the value simulated here is 40%.

The ratio of total (soluble and particulate non-soluble) Hg(II) to Hg(0) varies between 3 and 7%. Particulate non-soluble Hg(II) is about 3% of Hg(0), and soluble Hg(II) varies between 0.5% and 4% of Hg(0). The ratio of Hg(II) to Hg(0) decreases from day to day. This ratio of soluble Hg(II) to Hg(0) is consistent with available data. For example, *S.E. Lindberg and W.J. Stratton* [1998] measured Hg(II)/Hg(0) ratios of 2 to 8% in North America.

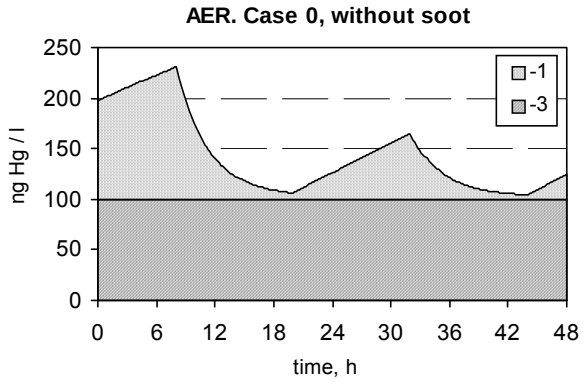

Figure 5.14. Hg liquid phase concentrations calculated by AER. Case 0 without soot in air.
1 – dissolved mercury; 3 – insoluble particulate mercury

Because the treatment of the adsorption of mercury to soot differs significantly among various models, it is of interest to conduct a simulation with no soot in order to remove this source of discrepancy among models. Therefore, the initial concentrations used in this simulation were identical to those used in the base case simulation except for the soot concentration that was set to zero. The results of this simulation without soot are showen in figure 5.14.

Table 5.3 presents the distribution of Hg species for daytime and nighttime conditions in case 0 without soot. In this simulation, all soluble Hg(II) is available for reduction to Hg(0) in the aqueous phase. As a result, the Hg(II) concentrations are lower in this simulation than in the base case simulation with soot. At the end of the daytime period, soluble Hg(II) is only 0.2% of total Hg. At night, the HO_2 reduction reaction does not take place and the Cl_2 oxidation reaction favors Hg(II) formation. As a result, soluble Hg(II) accounts for about 2% of total Hg at the end of the nighttime period.

These results demonstrate the importance of Hg adsorption to particulate matter and the need to obtain better estimates of the actual solution/particle partitioning of soluble Hg species.

The 48-hour simulations were initiated at midnight (i.e., using nocturnal concentrations for OH, Cl_2 and HO_2). We assumed daytime to occur from 8 a.m. to 8 p.m.

In the results presented below, we define Hg(II) as the sum of all oxidized mercury species including insoluble particulate mercury. We also define Hg(p) as the sum of all particulate mercury species including insoluble particulate mercury and soluble (i.e., adsorbed) particulate mercury.

Some additional calculations were performed to reveal sensitivity of the model to values of initial concentrations of gaseous Hg(II) and particulate mercury in air (see Chapter 4).

Table 5.3. Distribution of Hg species in the simulation with no soot[(a)]

Mercury species	Daytime[(b)]				Nighttime[(c)]			
	ng/m^3	M	% of Hg(0) or Hg(II)	% of total Hg	ng/m^3	M	% of Hg(0) or Hg(II)	% of total Hg
Total Hg(0)	1.75	NA	100.00	97.22	1.72	NA	100.00	95.55
Gas Hg(0)	1.75	NA	100.00	97.22	1.72	NA	100.00	95.55
Droplet Hg(0)	2.35×10^{-6}	2.34×10^{-14}	0.00	0.00	2.31×10^{-6}	2.30×10^{-14}	0.00	0.00
Total Hg(II)	5.32×10^{-2}	5.30×10^{-10}	100.00	2.96	8.33×10^{-2}	8.30×10^{-10}	100.00	4.63
Gas Hg(II)	7.93×10^{-5}	7.90×10^{-13}	0.15	0.00	8.27×10^{-4}	8.24×10^{-12}	0.99	0.0
Droplet Hg(II)	5.31×10^{-2}	5.30×10^{-10}	99.85	2.95	8.24×10^{-2}	8.22×10^{-10}	99.01	4.58
Hg^{2+}	3.81×10^{-9}	3.80×10^{-17}	0.00	0.00	3.98×10^{-8}	3.97×10^{-16}	0.00	0.0
$HgSO_3$	1.29×10^{-5}	1.28×10^{-13}	0.02	0.00	1.34×10^{-4}	1.34×10^{-12}	0.16	0.0
$Hg(SO_3)_2^{2-}$	2.18×10^{-3}	2.17×10^{-11}	4.10	0.12	2.26×10^{-2}	2.26×10^{-10}	27.25	1.26
$HgCl_2$	9.15×10^{-4}	9.13×10^{-12}	1.71	0.05	9.55×10^{-3}	9.52×10^{-11}	11.46	0.53
$Hg(OH)_2$	3.81×10^{-5}	3.80×10^{-14}	0.07	0.0	3.98×10^{-5}	3.97×10^{-13}	0.05	0.0
Hg(p) (soluble)	0.00	0.00	0.00	0.0	0.0	0.0	0.00	0.0
Hg(p) (non-soluble)	5.00×10^{-2}	NA	93.98	2.78	5.00×10^{-2}	NA	60.02	2.78

(a) Concentrations are provided in mass per volume of air (ng/m^3) and, for the aqueous phase, in moles per volume of water (M); NA = not applicable; percentage numbers may not add to 100% due to round-off and percentage numbers less than 0.005% are reported as 0.00%

(b) At time = 20 h

(c) At time = 32 h

Figure 5.15 shows the temporal variation of the total (i.e., gas, aqueous and particulate) concentration of Hg(II) per volume of air (ng/m^3), the aqueous concentration of Hg(II) per volume of air (ng/m^3) excluding particulate Hg(II) present in droplets, the particulate concentration of Hg(II) per volume of air (ng/m^3), and the ratio of Hg(II) (including particulate Hg) to Hg(0). In this case, Hg(p) is zero since there is no initial Hg(p) and no soot to adsorb Hg(II).

Concentrations of Hg(II) species are greater at night than during the day because the oxidation of Hg(0) by Cl_2 is zero during the day and the reduction of Hg(II) by HO_2 is zero at night. The rate of the aqueous oxidation of Hg(0) by OH is too low to have a significant effect on the diurnal cycle of Hg chemistry. The result of this diurnal variation in the red-ox Hg reactions is increased oxidation of Hg(0) at night and increased reduction of Hg(II) during the day. Consequently, the Hg(II)/Hg(0) ratio increases at night and decreases during the day. The Hg(II) concentrations are greater on the second day than on the first day because there is more time for Hg(0) oxidation during the second nocturnal period.

Table 5.4 presents the distribution of Hg species for daytime and nighttime conditions. Concentrations are presented for all species in mass per volume of air (ng/m^3) and, for aqueous-phase species, in moles per volume of water (M). Partitioning between the gas and

aqueous phases and Hg(II) speciation are also presented in percentage with respect to Hg(0) or Hg(II) as well as with respect to total Hg. Note that in table 5.4, particulate mercury is included in the droplet Hg(II) budget since it is assumed that (1) particulate mercury is oxidized mercury and (2) all particles are scavenged by the droplets.

The low solubility of Hg(0) leads to the majority of Hg(0) to be present in the gas phase, only about 0.0001% is present in the aqueous phase. On the other hand, only about 2% of soluble Hg(II) is present in the gas phase. Note that most gas-phase Hg(II) is $Hg(OH)_2$ because it is more volatile (less soluble) than $HgCl_2$.

At night, reduction of Hg(II) occurs only via $HgSO_3$ since HO_2 concentrations are set to zero; however, the kinetics of this reaction as measured by *L.E. van Loon et al.* [2000] is slow. Oxidation of Hg(0) occurs via the aqueous reaction with HOCl (83%), the aqueous reaction with O_3 (11%) and the gas-phase reaction with O_3 (6%). During the day, reduction of Hg(II) is governed by HO_2 (98%) and the $HgSO_3$ reaction is minor (2%). Since the Cl_2 concentration is set to zero during the day, the oxidation of Hg(0) occurs solely by reaction with O_3 in the aqueous phase (60%) and the gas phase (36%), and by reaction with OH in the aqueous phase (4%).

The speciation of Hg(II) does not change between day and night because it depends on the concentrations of SO_2, Cl^-, H^+ and particles and these concentrations remain constant. In droplets, soluble Hg(II) is primarily present as $Hg(SO_3)_2^{2-}$ (68%) and $HgCl_2$ (29%). The Hg(II) concentration varies between 0.002 and 0.03 ng/m^3. Accordingly, the ratio of total Hg(II) to Hg(0) varies between 0.1 and 1.8%.

The simulation results for case 2 are presented in figure 5.16 and table 5.5. Because the treatment of the adsorption of mercury to soot differs significantly among various models, it is of interest to conduct a simulation with soot in order to investigate this potential source of discrepancy among models. Therefore, the initial concentrations used in this simulation were identical to those used in the base case simulation except for the soot concentration that was set to 0.5 μgC/m^3. In this simulation, only dissolved Hg(II) is available for reduction to Hg(0) in the aqueous phase. As a result, the Hg(II) concentrations are greater in this simulation than in the case 1 simulation. At the end of the daytime period, Hg(II) is 0.3% of total Hg (compared to 0.1% in case 1). At night, the HO_2 reduction reaction does not take place and the Cl_2 oxidation reaction favors Hg(II) formation. As a result, Hg(II) accounts for about 2% of total Hg at the end of the nighttime period (compared to 1.8% in case 1). About 40% of soluble Hg(II) is adsorbed to particles. In droplets, soluble Hg(II) is primarily present as $Hg(SO_3)_2^{2-}$ (41% of soluble Hg(II)), $HgCl_2$ (17%), and adsorbed Hg(II) (40%).

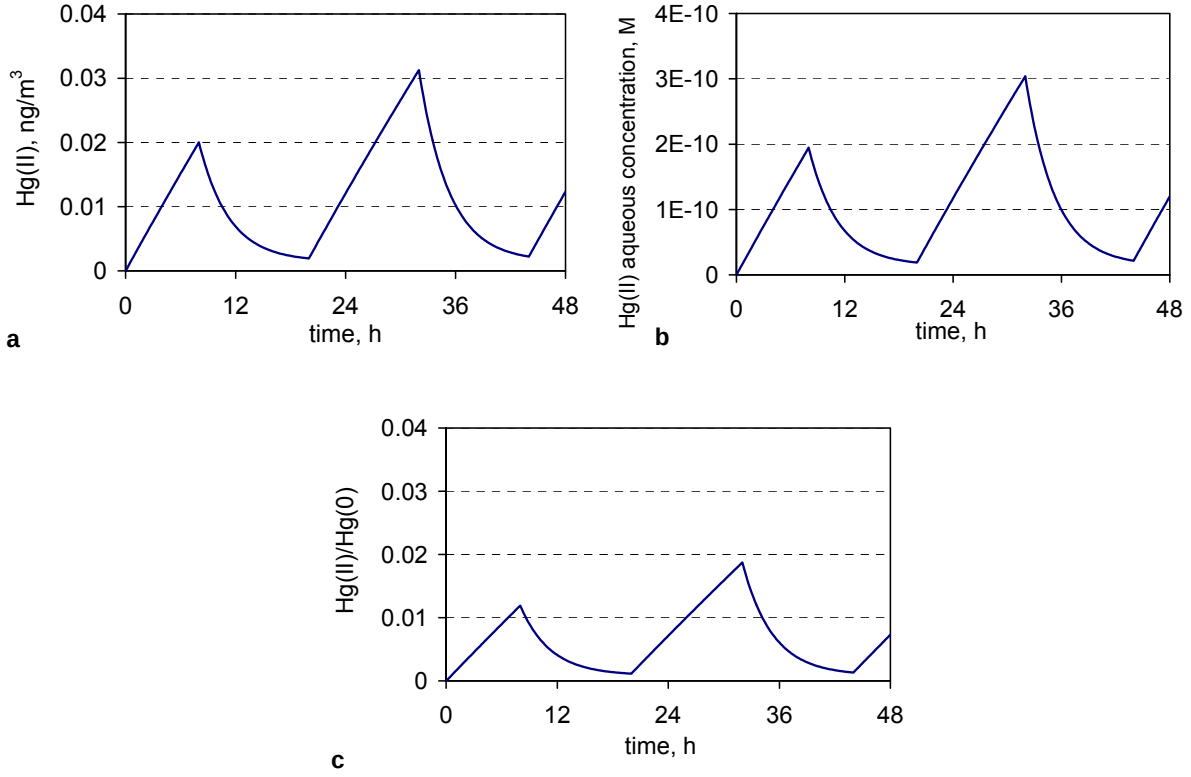

Figure 5.15. Simulation results for case 1: (a) Hg(II) total concentration (ng/m^3); (b) Hg(II) aqueous concentration (ng/m^3); (c) Hg(II)/Hg(0) ratio

Table 5.4. Distribution of Hg species in the case 1 simulation[(a)]

Mercury species	Daytime[(b)]				Nighttime[(c)]			
	ng/m^3	M	% of Hg(0) or Hg(II)	% of total Hg	ng/m^3	M	% of Hg(0) or Hg(II)	% of total Hg
Total Hg(0)	1.70	NA	100.0	99.9	1.67	NA	100.0	98.2
Gas-phase Hg(0)	1.70	NA	100.0	99.9	1.67	NA	100.0	98.2
Droptlet Hg(0)	2.29×10^{-6}	2.28×10^{-14}	0.0	0.0	2.25×10^{-6}	2.24×10^{-14}	0.0	0.0
Total Hg(II)	1.95×10^{-3}	NA	100.0	0.1	3.13×10^{-2}	NA	100.0	1.8
Gas-phase Hg(II)	5.55×10^{-5}	NA	2.8	0.0	7.77×10^{-4}	NA	2.5	0.0
Droplet Hg(II)	1.90×10^{-3}	1.89×10^{-11}	97.2	0.1	3.05×10^{-2}	3.04×10^{-10}	97.5	1.8
Hg^{2+}	2.33×10^{-9}	2.32×10^{-17}	0.0	0.0	3.74×10^{-8}	3.73×10^{-16}	0.0	0.0
$HgSO_3$	7.86×10^{-6}	7.84×10^{-14}	0.4	0.0	1.26×10^{-4}	1.26×10^{-12}	0.4	0.0
$Hg(SO_3)_2^{2-}$	1.33×10^{-3}	1.32×10^{-11}	68.0	0.1	2.13×10^{-2}	2.13×10^{-10}	68.3	1.3
$HgCl_2$	5.58×10^{-4}	5.57×10^{-12}	28.6	0.0	8.98×10^{-3}	8.95×10^{-11}	28.7	0.5
$Hg(OH)_2$	2.33×10^{-6}	2.32×10^{-14}	0.1	0.0	3.74×10^{-5}	3.73×10^{-13}	0.1	0.0
Hg(p) (soluble)	0.00	0.00	0.0	0.0	0.00	0.00	0.0	0.0
Hg(p) (non-soluble)	0.00	NA	0.0	0.0	0.00	NA	0.0	0.0

(a) Concentrations are provided in mass per volume of air (ng/m^3) and, for the aqueous phase, in moles per volume of water (M); NA = not applicable; percentage numbers may not add to 100% due to round-off and percentage numbers less than 0.05% are reported as 0.0%

(b) At time = 20 h

(c) At time = 32 h

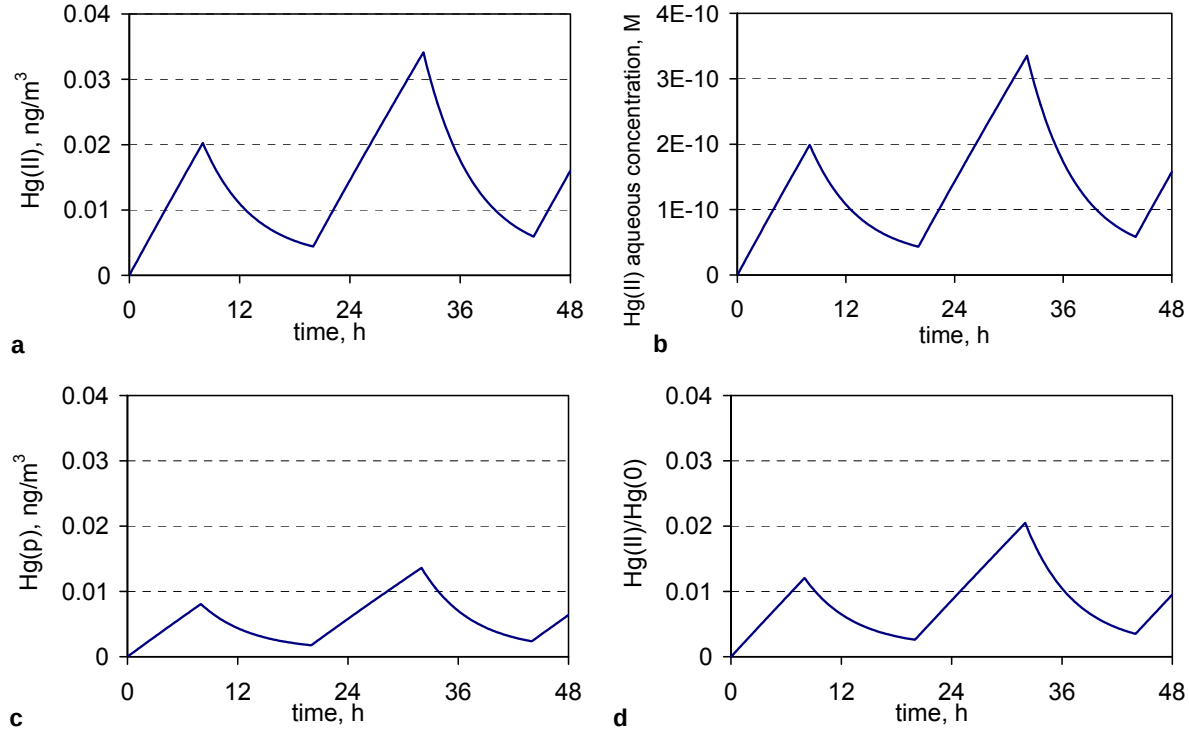

Figure 5.16. Simulation results for case 2: (a) Hg(II) total concentration (ng/m^3), (b) Hg(II) aqueous concentration (ng/m^3) (inluding adsorbed Hg(II) present in particles), (c) particulate Hg(II) concentration (ng/m^3), (d) Hg(II)/Hg(0) ratio

Table 5.5. Distribution of Hg species in the case 2 simulation[(a)]

Mercury species	Daytime[(b)]				Nighttime[(c)]			
	ng/m^3	M	% of Hg(0) or Hg(II)	% of total Hg	ng/m^3	M	% of Hg(0) or Hg(II)	% of total Hg
Total Hg(0)	1.70	NA	100.0	99.7	1.67	NA	100.0	98.0
Gas-phase Hg(0)	1.70	NA	100.0	99.7	1.67	NA	100.0	98.0
Droptlet Hg(0)	2.28×10^{-6}	2.28×10^{-14}	0.0	0.0	2.24×10^{-6}	2.24×10^{-14}	0.0	0.0
Total Hg(II)	4.40×10^{-3}	NA	100.0	0.3	3.41×10^{-2}	NA	100.0	2.0
Gas-phase Hg(II)	6.58×10^{-5}	NA	1.5	0.0	5.10×10^{-4}	NA	1.5	0.0
Droplet Hg(II)	4.34×10^{-3}	4.33×10^{-11}	98.5	0.3	3.36×10^{-2}	3.35×10^{-10}	98.5	2.0
Hg^{2+}	3.17×10^{-9}	3.16×10^{-17}	0.0	0.0	2.45×10^{-8}	2.45×10^{-16}	0.0	0.0
$HgSO_3$	1.07×10^{-5}	1.07×10^{-13}	0.2	0.0	8.29×10^{-5}	8.27×10^{-13}	0.2	0.0
$Hg(SO_3)_2^{2-}$	1.81×10^{-3}	1.80×10^{-11}	41.1	0.1	1.40×10^{-2}	1.40×10^{-10}	41.1	0.8
$HgCl_2$	7.60×10^{-4}	7.58×10^{-12}	17.3	0.0	5.89×10^{-3}	5.87×10^{-11}	17.3	0.3
$Hg(OH)_2$	3.17×10^{-6}	3.16×10^{-14}	0.1	0.0	2.45×10^{-5}	2.45×10^{-13}	0.1	0.0
Hg(p) (soluble)	1.76×10^{-3}	1.75×10^{-11}	39.9	0.1	1.36×10^{-2}	1.36×10^{-10}	39.9	0.8
Hg(p) (non-soluble)	0.00	NA	0.0	0.0	0.00	NA	0.0	0.0

(a) Concentrations are provided in mass per volume of air (ng/m^3) and, for the aqueous phase, in moles per volume of water (M); NA = not applicable; percentage numbers may not add to 100% due to round-off and percentage numbers less than 0.05% are reported as 0.0%

(b) At time = 20 h

(c) At time = 32 h

The relatively small effect of soot on Hg(II) concentrations (an increase of only 0.2% in the Hg(II)/Hg(0) ratio) is due to the fact that Hg(II) adsorption to soot is assumed to be reversible in our model. Therefore, as dissolved Hg(II) is reduced to Hg(0), some Hg(II) desorbs from the soot particles and becomes available for reduction. This reversible adsorption/desorption is consistent with the experiments conducted by Frontier Geosciences, Inc. where Hg(II) was shown to adsorb as well as desorb from atmospheric particulate matter [*Seigneur et al*., 1998]. These results demonstrate the importance of Hg adsorption to particulate matter and the need to obtain better estimates of the actual solution/particle partitioning of soluble Hg species.

The simulation results for case 3 are presented in figure 5.17 and table 5.6. Case 3 differs from case 1 by the initial concentration of insoluble Hg(p) of 0.04 ng/m^3. Since in our model, insoluble Hg(p) is not involved in the red-ox chemistry of mercury and does not adsorb Hg(II), the simulation results for case 3 differ from those obtained for case 1 only by the additional amount of Hg(p). As a result, the ratio of Hg(II)/Hg(0) has increased to 2.4% during the day and 4.1% at night. The distribution of soluble Hg(II) among the various oxidized mercury species is identical to that of case 1.

The simulation results for case 4 are presented in figure 5.18 and table 5.7. Case 4 differs from case 1 by the initial concentration of soluble Hg(II) of 0.005 ng/m^3. This intial Hg(II) concentration leads to slightly greater concentrations of Hg(II) on the first day. However, the mercury concentrations are very similar to those obtained in case 1 on the second day. This result is due to the fact that the red-ox mercury system is governed by reactions that bring the Hg(II) and Hg(0) concentrations toward equilibrium. Therefore, after 24 hours of simulation, the initial concentration of Hg(II) (which is a small amount of total Hg) has a negligible effect on the calculated speciation of mercury.

The simulation results for case 5 are presented in figure 5.19 and table 5.8. In this simulation, initial concentrations of soot, insoluble Hg(p), and soluble Hg(II) were included, with values equal to those used in cases 2, 3 and 4, respectively. This simulation is more likely to represent a real atmosphere since all relevant species are included with realistic concentrations. The concentration of Hg(II) (both soluble and insoluble) represents between 2 and 4% of total mercury. This ratio of soluble Hg(II) to Hg(0) is consistent with available data. For example, *S.E. Lindberg and W.J. Stratton* [1998] measured Hg(II)/Hg(0) ratios of 2 to 8% in North America.

The particulate mercury concentrations are consistent with values reported by Frontier Geosciences in their sorption experiments with atmospheric particulate matter suspended in water [*Seigneur et al*., 1998]. In those experiments, dissolved Hg(II) accounted for 3 to 22% of total Hg(II) in water; the value simulated here is 6% at the end of the daytime period and 27% at the end of the nighttime period. The sorption experiments suggested that the soluble fraction of Hg(II) adsorbed to particles was in the range of 9 to 55%; the value simulated here is 40%

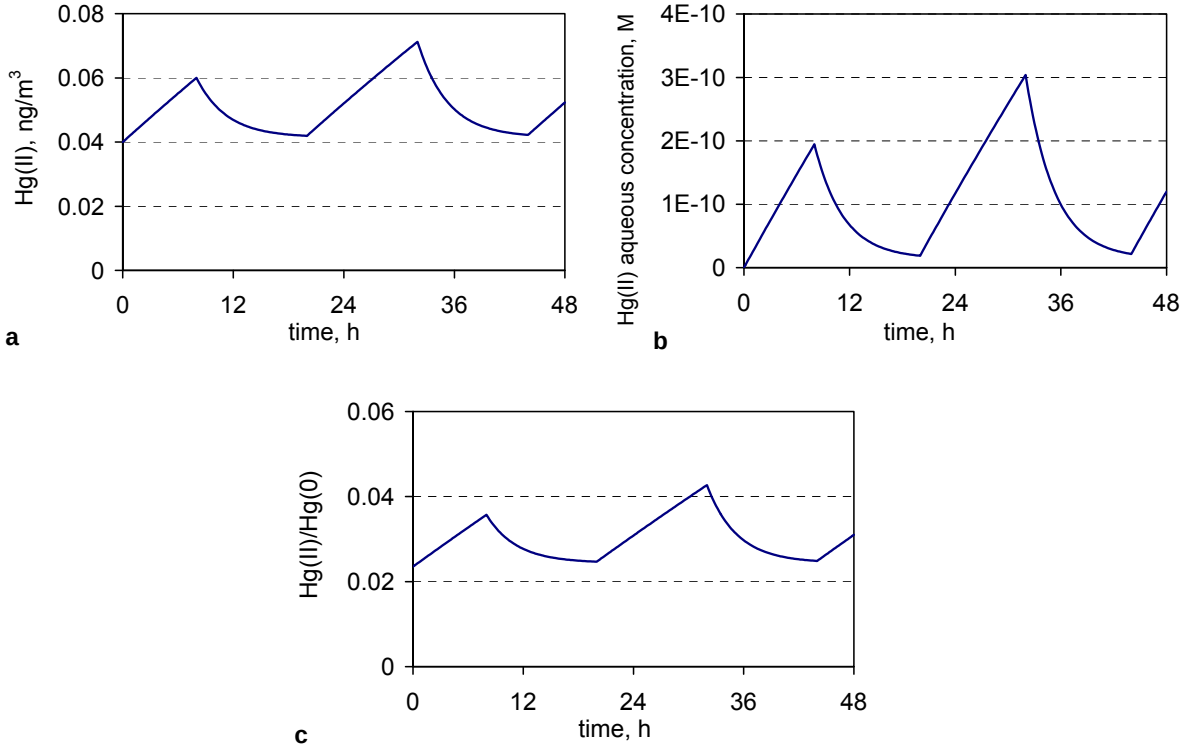

Figure 5.17. Simulation results for case 3: (a) Hg(II) total concentration (ng/m^3); (b) - Hg(II) aqueous concentration (ng/m^3) (excluding Hg(II) present in particles which is constant at 0.04 ng/m^3); (c) Hg(II)/Hg(0) ratio

Table 5.6. Distribution of Hg species in the case 3 simulation[(a)]

Mercury species	Daytime[(b)]				Nighttime[(c)]			
	ng/m^3	M	% of Hg(0) or Hg(II)	% of total Hg	ng/m^3	M	% of Hg(0) or Hg(II)	% of total Hg
Total Hg(0)	1.70	NA	100.0	97.6	1.67	NA	100.0	95.9
Gas-phase Hg(0)	1.70	NA	100.0	97.6	1.67	NA	100.0	95.9
Droptlet Hg(0)	2.29×10^{-6}	2.28×10^{-14}	0.0	0.0	2.25×10^{-6}	2.24×10^{-14}	0.0	0.0
Total Hg(II)	4.20×10^{-2}	NA	100.0	2.4	7.13×10^{-2}	NA	100.0	4.1
Gas-phase Hg(II)	5.55×10^{-5}	NA	0.1	0.0	7.77×10^{-4}	NA	1.1	0.0
Droplet Hg(II)	4.19×10^{-2}	4.18×10^{-10}	99.9	2.4	7.05×10^{-2}	7.03×10^{-10}	98.9	4.1
Hg^{2+}	2.33×10^{-9}	2.32×10^{-17}	0.0	0.0	3.74×10^{-8}	3.73×10^{-16}	0.0	0.0
$HgSO_3$	7.86×10^{-6}	7.84×10^{-14}	0.0	0.0	1.26×10^{-4}	1.26×10^{-12}	0.2	0.0
$Hg(SO_3)_2^{2-}$	1.33×10^{-3}	1.32×10^{-11}	3.2	0.1	2.13×10^{-2}	2.13×10^{-10}	30.0	1.2
$HgCl_2$	5.58×10^{-4}	5.57×10^{-12}	1.3	0.0	8.98×10^{-3}	8.95×10^{-11}	12.6	0.5
$Hg(OH)_2$	2.33×10^{-6}	2.32×10^{-14}	0.0	0.0	3.74×10^{-5}	3.73×10^{-13}	0.1	0.0
Hg(p) (soluble)	0.00	0.00	0.0	0.0	0.00	0.00	0.0	0.0
Hg(p) (non-soluble)	4.00×10^{-2}	NA	95.3	2.3	4.00×10^{-2}	NA	56.1	2.3

(a) Concentrations are provided in mass per volume of air (ng/m^3) and, for the aqueous phase, in moles per volume of water (M); NA = not applicable; percentage numbers may not add to 100% due to round-off and percentage numbers less than 0.05% are reported as 0.0%

(b) At time = 20 h

(c) At time = 32 h

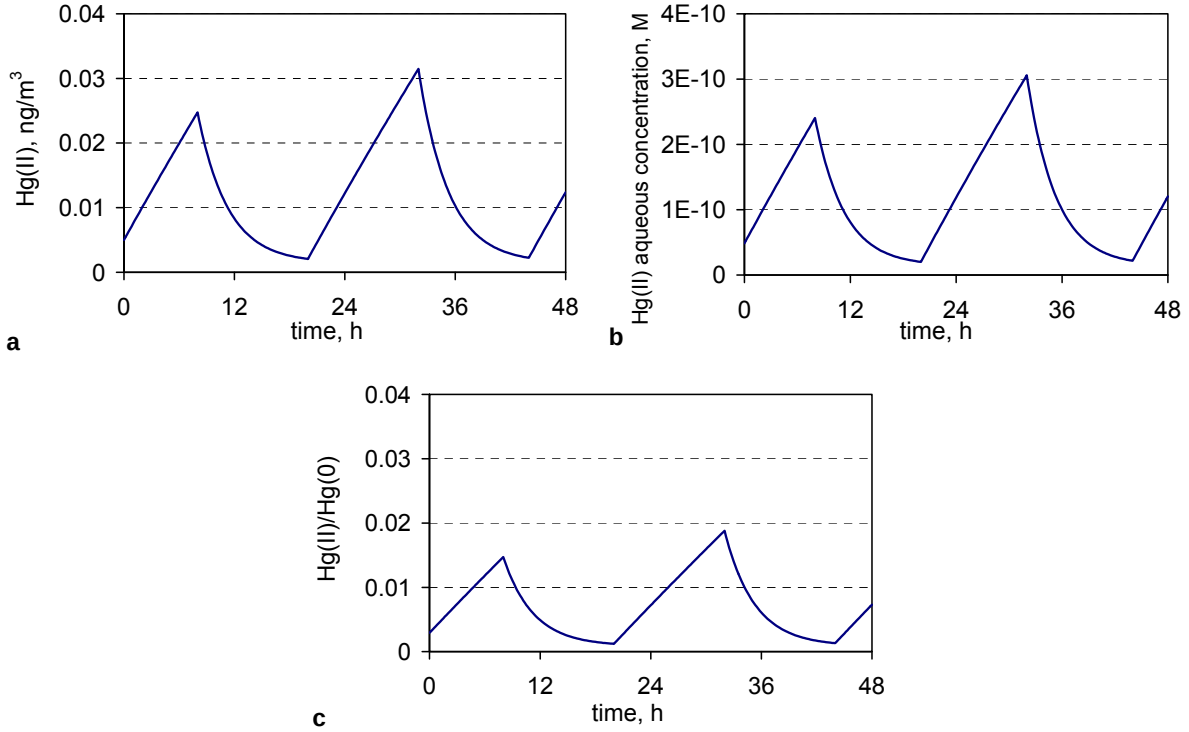

Figure 5.18. Simulation results for case 4: (a) Hg(II) total concentration (ng/m^3), (b) Hg(II) aqueous concentration (ng/m^3), (c) Hg(II)/Hg(0) ratio

Table 5.7. Distribution of Hg species in the case 4 simulation[(a)]

Mercury species	Daytime[(b)]				Nighttime[(c)]			
	ng/m^3	M	% of Hg(0) or Hg(II)	% of total Hg	ng/m^3	M	% of Hg(0) or Hg(II)	% of total Hg
otal Hg(0)	1.70	NA	100.0	99.9	1.67	NA	100.0	98.2
Gas-phase Hg(0)	1.70	NA	100.0	99.9	1.67	NA	100.0	98.2
Droptlet Hg(0)	2.29×10^{-6}	2.29×10^{-14}	0.0	0.0	2.25×10^{-6}	2.25×10^{-14}	0.0	0.0
Total Hg(II)	2.07×10^{-3}	NA	100.0	0.1	3.15×10^{-2}	NA	100.0	1.8
Gas-phase Hg(II)	5.57×10^{-5}	NA	2.7	0.0	7.82×10^{-4}	NA	2.5	0.0
Droplet Hg(II)	2.02×10^{-3}	2.01×10^{-11}	97.3	0.1	3.07×10^{-2}	3.06×10^{-10}	97.5	1.8
Hg^{2+}	2.33×10^{-9}	2.32×10^{-17}	0.0	0.0	3.74×10^{-8}	3.73×10^{-16}	0.0	0.0
$HgSO_3$	7.86×10^{-6}	7.84×10^{-14}	0.4	0.0	1.26×10^{-4}	1.26×10^{-12}	0.4	0.0
$Hg(SO_3)_2^{2-}$	1.33×10^{-3}	1.32×10^{-11}	64.0	0.1	2.13×10^{-2}	2.13×10^{-10}	67.8	1.3
$HgCl_2$	5.58×10^{-4}	5.57×10^{-12}	26.9	0.0	8.98×10^{-3}	8.95×10^{-11}	28.5	0.5
$Hg(OH)_2$	2.33×10^{-6}	2.32×10^{-14}	0.1	0.0	3.74×10^{-5}	3.73×10^{-13}	0.1	0.0
Hg(p) (soluble)	0.00	0.00	0.0	0.0	0.00	0.00	0.0	0.0
Hg(p) (non-soluble)	0.00	NA	0.0	0.0	0.00	NA	0.0	0.0

(a) Concentrations are provided in mass per volume of air (ng/m^3) and, for the aqueous phase, in moles per volume of water (M); NA = not applicable; percentage numbers may not add to 100% due to round-off and percentage numbers less than 0.05% are reported as 0.0%

(b) At time = 20 h

(c) At time = 32 h

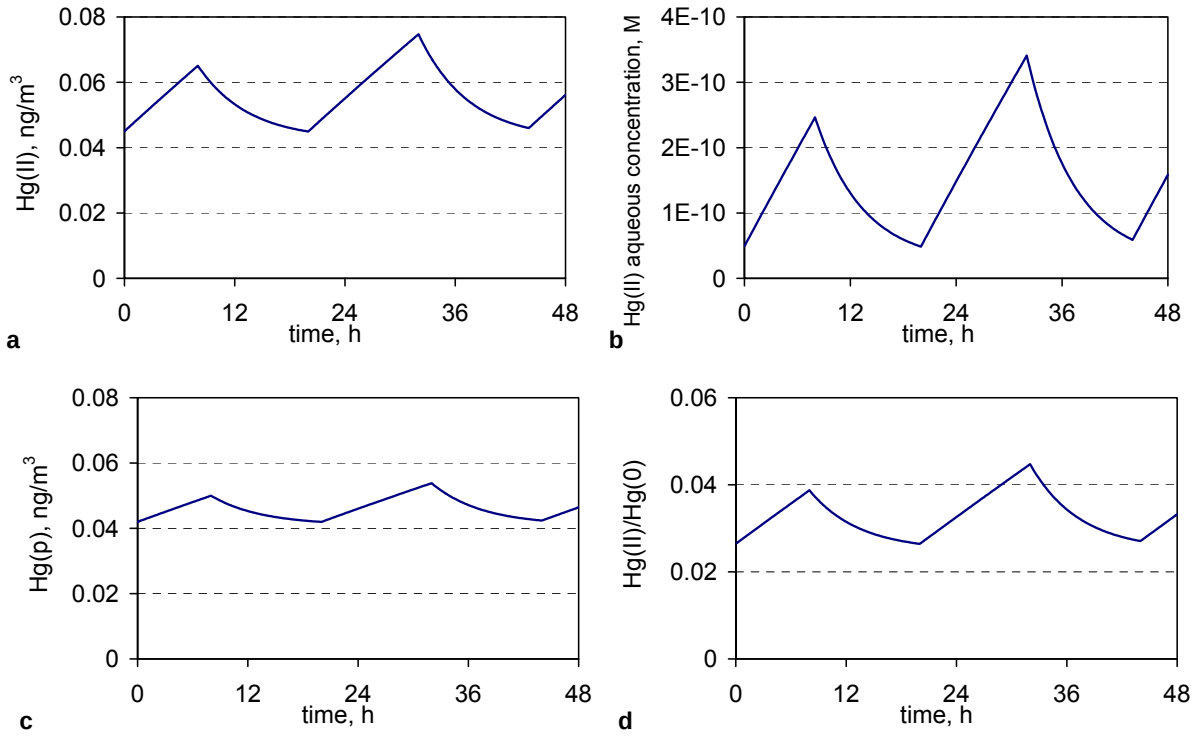

Figure 5.19. Simulation results for case 5: (a) Hg(II) total concentration (ng/m^3), (b) Hg(II) aqueous concentration (ng/m^3) (excluding insoluble Hg(II) present in particles), (c) insoluble particulate Hg(II) concentration (ng/m^3), (d) Hg(II)/Hg(0) ratio.

Table 5.8. Distribution of Hg species in the case 5 simulation[a]

Mercury species	Daytime[b]				Nighttime[c]			
	ng/m^3	M	% of Hg(0) or Hg(II)	% of total Hg	ng/m^3	M	% of Hg(0) or Hg(II)	% of total Hg
Total Hg(0)	1.70	NA	100.0	97.4	1.67	NA	100.0	95.7
Gas-phase Hg(0)	1.70	NA	100.0	97.4	1.67	NA	100.0	95.7
Droplet Hg(0)	2.29×10^{-6}	2.28×10^{-14}	0.0	0.0	2.25×10^{-6}	2.24×10^{-14}	0.0	0.0
Total Hg(II)	4.49×10^{-2}	NA	100.0	2.6	7.47×10^{-2}	NA	100.0	4.3
Gas-phase Hg(II)	7.39×10^{-5}	NA	0.2	0.0	5.19×10^{-4}	NA	0.7	0.0
Droplet Hg(II)	4.49×10^{-2}	4.47×10^{-10}	99.8	2.6	7.42×10^{-2}	7.40×10^{-10}	99.3	4.3
Hg^{2+}	3.17×10^{-9}	3.16×10^{-17}	0.0	0.0	2.45×10^{-8}	2.45×10^{-16}	0.0	0.0
$HgSO_3$	1.07×10^{-5}	1.07×10^{-13}	0.0	0.0	8.29×10^{-5}	8.27×10^{-13}	0.1	0.0
$Hg(SO_3)_2^{2-}$	1.81×10^{-3}	1.80×10^{-11}	4.0	0.1	1.40×10^{-2}	1.40×10^{-10}	18.8	0.8
$HgCl_2$	7.60×10^{-4}	7.58×10^{-12}	1.7	0.0	5.89×10^{-3}	5.87×10^{-11}	7.9	0.3
$Hg(OH)_2$	3.17×10^{-6}	3.16×10^{-14}	0.0	0.0	2.45×10^{-5}	2.45×10^{-13}	0.0	0.0
Hg(p) (soluble)	1.76×10^{-3}	1.75×10^{-11}	3.9	0.1	1.36×10^{-2}	1.36×10^{-10}	18.2	0.8
Hg(p) (non-soluble)	4.00×10^{-2}	NA	89.0	2.3	4.00×10^{-2}	NA	53.5	2.3

(a) Concentrations are provided in mass per volume of air (ng/m^3) and, for the aqueous phase, in moles per volume of water (M); NA = not applicable; percentage numbers may not add to 100% due to round-off and percentage numbers less than 0.05% are reported as 0.0%

(b) At time = 20 h

(c) At time = 32 h.

5.4. Results Obtained by MSCE-HM Model

The results for the basic set of initial parameters have been obtained with the three versions of the MSC-East module (see 2.4). To reveal a possible role of soot particles in mercury atmospheric chemistry each version was used twice: with soot particles in the modelled system and without them. The calculation results for mercury evolution in the liquid phase are plotted in figures 5.20 – 5.25. All dissolved mercury chemical species are combined into one form – “dissolved mercury”.

At the first moment particulate airborne mercury totally transfers to the liquid phase. Half of this mercury is instantly dissolved. The other half occurs in the liquid phase within insoluble particles. The main part of gaseous mercury chloride also transfers to the liquid phase in accordance with Henry`s law. Elemental mercury is distributed between the gas and liquid phase but only a small part transfers from air to water. All together these mercury forms produce initial mercury concentration in water of about 200 ng/l. This initial value is the same for all three model versions.

In all considered situations the concentration of mercury buried within the insoluble particles remains constant (50 ng/l) in the course of the modelled period. Another forms can evolve as a result of different chemical reactions. Figures 5.20 – 5.25 show that the versions of the model No. 1 and 2 give practically the same results: in the course of the simulated period the total mercury concentration is permanently rising from about 200 ng/l to 280 ng/l. The changing is practically linear during the 48-hour period under the prescribed conditions. This rising means continuos “pumping” of mercury to water drops from the ambient air. In accordance with the modelling scheme the ratio between dissolved and reversibly adsorbed mercury forms is constant in time (1 : 5). It is natural, that the concentration of insoluble mercury remains constant.

Very different picture has been obtained for version 3 (fig. 5.24 and 5.25) when the radicals play their very important role. In the course of the first six hours (nighttime) the total mercury concentration increases (like in versions 1 and 2). After sun rise the radicals appear and start to oxidize and reduce mercury. The oxidation process does not depend on occurrence of soot particles while reduction process is very fast when soot particles are absent. The reason for this is in the fact that absorbed mercury species cannot react with HO_2 radical. It results in very slow decreasing of the total mercury concentration in the liquid phase in the presence of soot particles (fig. 5.24). On the contrary, in the absence of soot particles the total mercury concentration drops rapidly from about 200 ng/l to 60 ng/l (fig. 5.25). In this case the main part of soluble oxidized mercury is reduced to elemental state, and it escapes from the liquid phase.

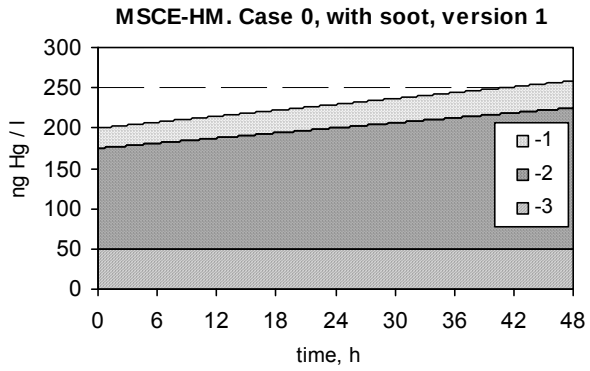

Figure 5.20. Hg liquid phase concentrations calculated by version 1 of MSCE-HM. Case 0 with soot in air. 1 – dissolved mercury; 2 – mercury absorbed on soot particles; 3 – insoluble particulate mercury

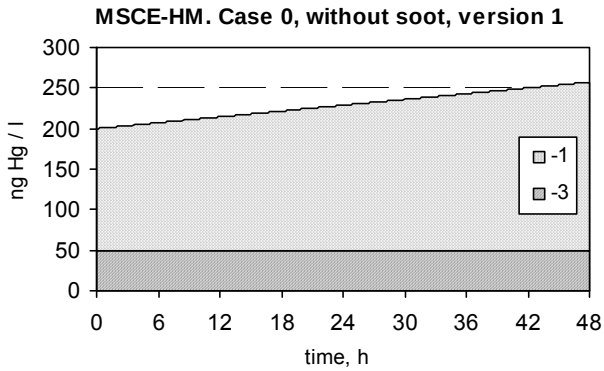

Figure 5.21. Hg liquid phase concentrations calculated by version 1 of MSCE-HM. Case 0 without soot in air. 1 – dissolved mercury; 3 – insoluble particulate mercury.

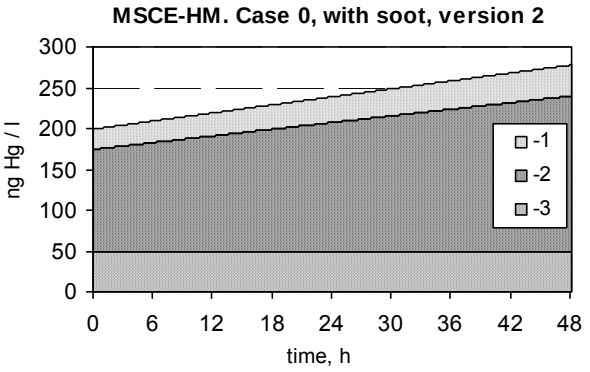

Figure 5.22. Hg liquid phase concentrations calculated by version 2 of MSCE-HM. Case 0 with soot in air. 1 – dissolved mercury; 2 – mercury absorbed on soot; 3 – insoluble particulate mercury.

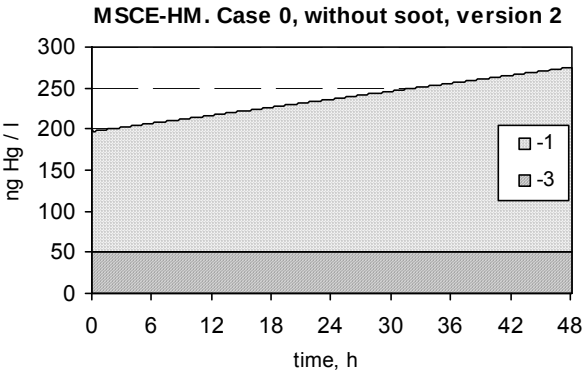

Figure 5.23. Hg liquid phase concentrations calculated by version 2 of MSCE-HM. Case 0 without soot in air. 1 – dissolved mercury; 3 – insoluble particulate mercury.

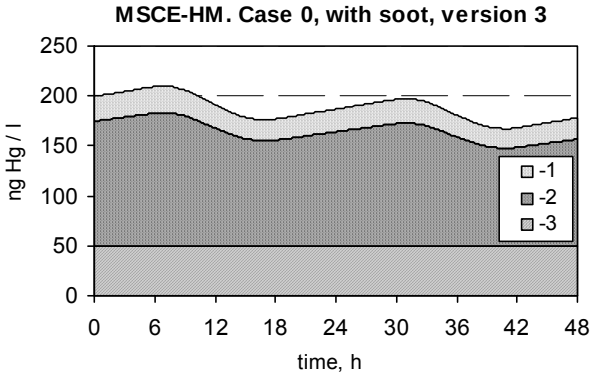

Figure 5.24. Hg liquid phase concentrations calculated by version 3 of MSCE-HM. Case 0 with soot in air. 1 – dissolved mercury; 2 – mercury absorbed on soot particles; 3 – insoluble particulate mercury.

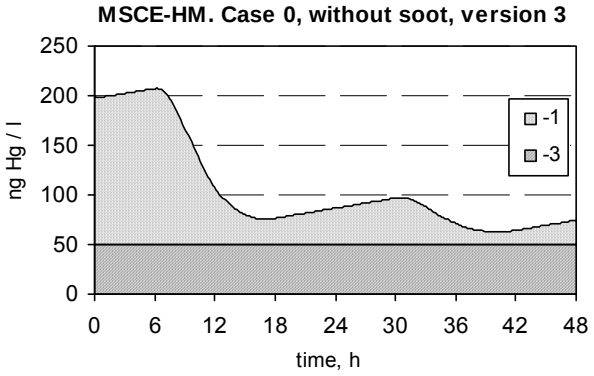

Figure 5.25. Hg liquid phase concentrations calculated by version 3 of MSCE-HM. Case 0 without soot in air. 1 – dissolved mercury; 3 – insoluble particulate mercury.

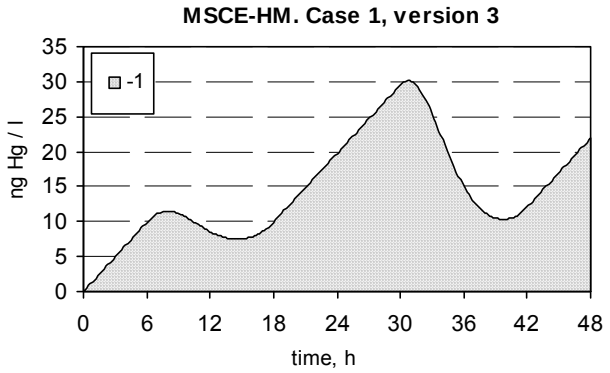

Figure 5.26. Hg liquid phase concentrations calculated by version 3 of MSCE-HM. Case 1.
1 – dissolved mercury

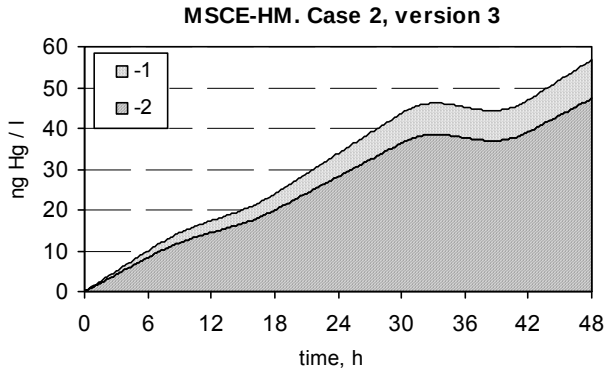

Figure 5.27. Hg liquid phase concentrations calculated by version 3 of MSCE-HM. Case 2.
1 – dissolved mercury;
2 – mercury absorbed on soot particles

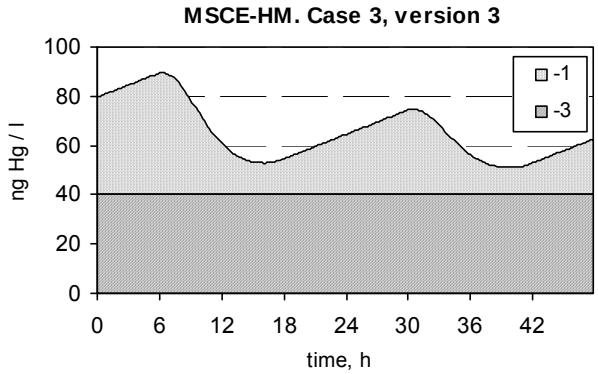

Figure 5.28. Hg liquid phase concentrations calculated by version 3 of MSCE-HM. Case 3. 1 – dissolved mercury; 3 – insoluble particulate mercury.

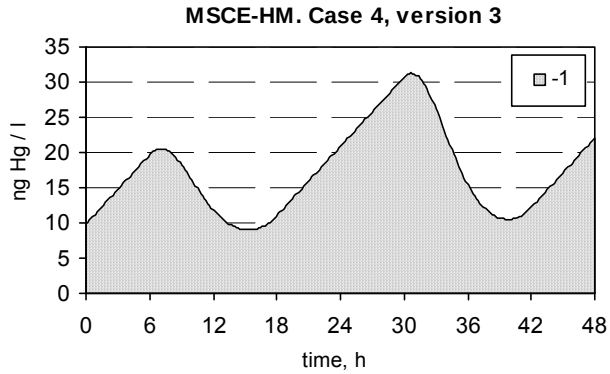

Figure 5.29. Hg liquid phase concentrations calculated by version 3 of MSCE-HM. Case 4.
1 – dissolved mercury.

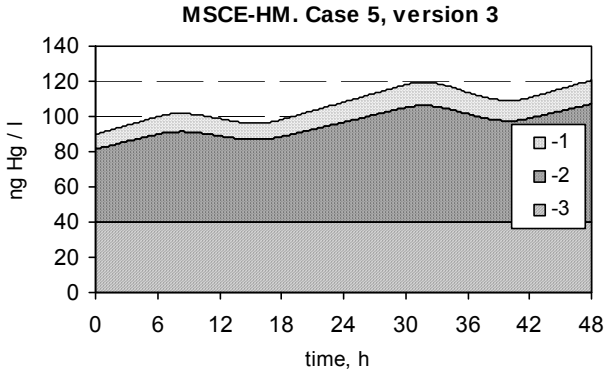

Figure 5.30. Hg liquid phase concentrations calculated by version 3 of MSCE-HM. Case 5.
1 – dissolved mercury; 2 – mercury absorbed on soot particles; 3 – insoluble particulate mercury.

To check the module sensitivity to the values of initial concentrations of gaseous and particulate mercury chloride some additional model runs have been performed. Five cases are considered (Chapter 4) using version 3 of the model.

In the first two cases initially there are no oxidized mercury (gaseous and particulate) in air. In both cases the total mercury concentration in the liquid phase generally rises (fig. 5.26 and 5.27). However, in the presence of soot particles (fig. 5.20) this increase is more pronounced. Again, the reason for this difference is in the fact that soot particles blockade the reduction reaction with HO_2 radical.

Initial presence of particulate mercury in air (case 3) leads to high concentration of mercury in the liquid phase (fig. 5.28) at the beginning of the simulation. During the daytime the concentration drops rapidly. By the second day a dynamic equilibrium is settled: the insoluble mercury concentration is constant and the soluble one varies in its diurnal cycle reaching maximum value by the end of night time.

Case 4 (fig. 5.29) is very similar to case 1 (fig. 5.26). The initial excess of soluble mercury is reduced during the first day. By the end of the first day the concentrations in both cases are practically equal, and later there is no difference between cases 4 and 1.

In the fifth case (fig. 5.30) the main part of mercury exists in water drops in the particulate form (insoluble and reversibly absorbed). The chemical system is practically in equilibrium, the diurnal cycle is slightly pronounced. The total mercury concentration remains during the simulation period on the level of 100 ng/l.

5.5. IVL Mercury Chemistry Model

The IVL Hg model was run for 5 scenarios following the scheme provided by MSC-E. The results are presented in the enclosed Excel files Resultsc1.xls to Resultsc5.xls. In Resultsc6.xls definitions of cases, units etc are given. Also results from model runs using a changed Herys law constant for Hg^0.

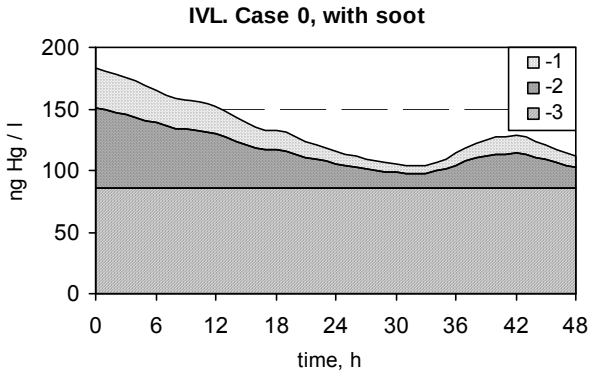

Figure 5.31. Hg liquid phase concentrations calculated by IVL model. Case 0 with soot in air.
1 – dissolved mercury; 2 – mercury absorbed on soot particles; 3 – insoluble particulate mercury

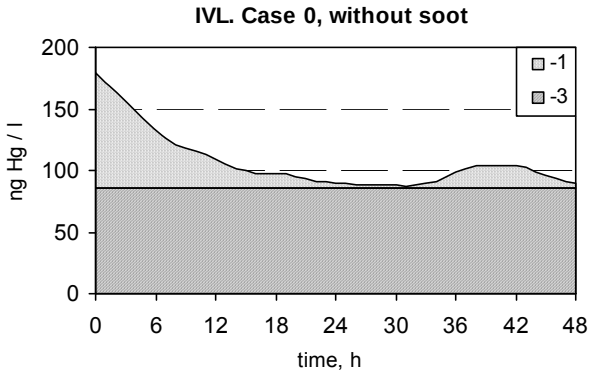

Figure 5.32. Hg liquid phase concentrations calculated by IVL model. Case 0 without soot in air.
1 – dissolved mercury; 3 – insoluble particulate mercury.

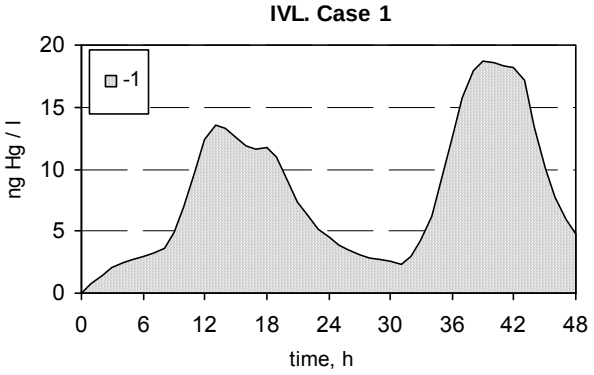

Figure 5.33. Hg liquid phase concentrations calculated by IVL model. Case 1.
1 – dissolved mercury.

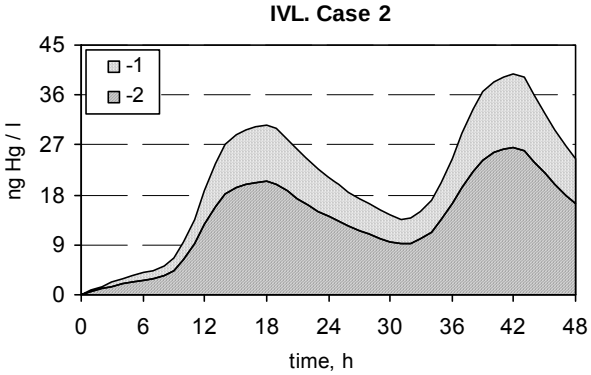

Figure 5.34. Hg liquid phase concentrations calculated by IVL model. Case 2.
1 – dissolved mercury; 2 – absorbed on soot particles mercury.

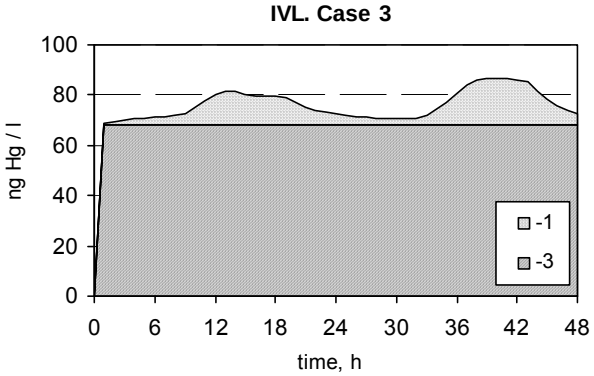

Figure 5.35. Hg liquid phase concentrations calculated by IVL model. Case 3.
1 – dissolved mercury; 3 – insoluble particulate mercury.

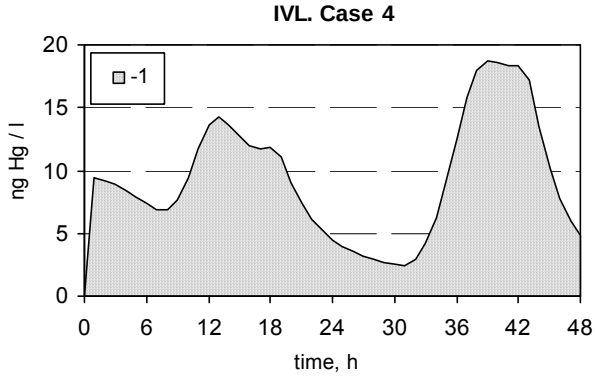

Figure 5.36. Hg liquid phase concentrations calculated by IVL model. Case 4.
1 – dissolved mercury.

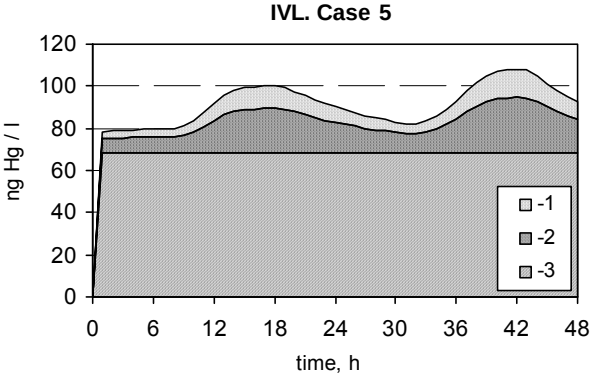

Figure 5.37. Hg liquid phase concentrations calculated by IVL model. Case 5.
1 – dissolved mercury; 2 – absorbed on soot particles mercury; 3 – insoluble particulate mercury.

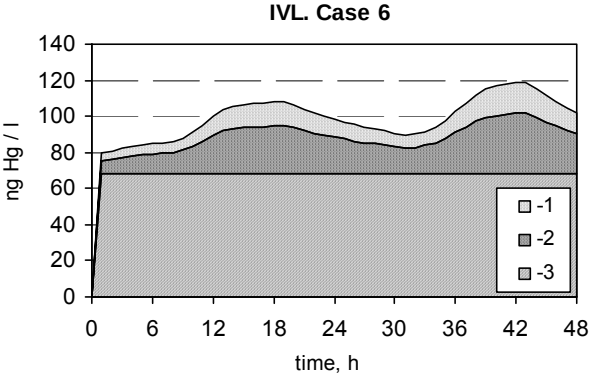

Figure 5.38. Hg liquid phase concentrations calculated by IVL model. Case 5. (New Henry's Law = 0.368 (M/Atm)) 1 – dissolved mercury; 2 – absorbed on soot particles mercury; 3 – insoluble particulate mercury.

6. COMPARISON OF THE RESULTS

As a result of calculations carried out by each group participated in the intercomparison study a huge volume of information on the content of different physical-chemical mercury forms in the gaseous and liquid phase has been obtained. In view of the fact that at the first phase of the mercury model intercomparison mercury concentration evolution in cloud droplets is of a primary interest, a special attention is payed on the behaviour of different mercury forms in the liquid phase.

It was a primordial assumption that soot particles play a significant role in the mercury behaviour in the atmosphere. For this reason the intercomparison program was started from finding out differences in interpretation of sorption processes of mercury compounds by soot in the aqueous environment. In the course of the study it was determined that for the comprehension of results it is important to presume initial concentration values of inorganic mercury compounds both gaseous and in the content of solid particles. Additional calculations with initial values measured under real conditions have been carried out.

All the participants used an identical set of initial parameters, however, the interpretation of many processes in models is different. The number of possible chemical reactions considered is different as well – from purely analytical solution (MSCE-HM, version 2) to the calculation scheme with 180 reactions between 90 individual species (model IVL).

At the consideration of calculation results obtained under basic variant (case 0) practical coincidence of initial mercury concentration in the liquid phase engages our attention. It means that all the groups use approximately identical parameters of mechanisms of physical-chemical transition of different mercury forms from the gas phase to the liquid one. In all schemes the equilibrium between the phases is set up instantly. The results at the initial moment obtained by the model of GKSS are somewhat different. It is explained by the fact that as distinct from other models GKSS model is dynamic (it considers mercury chemistry together with cloud mixing) and it takes a spin-up period of about 6 hours for dynamic equilibrium establishment in a cloud layer.

With the availability of soot particles in the system further evolution of liquid phase mercury concentrations in different models goes on in a different way. In GKSS model after the spin-up period mercury concentration in drops very slowly decreases. In MSCE-HM model (version 1 and 2) the concentration is somewhat increasing. In the first approximation in both cases mercury concentration in the liquid phase may be considered to be practically constant. However, absolute values obtained by GKSS model are significantly lower than in MSCE-HM model (version 1 and 2). It is explained by the fact that in GKSS model initially

mercury in sub-cloud layer is almost absent and in the course of layer mixing general dilution of mercury content in sub-cloud and cloud layers takes place. On the whole the dynamics of mercury behaviour in the liquid phase for these two models may be considered to be similar.

In the availability of soot AER and IVL models demonstrate a noticeable (about 2 times) decrease of concentrations in the liquid phase during the considered period. In CMAQ model mercury concentration in droplets decreases more rapidly (about 5 times during 48 hours). MSCE-HM model (version 3) also shows the concentration decrease but it is insignificant. A day-time cycle of liquid phase mercury evolution is characteristic of all these models.

The key mechanism of the influence of soot particles on mercury liquid phase chemistry is in the fact that sorbed molecules do not interact with reducing agents (sulphite-ion, hydroxyl radical). Hence in this case the oxidation process prevails the reduction one.

It is also important that in the reduction mechanism through sulphite ion the reduction rate depends upon quantity of chloride ions in the solution. This mechanism operates only at very low chloride concentrations when the reactions of the formation of several unstable sulphite-mercury complexes can be noticeably realized. At the observed chloride concentrations mainly chloride-mercury complexes are formed slowing down drastically the reduction according to sulphite-ion mechanism. On the contrary the reduction reaction with hydroperoxide radical takes place with all dissolved mercury compounds.

In any case at the prescribed initial parameters in an isolated cloud system volume sooner or later the equilibrium between the gaseous and liquid phase will be set up. Radical reactions can cause intra-diurnal disturbances of equilibrium but the next diurnal cycle will be similar to the previous one. The consideration of these or those reactions, the selection of appropriate values of reaction rates will define the time of equilibrium establishment and its level (i.e. the value of concentration ratios between different phases).

All of the preceding explains the fact that GKSS and MSCE-HM models (version 1 and 2) reveal the independence of total mercury concentrations in the liquid phase on soot availability. These models do not consider radical reactions, and at sufficiently high concentration of chloride the reduction process according to sulphite-ion mechanism does not practically take place. Thus during the whole calculation period the oxidation mechanism prevails leading to mercury accumulation in a drop independent of soot availability or its lack in the system.

In models AER, CMAQ and IVL the reaction of hydroperoxide radical is the basic reaction of reduction. It is responsible for prevailing of reduction over oxidation, and as a result the total concentration rapidly decreases in the day-time. The availability of soot, however, drastically slows down the process since hydroperoxide radical does not react with sorbed molecules. In

the dark time oxidation independent of soot availability prevails thereby increasing total mercury concentration in a drop.

The difference in the character of mercury concentration evolution is also defined by the accepted ratio of sorbed and dissolved fractions. In GKSS model (as well as in MSCE-HM model) it is assumed that in the soot availability the main fraction of mercury is sorbed and essentially lower part (about 17%) is present in solution, and it is accessible for chemical reactions. In CMAQ and AER model this ratio is about 55-60%. It is natural that in these models a considerable part of soluble mercury compounds is available for reduction reaction. Therefore even when soot is present mercury concentration in a drop sharply decreases. IVL model is in the intermediate position: it is accepted that about 2/3 of mercury is sorbed.

An important (if not most important) difference in the models is the interpretation of physical-chemical properties of aerosol particles mainly in terms of possibilities of mercury compound transition from the solid particle phase to the solution inside a drop. CMAQ model assumed that all mercury contained in aerosol particles when transferred into the liquid phase is dissolved and then it participates in chemical processes. On the contrary AER model assumes that mercury contained in aerosol particles is completely insoluble in water and consequently is not susceptible to any chemical evolution inside a drop. The IVL and MSCE-HM models take an intermediate position – in the IVL one insoluble mercury accounts for 85%, in the MSCE-HM one equal fractions of soluble and insoluble mercury are assumed. In the dynamic GKSS model after each cycle of drop evaporation, aerosol particles are produced which can again enter a drop in the next cycle. In the process of simulated evaluation the ratio of soluble and insoluble fractions is varied but in general it is close to 50:50%.

Different interpretation of solubility of aerosol mercury in an essential extent defines the concentration evolution character in a drop. It is natural that the more insoluble mercury fraction is the more stable in time total concentration value. In AER model on the second day of evolution the contribution of insoluble part varies from 65% at night to 95% in the day-time. In IVL model the contribution of insoluble fraction also reaches 95%. If there is no contribution of chemically inertial insoluble share (CMAQ model) or it is not dominating (MSCE-HM, version 3) then in the absence of soot a rapid decrease of total mercury concentration in cloud drops due to reduction is observed.

The consideration of calculation results the basic variant showed that all the models make allowance for the same main physical-chemical processes which potentially can take place in the cloud system. The principal difference lies in the consideration of radical reactions, in evaluation of the extent of mercury sorption on soot particles and in the interpretation of

solubility of mercury compounds contained in particles. The inclusion of mercury oxidation reactions due to molecular chlorine dissolution in water is not of a principal character – they take place in nighttime only and on the mean diurnal basis they are less effective than reactions of oxidation by dissolved ozone.

All the models demonstrated that to a considerable extent mercury concentration evolution in the liquid phase is defined by initial values of oxidized mercury concentrations in air. Recent experimental data have indicated that these values are lower than those taken in the basic variant of model calculations. Especially it is characteristic of gaseous inorganic mercury. For this reason calculations have been carried out both with more realistic initial concentrations of oxidized mercury and without oxidized forms at all. It allowed clarifying how different models respond to initial parameters.

The consideration of cases 1 and 4 is very indicative when originally there is no solid particles. In the first case mercury in the liquid phase appears only due to reactions of elemental form oxidation. Table 6.1 shows the calculated mercury concentrations in the liquid phase averaged over the second day of evolution when actually equilibrium between oxidation and reduction reactions is set up. As it follows from table 6.1 all models (but GKSS) predict that initial lack (case 1) or relatively low initial content of gaseous oxidized mercury in the system (case 2) does not inflict any influence upon the simulated value on the second day of evolution. GKSS model does not consider radical reduction reaction therefore mercury concentration is slowly increasing. In spite of the distinction between models in the interpretation of gas and liquid phase reactions the obtained values are rather close to each other.

Table 6.1. Liquid phase mercury concentrations averaged for the second day of the calculated evolution, ng Hg/l

Model	case 1	case 2	case 3	case 4	case 5
CMAQ	10	17	10	10	35
GKSS	15	15	75	20	80
AER	25	35	110	25	115
MSCE-HM (version 3)	20	45	70	20	120
IVL	10	25	80	10	90

Significant differences in results are noted for cases when the solid phase is prescribed. It is appropriate both for soot particles capable to adsorb reversibly dissolved mercury compounds and for particles contained insoluble mercury. As seen from table 6.1 discrepancies of modelled values for the calculated evolution in the second day may be

essential. For case 2 (initial lack of oxidized mercury, availability of soot) the MSCE-HM model gives the highest concentrations, and the GKSS one – the lowest concentrations. However, it should be mentioned that the difference is not of a dramatic character and it is within the range of a factor of 2 of the average value.

For cases 3 and 5 in which the different interpretation of mercury solubility is principal, CMAC model results differ appreciably from other results. Since this model assumes that all mercury is soluble and the fraction of adsorbed mercury is not high, reduction reactions play the main role leading to the lowest concentration values. The results of other models are within a relatively narrow range ($\pm$30% of the average). It may be considered as an excellent coincidence.

Additional calculations (GKSS-cases 6,7 and 8) were performed with GKSS dynamic model. In these cases along with the conditions defined in case 5 mercury washout from the modelled reservoir by continuous rain of different intensity (from 0.07 to 0.22 mm/h) is assumed. The calculation results point out that in these cases mercury concentration in cloud system liquid phase decreases steadily. At precipitation intensity of about 0.2 mm/hr and at rain duration of 2 days the concentration reaches about 10 ng/l. This value actually does not differ from those measured in Hamburg region (Germany) under similar meteorological conditions (prolonged rain of slight and average intensity). This agreement of calculated and observed data points out to the fact that model can adequately describe atmospheric physical-chemical processes associated with mercury.

Besides using IVL model the effect of Henry's law constant for Hg(0) on mercury behaviour in the liquid phase is investigated (IVL-case 6). This study is based on parameters of case 5. Recently refined value on Henry's law constant for elemental mercury is 0.368 M/atm. Henry constant value changes but slightly affects total mercury concentration in a drop. The effect, however, was masked by a considerable contribution of insoluble mercury (see fig. 5.30 and 5.31). If we consider only dissolved mercury, the effect of Henry constant alternation may be noticeable (more than 30%).

SUMMARY AND MAIN CONCLUSIONS

A model intercomparison study of the EMEP/MSC-E model for atmospheric mercury species with the most advanced models of different scientific groups around the world is being performed in four consecutive stages. The main objectives of the study are

- to evaluate the EMEP/MSC-E model formulated under assumptions of simplified mercury chemistry against other more comprehensive mercury simulation models

and

- to provide a possibility for EMEP/MSC-E to improve its model by an approach that adopts more advanced individual physical and chemical mercury processes from the other models without requiring significantly more computational resources to keep the model on an operational level for LRTAP Convention purposes.

Stage I of the intercomparison study described in this report has been performed involving five scientific groups using their atmospheric mercury chemistry modules and the closest possible approximation to the agreed input parameters. Results from individual modules in terms of 48 h time evolution of aqueous phase concentrations in cloud droplets for a variety of initial concentrations of mercury species in ambient air have been intercompared.

A comparative evaluation of the chemistry module performances led to 3 main issues:

In general, results from all models in terms of total aqueous mercury concentrations agree within a factor of about two, suggesting that there are no significant processes missing from their formulations. However, the results do show some differences that indicate important uncertainties regarding the reduction-oxidation balance of aqueous mercury and the fraction of aqueous mercury that is sorbed to suspended particles.

One of the modules incorporating a state-of-the-science parameterization of cloud processes including precipitation demonstrated its capabilities to reproduce results from a field measurement campaign in a moderately polluted area in Central Europe consisting of simultaneous measurements of 3 mercury species in ambient air, mercury concentration in precipitation and precipitation rates. Model predicted total concentrations in precipitation agree well with observed values and aqueous concentrations obtained with the same initial conditions but with a zero precipitation rate are close to those predicted by the other modules. These results suggest that all modules have a potential to reproduce observed concentrations reasonably well justifying their ultimate use in the full models.

There are indications from the comparative chemistry module testing that results from the MSC-E model with a simplified chemical equation set do not substantially differ from those

obtained by more comprehensive models justifying its use in the full MSC-E model in the following stages of the intercomparison. However, firm conclusions cannot only be drawn when results from the three following stages of the model intercomparison will be available and it remains to be seen if the model then can maintain its capabilities to address effectively the scientific and political questions of the LRTAP Convention.

Overall, the intercomparison study described in this Technical Note represents a first attempt to synthesize the current knowledge of atmospheric mercury chemistry into model systems that can be generally used to understand the regional atmospheric transport and fate of mercury and that lead to an adequate operational tool for the quantification of mercury transboundary fluxes in Europe.

Acknowledgements

The AER/EPRI mercury chemistry model was developed under funding from EPRI (Contract WO3218-08, Dr. Leonard Levin, EPRI Project Manager).

References

Acker K., Moller D., Wieprecht W., Kalass D. and R.Auel [1998] Investigations of ground-based clouds at the Mt. Brocken. Fresenius, *Anal. Chem*, v.361, pp.59-64

Calhoun, J.A. and E. Prestbo [1998] Kinetic study of the gas phase oxidation of elemental mercury Hg by molecular chlorine (Cl_2), Frontier Geosciences, Inc., Seattle, WA, unpublished manuscript.

Constantinou E., Wu X.A. and C. Seigneur [1995] Development and application of a reactive plume model for mercury emissions. WASP, v.80, N 1-4, pp.325-335.

Hall B. and N. Bloom [1993] Report to EPRI, Palo Alto, CA.

Hall B. [1995] The gas-phase oxidation of elemental mercury by ozone, *Water Air Soil Pollut*., v.80, pp.301-315.

Herrmann H., B. Ervens, H.-W.Jacobi, R.Wolke, P. Nowacki and R. Zellner [2000] CAPRAM2.3: A chemical aqueous phase radical mechanism for tropospheric chemistry. J*. of Atm. Chem*., v.36, p.231-284.

Gårdfeldt et al. [2001] Private communication to John Munthe.

Iverfeldt A., Occurrence and turnover of atmispheric mercury over the Nordic countries. *Water, Air and Soil Pollution*, Vol. 56, pp. 252-265.

Kosak-Channing L.F. and G.R. Helz [1983] Solubility of ozone in aqueous solutions of 0-0.6 M ionic strength at 5-30°C, *Environ. Sci. Technol*., v.17, pp.581-591.

Lin C.-J. and S.O. Pehkonen [1997] Aqueous free radical chemistry of mercury in the presence of iron oxides and ambient aerosol. *Atm. Environ*., v.31, N 24, pp.4125-4137.

Lin C.J. and S.O. Pehkonen [1998] Oxidation of elemental mercury by aqueous chlorine ($HOCl/OCl^-$): Implications for tropospheric mercury chemistry, *J. Geophys. Res*., v.103, pp.28093-28102.

Lind J.A. and G.L. Kok [1986] Henry's law determinations for aqueous solutions of hydrogen peroxide, methylhydroperoxide, and peroxyacetic acid, *J. Geophys. Res.*, v.91, pp.7889-7895.

Lindberg S.E. and W.J. Stratton [1998] Atmospheric mercury speciation: Concentrations and behavior of reactive gaseous mercury in ambient air, *Environ. Sci. Technol.*, v.32, pp.49-57.

Lindqvist O. and H. Rodhe [1985] Atmospheric mercury – a review, Tellus, v.37B, pp.136-159.

Liu X., G.Mauersberger and D.Moller, 1997. The effects of the cloud processes on the tropospheric photochemistry: An improvement of the EURAD model with a coupled gaseous and aqueous chemical mechanism, J.*Atmos. Environ*., v.31, pp.3119-3135.

Loon van L., E.Mader and S.L.Scott [2000] Reduction of the aqueous mercuric ion by sulfite: UV spectrum of $HgSO_3$ and its intramolecular redox reactions, *J. Phys. Chem.*, v.104, pp.1621-1626.

Lu J., W. H. Schroeder, T. Berg, J. Munthe, D. Schneeberger and F. Schaedlich [1998] A device for sampling and determination of total particulate mercury in ambient air, *Anal. Chem.*, v.70, pp.2403-2407.

Lurie Yu.Yu. [1971] Handbook for Analytical Chemistry. Moscow, «Khimiya», 454 p.

Marsh A.R.W. and W.J. McElroy [1985] The dissociation constant and Henry's Law constant of HCl in aqueous solution, *Atmos. Environ.*, v.19, pp.1075-1080.

McArdle J.V. and M.R. Hoffmann [1983] Kinetics and mechanism of the oxidation of aquated sulphur dioxide by hydrogen peroxide at low pH, *J. Phys. Chem*., v.87, pp.5425-5429.

Munthe J., Z.F. Xiao and O. Lindqvist [1991] The aqueous reduction of divalent mercury by sulfite, *Water Air Soil Pollut*., v.56, pp.621-630.

Munthe J. [1992] The aqueous oxidation of elemental mercury by ozone, *Atmos. Environ*., v.26A, pp.1461-1468.

Pai P., Karamchandani P. and Ch. Seigneur [1997] Simulation of the regional atmospheric transport and fate of mercury using a comprehensive Eulerian model. *AE*, 31, No 17, pp. 2717-2732.

Pehkonen, S.O. and C.J. Lin [1998] Aqueous photochemistry of divalent mercury with organic acids, *J. Air Waste Manage. Assoc*., v.48, pp.144-150.

Petersen G., Munthe J., Pleijel K., Bloxam R. and A.V.Kumar [1998] A comprehensive Eulerian modeling framework for airborne mercury species: Development and testing of the tropospheric chemistry module (TCM). *Atm. Environ.*, v. 32, No.5, pp.829-843.

Pleijel K. and J.Munte [1995] Modeling the atmospheric mercury cycle - chemistry in fog droplets. *Atm. Environ.,* v. 29, No. 12, pp. 1441-1457.

Raymond D. J. and A.M.Blyth [1986] A Stochastic Mixing Model for Non-precipitating Cumulus Clouds, *J. of Atm. Sci.*, v.3, pp.2708-2718.

Ryaboshapko A., Ilyin I., Gusev A., Afinogenova O., Berg T. and A.G. Hjellbrekke [1999] Monitoring and modelling of lead, cadmium and mercury transboundary transport in the atmosphere of Europe. Joint report of EMEP centers MSC-E and CCC. MSCE report No 1/99.

Ryaboshapko A. and V.Korolev [1997] Mercury in the atmosphere: estimates of model parameters. Meteorological Synthesizing Centre - East, EMEP/MSC-E Report 7/97, August 1997, Moscow, 60 p.

Sander R. [1997] Henry's law constants avaiable on the Web. EUROTRAC Newsletter, No. 18, pp. 24-25, http://www.science.yorku.ca/cac/people/sander/res/henry.html

Sanemasa I. [1975] The solubility of elemental mercury vapor in water, *Bull. Chem. Soc. Jpn*., v.48, pp.1795-1798.

Schroeder W.H. and J.Munthe [1998] Atmospheric mercury - an overview. *Atm. Environ*., v.32, N.5, pp. 809-822.

Seigneur C., H.Abeck, G. Chia, M. Reinhard, N.S. Bloom, E. Prestbo and P. Saxena [1998] Mercury adsorption to elemental carbon (soot) particles and atmospheric particulate matter, *Atm. Environ.*, v.32, pp.2649-2657.

Seigneur C. and K.Lohman [1999] Comparison of several chemical mechanisms for atmospheric mercury concentrations. In: Mercury as a Global Pollutant. 5th International Conference, Rio de Janeiro, May 23-28, 1999. Book of abstracts, p. 90.

Seigneur C. and P. Saxena [1988] A theoretical investigation of sulfate formation in clouds, *Atm. Environ.*, v.22, pp.101-115.

Seigneur C., Wrobel J. and E.Constantinou [1994] A chemical kinetic mechanism for atmospheric inorganic mercury. *Environ. Sci. and Technol.,* v.28, No. 9, pp.1589-1597.

Seigneur C., X.A. Wu, E. Constantinou, P. Gillespie, R.W. Bergstrom, I. Sykes, A. Venkatram and P. Karamchandani [1997] Formulation of a second-generation reactive plume & visibility model, *J. Air Waste Manage. Assoc.*, v.47, pp.176-184.

Shia R.L., C. Seigneur, P. Pai, M. Ko and N.D. Sze [1999] Global simulation of atmospheric mercury concentrations and deposition fluxes, *J. Geophys. Res.*, v.104, pp.23747-23760.

Sillen G.L. and A.E. Martell [1964] Stability Constants of Metal Ion Complexes; Special Publication of the Chemical Society: London, p. 17.

Smith R.M. and A.E. Martell [1976] Critical Stability Constants, Vol. 4, Inorganic Complexes, Plenum Press, New York.

Sommar J., K. Gårdfeldt, X. Feng and O. Lindqvist [1999] Rate coefficients for gas-phase oxidation of elemental mercury by bromine and hydroxyl radicals, in Mercury as a Global Pollutant – 5th International Conference, May 23-28, 1999, Rio de Janeiro, Brazil.

Tokos J.J.S., B. Hall, J.A. Calhoun and E.M. Prestbo [1998] Homogenous gas-phase reaction of Hg^0 with H_2O_2, O_3, CH_3I, and $(CH_3)_2S$: Implications for atmospheric Hg cycling, *Atm. Environ*., 32, 823-827.

Xiao Z.F., Munthe J., Stro:mberg D. and O.Lindqvist [1994] Photocemical Behavior of Inorganic Mercury Compounds in Aqueous Solution. In: Mercury Pollutiom: Integration and Synthesis, ed. by C.J. Watras and J.W.Huckabee, Lewis Publishers, Boca Raton, pp. 581-592.

Young T. R. and J.P.Boris [1977] A Numerical Technique for Solving Stiff Ordinary Differential Equations Associated with the Chemical Kinetics of Reactive Flow Problems, *J. of Physical Chemistry*, v.81, pp.2424-2427.